

Intercellular metabolite communication via Panx1 coordinates inflammation

Christopher Bernardo Medina

Madison, New Jersey

B.S., Siena College, 2013

A dissertation presented to the Graduate Faculty of the University of Virginia in Candidacy for the Degree of Doctor of Philosophy

Department of Microbiology, Immunology, and Cancer Biology

University of Virginia

May 2020

Abstract

Throughout the years evolution has shaped and molded the human species. This is highlighted by conserved genes and mechanisms that exist within us, including those involved in protecting our system from pathogen, disease, and insult. At the crux of this protection is inflammation, which is essential for survival. However, while inflammation is required to protect from foreign insults and even sterile injury, proper resolution must also occur. Unchecked inflammatory responses can cause excessive damage to the areas affected, and magnify health complications. Therefore, mechanisms that regulate and dampen inflammation are as important as inflammation itself. Here, in this dissertation, I have focused on how pannexin 1 channels regulate inflammatory responses in two different settings: the process of apoptosis, and the function of T regulatory cells in airway inflammation.

The first part of this dissertation examines how apoptotic cells can remain immunologically silent. I describe one mechanism by which apoptotic cells, with an intact cell membrane, can regulate and orchestrate the specific release of metabolites. Such extracellular metabolites, in turn, are able to signal to the surrounding cells to maintain an anti-inflammatory state within the tissue. Some of these metabolites were quite potent in their signaling capacity and we could combine a few select metabolites and harness their properties for therapeutic potential in several disease models.

In the second part of this dissertation, I describe a novel mechanism by which T_{eff} and T_{reg} cells can communicate via extracellular adenine nucleotides. This occurs to optimally mediate suppression of the immune response by T_{reg} cells to inhibit excessive proliferation of T_{eff} cell during airway inflammation. This crosstalk was dependent on

Panx1 channels for ATP release via either T_{eff} or T_{reg} cells and in turn regulated the severity of allergic airway inflammation. Collectively, the data from my dissertation suggest novel mechanisms by which apoptotic cells and Panx1 can mediate intercellular communication between cells which is important for the proper control of inflammation. This has implications for several inflammatory disorders and identifies ways we may be able to harness certain aspects of Panx1 for therapeutic benefit. It also advances the Pannexin field by widening the scope through which we view Panx1, as not just an ATP release channel.

Acknowledgements

First, I would like to thank my mentor Ravi. I have enjoyed my time in his lab to the fullest. Ravi has always been the most positive person in the lab and his love for science is extremely contagious. I admire the manner in which Ravi has formed such an amazing lab with great people and the way in which he is able to adapt himself to every individual's mentoring necessities. During my time here, Ravi has taught me so much and helped me grow into the scientist I am today. I was given the freedom to explore, learn, fail, and ultimately succeed. I believe this type of 'controlled' freedom as a graduate student has shown me how to think individually about scientific problems, but at the same time work together in groups to solve the question at hand. I will always be grateful for my time under Ravi and hope in the future I can become a mentor as respectful, creative, and inspiring.

Secondly, I'd like to thank all my fellow lab mates who were instrumental throughout my PhD. Everyone in the lab has been an extremely important part of my PhD adventure. The lab was always there to; help with experiments, think through the problem when I hit a roadblock, have a beer, bounce ideas off of, discuss science, argue about whose experiment was better, and have another beer. Claudia Han mentored me through my rotation and helped me get up and running in the lab when I first started. Postdocs, Iker, Chris Lucas, Sho, Justin and Sanja taught me so much on a daily basis, from how to perform experiments to how to think about science. Brady and Kristen who were always there to discuss science and were great bay 2 members.

I'd also like to thank my committee members, Young Hahn, Ulrike Lorenz, Bimal Desai, Hui Zong and Doug Bayliss. It was always great and insightful having committee meetings with this group. I've enjoyed working with Young Hahn since my first rotation

and really admire the way she thought about science and probed my work throughout the years. Hui Zong was helpful throughout the generation of the different mouse models we derived. Bimal always knew how to ask the toughest questions, and this helped me develop my 'on-the-spot' critical thinking skills. Ulrike was always available for discussion, especially during my T_{reg} project. Lastly, I have had the pleasure of working a lot with Doug throughout the years, which has led to several fruitful collaborations. Doug is an amazing scientist and person (and as I've seen – basketball player) and I've really enjoyed learning from him. Additionally, I'd also like to thank Doug's Post-doc Eva, who also taught me so much and was an exceptional scientist that I enjoyed working with for several years.

Lastly, I'd like to thank my family who have always supported me and believed in me, even my brother who would constantly ask for medical advice. They sacrificed so much to give me the opportunity to excel in life and I will always be grateful. They have always and will always continue to push me and support me through every aspect of life.

Table of Contents

Title Page

Abstract

Acknowledgments

List of Figures

List of Tables

List of Abbreviations

Chapter I

1.1. Apoptotic cell clearance

1.1.1. Apoptosis

1.1.2. Engulfment

1.2. Apoptotic cell secreted factors and their signaling

1.2.1. Lysophosphatidylcholine (LPC)

1.2.2. Sphingosine-1-phosphate (S1P)

1.2.3. Fractalkine (CX3CL1)

1.2.4. Nucleotides

1.2.5. Other find-me signals

1.2.6. In-vivo relevance

1.2.7. Additional functions of find-me signals

1.2.8. Open questions in the field

1.3. Pannexin 1

1.3.1. Panx1 channel properties

1.3.2. Panx1 in disease pathogenesis

1.4. Focus of this work and key hypothesis.

1.4.1. Publications arising from my work under Dr. Ravichandran

Chapter II

2.1. Abstract

2.2. Introduction

2.3. Materials and methods

2.3.1. Reagents

2.3.2. Mice

2.3.3. Apoptosis induction

2.3.4. Metabolite detection

2.3.5. Flow cytometry of apoptosis and Panx1 activation

2.3.6. Metabolomics analysis of apoptotic supernatant and cell pellet

2.3.7. Metabolite flux experiments with ¹³C-arginine labeling

2.3.8. RNA-sequencing

2.3.9. Quantitative RT-PCR analysis

2.3.10. Thymic myeloid cell isolation and gene expression

2.3.11. Memix preparation and *in vivo* treatment

2.3.12. K/BxN induced arthritis

2.3.13. Lung Transplant Rejection Model

2.3.14. Histology

2.3.15. Statistical analysis

2.4. Results

2.4.1. Apoptotic cell secretome

2.4.2. Orchestrated metabolite release

2.4.3. Metabolites as extracellular signaling molecules

2.4.4. Therapeutic potential of apoptotic cell released metabolites

2.5. Discussion

2.6. Acknowledgements and Author Contributions

2.6.1. Acknowledgements

2.6.2. Author Contributions

Chapter III

3.1. Abstract

3.2. Introduction

3.3. Materials and methods

3.3.1. Mice

3.3.2. Generation of Panx1-transgenic mice

3.3.3. HDM-induced allergic airway inflammation

3.3.4. Immunostaining and cell count

3.3.5. Lung histology and immunohistochemical staining

3.3.6. Quantitative RT-PCR

3.3.7. Western Blotting

- 3.3.8. CD4 T cell Isolation
- 3.3.9. Apoptosis measurement
- 3.3.10. T cell Activation and Suppression Assays
- 3.3.11. Statistical analysis

3.4. Results

- 3.4.1. Global Panx1 knockout mice exhibit increased disease during AAI
- 3.4.2. Panx1 expression on T cells is necessary to control inflammation during AAI
- 3.4.3. Panx1 does not play a cell intrinsic role during T cell activation or on T_{reg} cells
- 3.4.4. Intercellular T cell communication via Panx1 optimizes the suppressive capacity of T_{reg} cells
- 3.4.5. Panx1 expression on T cells is sufficient to control AAI

3.5. Discussion

3.6. Acknowledgements and Author Contributions

- 3.6.1. Acknowledgements
- 3.6.2. Author Contributions

Chapter IV

4.1. Metabolites released from apoptotic cells

- 4.1.1. Significance of findings – apoptosis
- 4.1.2. Future direction – metabolic adaptations during apoptosis
- 4.1.3. Future directions – metabolites as extracellular signaling molecules
- 4.1.4. Significance of findings – Panx1 field
- 4.1.5. Future directions – Panx1-dependent metabolite release

4.2. Panx1 in AAI

4.2.1. Significance of finding

4.2.2. Future directions

References

List of Figures

Chapter I

Figure 1.1: Processes involved in apoptotic cell engulfment

Figure 1.2: ‘Find-me’ signals.

Figure 1.3: Pannexin 1 channels.

Chapter II

Figure 2.1: Conserved metabolite secretome from apoptotic cells.

Figure 2.2: Metabolite release from apoptotic Jurkat cells.

Figure 2.3: Reciprocal metabolite changes between apoptotic supernatant and pellet.

Figure 2.4: Conserved metabolite release during apoptosis.

Figure 2.5: Panx1 activation and inhibition during cell death.

Figure 2.6: Panx1 inhibition does not influence apoptotic cell death.

Figure 2.7: Panx1 activation and continued metabolic activity of dying cells orchestrates metabolite release.

Figure 2.8: Panx1-dependent metabolite release during apoptosis.

Figure 2.9: Conserved Panx1 secretome.

Figure 2.10: Transcriptional and metabolic changes during apoptosis.

Figure 2.11: Metabolites from apoptotic cells influence gene programs in live cells.

Figure 2.12: Transcriptional changes on surrounding phagocytes induced by Panx1-dependent metabolite release during apoptosis.

Figure 2.13: In-vivo thymic cell death analysis and supernatant effects during arthritis.

Figure 2.14: Panx1-dependent metabolite release during apoptosis modulates phagocyte gene expression *in vivo* and can alleviate inflammation.

Chapter III

Figure 3.1: *Panx1*^{-/-} mice exhibit increased inflammation during HDM-induced AAI.

Figure 3.2: *Panx1*^{-/-} mice exhibit increased histological disease severity.

Figure 3.3: *Panx1*^{-/-} mice do not contain increased number of apoptotic cells.

Figure 3.4: Panx1 gene expression in different cell types.

Figure 3.5: Panx1 expression on T cells limits inflammation during disease.

Figure 3.6: Cre expression or Panx1 deletion using *Cx3cr1-cre* does not affect inflammation during AAI.

Figure 3.7: Panx1 deletion does not intrinsically effect T effector cell activation.

Figure 3.8: Panx1 deletion does not intrinsically affect CD4 T effector cell downstream TCR signaling or proliferation.

Figure 3.9: T regulatory cell Panx1 deletion does not affect inflammation during airway inflammation.

Figure 3.10: A non-cell autonomous role for Panx1-released extracellular ATP during Treg dependent suppression of T effector cell proliferation.

Figure 3.11: *In vivo* T cell proliferation.

Figure 3.12: Panx1 expression on T cells is sufficient to limit excessive inflammation during AAI.

Figure 3.13: Generation and validation of *Panx1*^{Tg} mice

Chapter IV

Figure 4.1: Summary of Findings – metabolites released from apoptotic cells

Figure 4.2: Summary of Findings – Panx1 in allergic airway inflammation

List of Tables

Chapter I

Table 1.1: Efforts to define function of ‘find-me’ signals *in vivo*.

Table 1.2: ‘Find-me signals’ and possible supplementary actions they can play during apoptotic cell clearance.

Chapter II

Table 2.1: Reported extracellular function of metabolites.

List of Abbreviations

Lysophosphatidylcholine (LPC)

Sphingosine-1-phosphate (S1P)

Fractalkine/CX3CL1 (FKN)

Adenosine ribosomal protein S19 (RP S19)

Endothelial monocyte activating polypeptide II (EMAPII)

Tyrosyl tRNA synthetase (TyrRS)

Calreticulin(CRT)

Intracellular cell adhesion molecule 3 (ICAM3)

Death Domain 1 α (DD1 α)

LDL receptor-related protein 1 (LRP1)

Brain-specific angiogenesis inhibitor 1 (BAI1)

T cell immunoglobulin mucin domain (TIM)

Growth arrestin-specific (GAS6)

Milk fat globule EGF factor 8 (MFGE8)

Tyro-Axl-Mer (TAM)

Engulfment and cell motility (ELMO)

Downstream of Crk (DOCK180)

Vacuolar sorting protein (Vsp)

Calcium-independent phospholipase A2 (iPLA₂)

Secretory PLA₂ (sPLA₂)

ATP-binding cassette transporter (ABCA1)

Sphingosine kinase 1/2 (SphK1/2)

S1P receptor (S1PR)

G-protein coupled receptor 2A (G2A)

CX3C chemokine receptor 1 (CX3CR1)

Pannexin (Panx)

Purinergic receptors (P2X/P2Y)

Phosphatidylserine (PtdSer)

Tumor necrosis factor (TNF)

Interleukin (IL)

Macrophage inflammatory protein (MIP)

Natural killer (NK)

High mobility group box (HMGB)

Central nervous system (CNS)

Prostaglandin (PGE)

Dendritic cell (DC)

Experimental autoimmune encephalomyelitis (EAE)

Apolipoprotein (ApoE)

Low-density lipoprotein (LDL)

High density lipoprotein (HDL)

N-methyl-D-aspartic acid receptor (NMDA)

G-protein coupled receptors (GPCR)

Alpha-1D adrenergic receptor (α_{1D})

Purinoreceptors-2Y (P2Y)

purinoreceptors-2X (P2X)

Bone-marrow derived macrophages (BMDM)

Ultraviolet (UV)

Adenosine tri/monophosphate (ATP/AMP)

Guanosine monophosphate (GMP)

Glycerol 3-phosphate (G3P)

Trovafloxacin (Trovan)

Spironolactone (Spiro)

Spermidine synthase (SRM)

Pannexin-1 dominant negative (Panx1-DN)

Dexamethasone (Dex)

Dihydroxy acetone phosphate (DHAP)

Inosine monophosphate (IMP)

Fructose 1,6-bisphosphate (F1,6BP)

Extracorporeal photopheresis (ECP)

Allergic airway inflammation (AAI)

Extracellular ATP (eATP)

House dust mite (HDM)

T regulatory cell (T_{reg})

T effector cell (T_{eff})

Bronchoalveolar lavage (BAL)

Bronchoalveolar lavage fluid (BALF)

Peripheral blood mononuclear cells (PBMC)

Hematoxylin and Eosin (H&E)

Phosphate buffered saline (PBS)

Interleukin 4 (IL-4)

Adenosine diphosphate (ADP)

5'-ethynyl-2'-deoxyuridine (EdU)

Wild type (WT)

Knockout (KO)

Internal ribosome entry site (IRES)

Green fluorescent protein (GFP)

Transgene (Tg)

Danger associated molecular pattern (DAMP)

Receptor-interacting serine/threonine protein kinase 3 (RIPK3)

Mixed lineage kinase domain like pseudo kinase (MLKL)

Tricarboxylic acid cycle (TCA)

Tobacco etch virus protease (TEVp)

Chapter I

Introduction

This work has been adapted and extended from my review published in Cell Death and Differentiation: Christopher B. Medina and Kodi Ravichandran.

1.1. Apoptotic cell clearance

Billions of cells are known to turn over in our body on a daily basis as part of development, routine homeostasis, and pathogenic conditions (Henson, 2005). For example, in the thymus and bone marrow, excess lymphoid, myeloid, and erythroid lineage cells that are not considered to move further in development constantly undergo cell death. Whether dying cells come from physiological or pathological consequences, efficient clearance of these cells by professional (macrophages and dendritic cells) or non-professional (epithelial cells and fibroblasts) phagocytes must occur (Ravichandran, 2011). Additionally, the clearance of dying cells is actively immunosuppressive, protecting the body from a break in tolerance to self-antigens (Ipseiz et al., 2014). Failure to sustain efficient clearance results in the secondary necrosis which can lead to exacerbated inflammation and autoimmune diseases (Miyanishi et al., 2007; Nagata et al., 2010). For these reasons both the dying cell and the phagocyte communicate and engage each other to ensure successful engulfment.

1.1.1. Apoptosis

One way in which cellular turnover occurs is through apoptosis, one type of programmed cell death (Henson and Hume, 2006). Although different types of cell death exist (Kroemer et al., 2009), the majority of what is known about cell clearance involves the engulfment of caspase-driven apoptotic cells. Apoptosis can be initiated by intrinsic or

extrinsic pathways, such as genotoxic stress or receptor mediated death, respectively. The activation of caspases during apoptosis leads to many cellular changes such as DNA fragmentation, plasma membrane alterations, and the regulated release of cellular contents (Elmore, 2007).

1.1.2. Engulfment

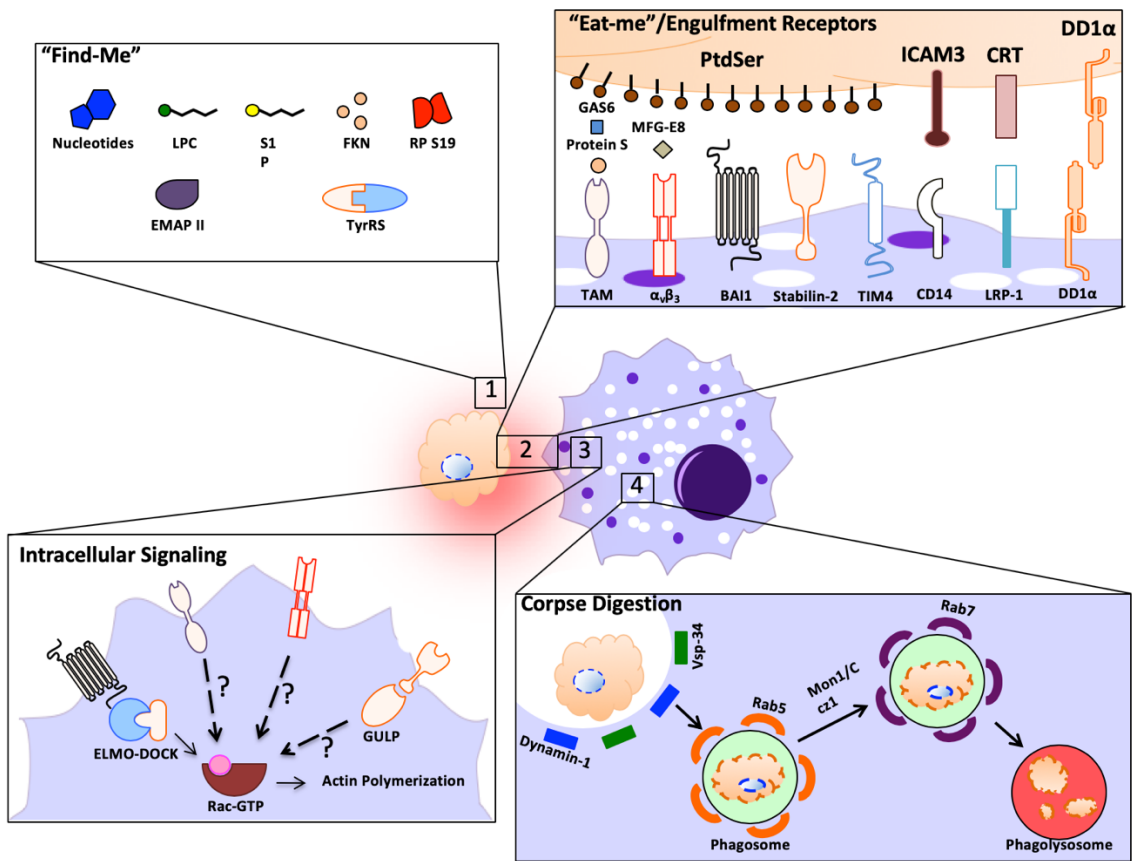
Proper apoptotic cell clearance occurs through several steps: migration toward the dying cell, recognition/binding to the apoptotic target, phagocytosis of the target, and digestion of the corpse (Poon et al., 2014b)(**Figure 1.1**). Apoptotic cells first release find-me signals to promote phagocyte migration to the proximity of cells undergoing death. The phagocytes then specifically recognize the dying cells via ‘eat-me’ signals, the best studied being phosphatidylserine (PtdSer). PtdSer is a phospholipid that is usually found on the inner leaflet of the plasma membrane, but flips to the outer membrane upon apoptosis induction through the activation and deactivation of scramblases and flippases, respectively (Segawa and Nagata, 2015). Other less-characterized recognition signals are shown in **Figure 1.1 (panel 2)** as well as the respective receptors they engage on phagocytes. Different factors such as the cell type undergoing death, the pathological or physiological stimulus, or the duration of this fatal process can affect the landscape of eat-me signals exposed.

Many different receptors and soluble molecules have been linked to PtdSer recognition, and this recognition occurs either directly or indirectly. Direct recognition can occur via brain-specific angiogenesis inhibitor 1 (BAI1) (Park et al., 2007), Stabilin-2 (Park et al., 2008a), and members of the T cell immunoglobulin mucin domain (TIM) (Kobayashi et al., 2007; Miyanishi et al., 2007; Nakayama et al., 2009); alternatively, bridging

molecules such as GAS6/Protein S and milk fat globule EGF factor 8 (MFGE8) can bind to the PtdSer exposed on the apoptotic cells, and in turn be recognized by members of the Tyro-Axl-Mer (TAM) family and $\alpha_v\beta_3$ integrin, respectively, on the phagocyte (Hanayama et al., 2002; Ishimoto et al., 2000). While some of these receptors only serve as a tether to the apoptotic cells (such as TIM4, TIM1), others can initiate intracellular signaling to induce phagocytosis (Flannagan et al., 2014). Receptors such as BAI1 can signal intracellularly through the ELMO1-DOCK180-Rac signaling module to stimulate cytoskeletal rearrangement and engulfment (Park et al., 2007). On the other hand, Stabilin-2 has been reported to require the adaptor protein GULP and thymosin β_4 to engulf apoptotic cells (Lee et al., 2008; Park et al., 2008b). Once internalized, phagolysosome maturation occurs through the action of several Rab-family GTPases, eventually leading to the degradation of the ingested cell corpse (Kinchen et al., 2008). The reason for the involvement of numerous PtdSer receptors is unknown, although not all receptors are expressed or needed in any given cell. While it is tempting to infer that the redundancy may provide compensatory mechanisms, *in vivo* genetic models of single PtdSer receptor knockout mice do contain defects in cell clearance that can lead to autoimmune disease (Arandjelovic and Ravichandran, 2015; Lee et al., 2016; Ramirez-Ortiz et al., 2013). This suggests that not all PtdSer receptors can fully compensate for one another. Instead, different PtdSer receptors may be ‘qualitatively different’ and important in specific cell types, tissue contexts, or inflammatory environments (Penberthy and Ravichandran, 2016; Penberthy et al., 2017). Whether individual or a combination of different recognition receptors affect the overall efficiency of engulfment or the responses from a phagocyte remains to be elucidated.

Figure 1.1: Processes involved in apoptotic cell engulfment.

1. Apoptotic cells are capable of releasing several different 'find-me' signals to attract phagocytes toward dying cells. 2. Phagocytes express an array of different receptors that recognize ligands on apoptotic cells. This can occur through direct binding to the dying cell or through soluble intermediates called bridging molecules. 3. Engulfment receptors that are bound to PtdSer can initiate intracellular signaling leading to Rac1 activation and cytoskeletal rearrangement. The specific mechanism by which signaling is mediated downstream of each receptor is not fully defined. 4. Once internalized, phagosome maturation to the phagolysosome through recruitment of Vps34/Dynamin1 as well as Rab5, Mon1/Ccz1, and Rab7 proteins leads to eventual corpse degradation.



1

2

3

4

1.2. Apoptotic cell secreted factors and their signaling

Much work has been done to understand how phagocytes mediate clearance as well as influence their immediate environment during cell clearance. However, before engulfment can occur, a key step is for the phagocyte to ‘find’ the dying cells among the sea of living cells. How this is achieved is a fascinating question that is just beginning to be delineated.

Both non-professional phagocytes and resident professional phagocytes can clear dying cells under homeostatic conditions. While neighboring cells may not need to ‘migrate’ toward an apoptotic cell to engulf, motile phagocytes such as a resident macrophage likely requires migration towards the dying cell. During situations where a large amount of apoptosis might be occurring, such as in an inflammatory setting, additional professional phagocyte migration and their inherent increased engulfment capability is necessary to cope with the apoptotic corpse overload. Moreover, in many cases, healthy neighboring cells (e.g. thymocytes) are unable to clear their dying brethren, and therefore, migration of resident professional phagocytes within a tissue is required.

It is now well established that apoptotic cells can release mediators that induce phagocyte attraction to the proximity of the dying cell to facilitate efficient clearance (Peter et al., 2010b). Interestingly, many of these factors also contain several extracellular signaling capabilities (Idzko et al., 2014; Ishii et al., 2004; Rosen et al., 2009), indicating that they may play additional roles beyond simply inducing phagocyte migration. One possibility is that these recruitment / find-me signals also influence the cell clearance microenvironment, or even affect the ability of phagocytes to engulf apoptotic cells. It is

also possible that these find-me signals not only recruit the right phagocytes but also 'prepare' the environment for clearance.

Apoptotic (and/or necrotic) cells can release different mediators (Muñoz et al., 2010; Peter et al., 2010b) (**Figure 1.2**). While some of these are better characterized, in-depth understanding of others is still required. The section below describes four find-me signals that are currently better detailed for their role in phagocyte attraction and beyond.

1.2.1. Lysophosphatidylcholine (LPC)

One of the first identified recruitment signals for apoptotic cell engulfment was lysophosphatidylcholine (LPC) (Lauber et al., 2003). Lauber et. al. showed that the cell supernatants taken from apoptotic MCF7 human breast carcinoma cell line could induce phagocyte migration. The authors linked soluble LPC released by dying cells as the factor responsible for mediating recruitment. Unlike LPC, other lysophospholipids or metabolic derivatives of LPC were unable to induce phagocyte chemotaxis (Peter et al., 2008). This release of LPC was an active process and was not simply leakage of cellular contents as the membrane integrity was intact. LPC release was dependent on caspase-3 mediated activation of calcium-independent phospholipase A2 (iPLA₂) (Lauber et al., 2003), which can hydrolyze membrane lipid phosphatidylcholine (PC). However, it is not known whether the LPC generation during apoptosis occurs intracellularly, extracellularly, or both, as the perturbed membrane structure is susceptible to secretory PLA₂ activity (Atsumi et al., 1997). Later, it was shown that ABCA1 might be important for the release of lysophospholipids during apoptosis, as knockdown of ABCA1 resulted in the reduced migration of macrophages toward apoptotic cell supernatants. However, the authors did not show that this was caused by a reduction of LPC in the supernatants as other

lysophospholipids may have also been affected (Peter et al., 2012). This linkage of LPC release to ABCA1 is of interest since among the many evolutionarily conserved genes linked to apoptotic cell clearance, the ABCA1 homologue CED-7 in *C. elegans* is the one player known to be required in both the apoptotic and engulfing cells to mediate efficient clearance (Wu and Horvitz, 1998).

Subsequently, the G-protein-coupled receptor G2A was suggested as the target for LPC (Yang et al., 2005). Unlike its relative G-protein-coupled receptor (GPCR) GPR4, another target of LPC, knockdown of G2A was able to decrease migratory capacity of phagocytes to apoptotic cell supernatants (Peter et al., 2008). However, it is important to note that other phospholipids were able to neutralize migration to pure LPC in a G2A dependent manner. It is possible that a balance of different lysophospholipids released from apoptotic cells can affect migration. However, there is some controversy in the G2A field on whether LPC is a ligand for the G2A receptor (Witte et al., 2005), as LPC has been shown to inhibit G2A mediated signaling, including actin polymerization (Murakami et al., 2004). Furthermore, studies have shown that G2A receptor signaling may be dependent on other oxidized fatty-acids (Obinata et al., 2005) for specific interactions with intracellular G-proteins and GPCRs (Lin and Ye, 2003). The effects of LPC or other lysophospholipids on migration may depend on the specific phagocyte, due to differential expression of GPCRs and G-proteins in different cell types.

1.2.2. Sphingosine-1-phosphate (S1P)

Another lysophospholipid that has been shown to function as a find-me signal during apoptosis is sphingosine-1-phosphate (S1P). It had already been shown that apoptotic cells can release S1P (Hait et al., 2006), but its function as a lipid attraction signal during

cell death was not reported until 2008. Gude et al. (2008) suggested that sphingosine kinase 1 (SphK1) was upregulated during apoptosis and this, in turn, led to the increased secretion of S1P. Concomitantly, purified S1P was able to induce phagocyte chemotaxis. However, it is important to note that it was never directly shown that S1P from the apoptotic supernatants was the chemotactic factor. Additionally, though the authors showed that there was no increase in extracellular SphK1 (Gude et al., 2008), suggesting that the S1P generation occurred within a cell, they did not rule out any actions of SphK2. Of note, SphK2 has since been shown to be secreted during apoptosis in a caspase dependent manner, possibly leading to extracellular generation of S1P (Weigert et al., 2010; 2006). Therefore, a complete understanding of S1P release during apoptosis, and its importance in phagocyte migration remains to be further characterized.

While there are known receptors for S1P (S1PR₁₋₅), the specific GPCR involved in phagocyte migration has not yet been delineated. Phagocytes can also express more than one S1P receptor, some of which might compensate for each other, making it difficult to determine the receptor(s) involved. Cell type specific expression as well as concentration of S1P may be key factors in determining which receptor mediates phagocyte migration (Rosen et al., 2009).

1.2.3. Fractalkine (CX3CL1)

It has been observed that apoptotic cells can undergo membrane blebbing and release small vesicles during the death process. Truman et. al. showed that these blebs can participate in monocyte chemotaxis toward apoptotic germinal center B cells (Segundo et al., 1999). It was also shown that Fractalkine/CX3CL1 (FKN) associated with apoptotic microparticles was a chemotactic factor (Truman et al., 2008). This 90kDa membrane-

associated chemokine appears to be processed to a 60kDa form during the early stages of apoptosis (presumed to occur via extracellular proteases) in B cells and released with PtdSer exposing microparticles. While the precise mechanism of release for the microparticle-associated fractalkine is not known, phagocyte migration was dependent on the chemokine receptor CX3CR1 (the receptor for fractalkine), as CX3CR1-deficient macrophages failed to migrate toward apoptotic B cells.

Interestingly, it has been shown that FKN shedding or cleavage by ADAM17/ADAM10 can lead to production of a soluble 90kDa form of the protein in the absence or presence of apoptosis (Hundhausen et al., 2003; Truman et al., 2008). Why the soluble 90kDa fragment does not confer similar migratory effects during cell death remains to be determined. It is possible that PtdSer found on microparticles could further enhance chemotaxis. A 55kDa soluble form of FKN is shown to occur through cathepsin S processing, however this is not microparticle bound (Fonović et al., 2013). Therefore, the precise mechanism through which apoptosis is able to differentially regulate the 60kDa FKN processing and packaging into microparticles currently remains unclear (Schulte et al., 2007). Intriguingly, compared to the mature glycosylated FKN (90kDa), the unglycosylated intracellular form is ~50-60kDa (Garton et al., 2001). It is enticing to speculate that apoptosis may inhibit glycosylation of FKN, which could result in increased unglycosylated protein. In turn, intracellular vesicles liberated during membrane blebbing could entail a possible mechanism of FKN release. Alternatively, it has also been shown that caspase-3 is also present in microparticles (Böing et al., 2008), indicating that this cleavage process may happen after the particles have already been released.

1.2.4. Nucleotides

Nucleotides can also serve as find-me signals (Elliott et al., 2009). Both adenosine triphosphate (ATP) and uridine triphosphate (UTP) can be released from apoptotic cells in a time- and caspase-dependent manner. Breakdown of these nucleotides by apyrase treatment, resulted in impaired migration (*in vitro* and *in vivo*) and defective cell clearance of apoptotic thymocytes (Elliott et al., 2009). It was determined that the regulated release of nucleotides from apoptotic cells occurred while the membrane was still intact, and this release occurred through the plasma membrane Pannexin-1 (Panx1) channel (Chekeni et al., 2010). While nucleotide release through the pannexin channels is perhaps the best detailed to date among the find-me signals, there are still several questions that remain. For example, similar levels of UTP and ATP are released from apoptotic cells, even though the intracellular concentration of ATP is much higher (Peter et al., 2010a). Whether Panx1 is more selective for UTP (difficult to explain by the current understanding of channel properties of Panx1), if UTP is somehow more accessible for release, or if ATP is metabolized intracellularly (Yamaguchi et al., 2014) during apoptosis remains to be sorted. While ATP remains the most studied metabolite released from Panx1, the channel forms a rather non-selective pore, allowing the passage of molecules up to 1 kDa in size (Wang et al., 2007). Therefore, it will be interesting to determine whether Panx1 is involved in the release of any other find-me signal mediators that may either cooperate with nucleotides for phagocyte attraction, or alternatively, serve additional functions during cell clearance. In this context, intracellular AMP is also released through the pannexin channels during apoptosis (Yamaguchi et al., 2014).

As there are many purinergic receptors that recognize extracellular nucleotides, including ionotropic P2X receptors (ATP-gated ion channels, although requiring much

greater concentration of ATP, see below) and metabotropic P2Y receptors (G-protein coupled receptor), they can play a wide variety of functions (Idzko et al., 2014). Elliot et al. (2009) was able to demonstrate that the purinergic receptor P2Y2 was involved in mediating phagocyte chemotaxis, as P2Y2 receptor knockout mice showed decreased migration towards apoptotic cell supernatant in a murine air pouch model of migration and also in the context of apoptotic thymocyte clearance. It will be important to determine what other effects the release of ATP/UTP can have on the phagocytes during engulfment as immune cells such as macrophages are known to express several purinergic receptors (Junger, 2011).

1.2.5. Other find-me signals

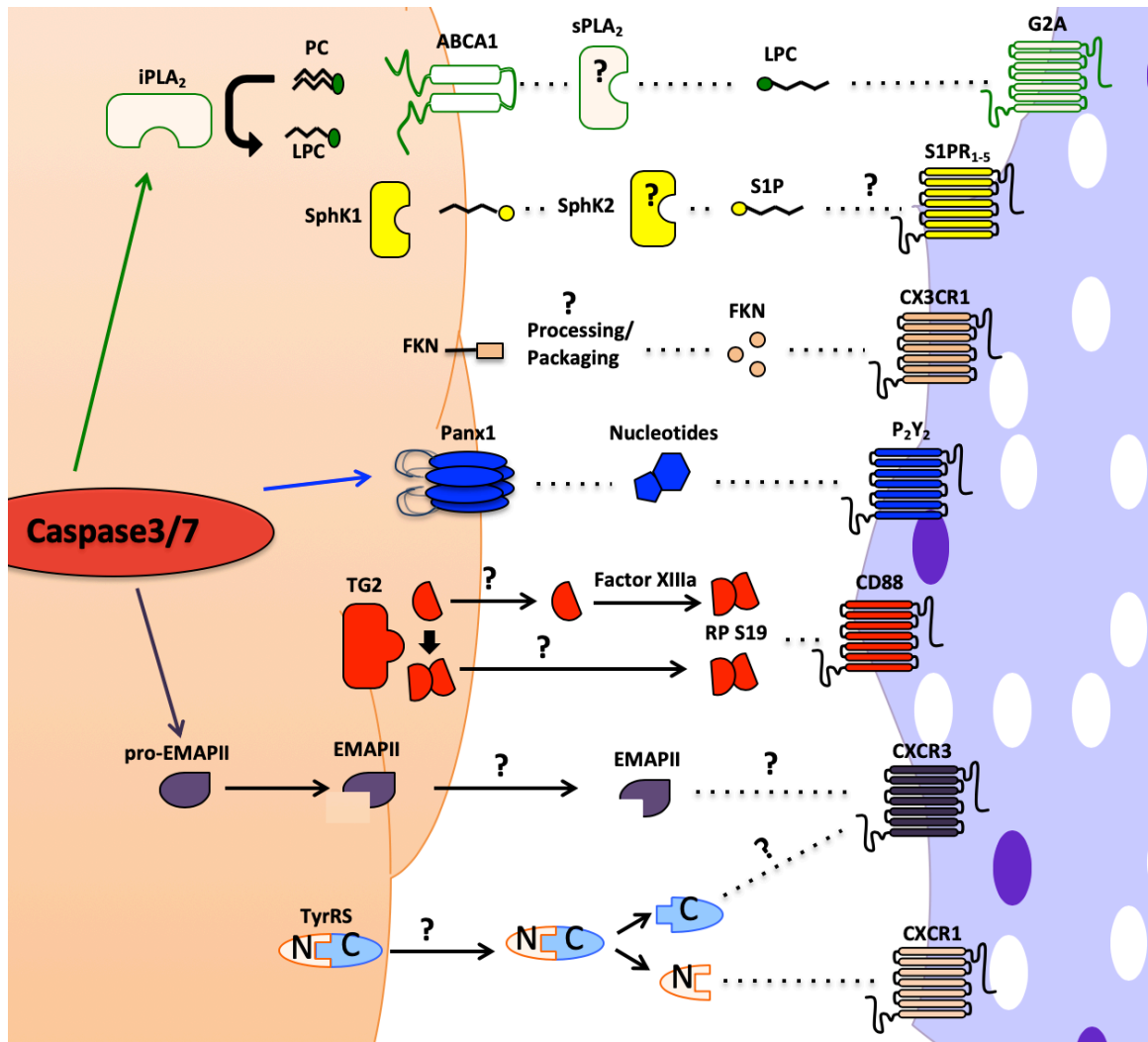
Apoptotic cells have also been shown to release other soluble mediators to induce phagocyte migration (**Figure 1.2**). One of the first attraction signals discovered was the dimer of ribosomal protein S19 (RP S19) (Horino et al., 1998). Only the cross-linked dimer [formed by transglutaminase 2 intracellularly (Nishimura et al., 2001) or by factor XIIIa extracellularly (Nishiura et al., 1999)], but not monomers (Nishimura et al., 2001) of S19, induced monocyte migration. CD88, the C5a receptor on monocytes was linked to sensing of S19 and the migration of monocytes (Nishiura et al., 1998). Although neutrophils also express CD88, the dimer RP S19 did not induce neutrophil chemotaxis. This is thought to be a consequence of a C-terminal moiety, which is able to antagonize the polymorphonuclear leukocyte receptor (Shrestha et al., 2003). While the chemotactic properties of RP S19 have been established, how the factor is released during apoptosis remains unknown. Additionally, whether this can be recapitulated under physiological

apoptotic stimuli remains to be shown, as the authors used hyperthermia (43° C for 60 min) to induce cell death.

Two other attraction molecules that share homology include endothelial monocyte activating polypeptide II (EMAPII) and human tyrosyl tRNA synthetase (TyrRS). Both attraction molecules require proteolytic processing to gain their chemotactic properties (Knies et al., 1998). While EMAPII requires processing from the pro-EMAPII form, most likely through caspase-7 cleavage (Behrendorf et al., 2000), TyrRS cleavage is thought to occur by extracellular neutrophil released elastase (Wakasugi and Schimmel, 1999). Of note, the C-terminal cleavage product of TyrRS shares homology (49%) with EMAPII (Kleeman et al., 1997) indicating that there may be redundancy with the effects of these attraction signals. It was determined that the N-terminal fragment of TyrRS (mini TyrRS) can stimulate phagocyte migration via the membrane protein CXCR1 (IL-8 receptor), but the receptor for the EMAPII like C-terminal fragment of TryRS is unknown. EMAPII can facilitate the migration of endothelial progenitor cells, which are derived from monocytes, through CXCR3; however, this has not been shown in the context of apoptotic cell clearance or other phagocytes (Hou et al., 2006). Unfortunately, EMAPII and TyrRS release was shown to occur relatively late in the apoptotic process, suggesting that it may be released during secondary necrosis of these cells (Behrendorf et al., 2000; Knies et al., 1998).

Figure 1.2: 'Find-me' signals.

The different find-me signals released from apoptotic cells, their known or putative mechanism of release, and the possible receptors on phagocytes that can regulate chemotaxis.



1.2.6. In-vivo relevance

The growing field of find-me signals has garnered much interest in the field. However, to fully understand the importance of these signals and regulation of cell clearance, many of these have to be better characterized *in vivo*. Unlike other components of the engulfment machinery (i.e. PtdSer receptors), where the generation of transgenic and knockout mice can help determine their involvement (Ravichandran and Lorenz, 2007), many of the signals such as LPC, S1P, ATP released from apoptotic cells cannot be genetically knocked out. Instead, knock out of specific enzymes required for their production (Allende et al., 2004), release (Qu et al., 2011), or recognition (Combadiere et al., 2003) (which can be indirect and less specific) has to be used in an attempt to address these issues.

To gain insight as to whether the failed release or recognition of these find-me signals affects the overall process of cell clearance *in vivo*, and in turn physiological or pathological conditions, the examination of specific knockout mice is required. For example, defective apoptotic cell clearance is thought to be involved in atherogenesis (Elliott and Ravichandran, 2010; Tabas, 2010), and intriguingly FKN deficiency has been associated with this disease (Combadiere et al., 2003; Saederup et al., 2008) (**Table 1.1**). To what extent FKN released during apoptosis is involved in this pathogenesis has not been determined. The deficiency of CX3CR1 (the FKN receptor) has also been associated with a decreased number of macrophages in B cell germinal centers (Truman et al., 2008). Although the recruitment of these macrophages was affected, there was no increase in the amount apoptotic B cells, indicating that the reduced number of macrophages was still

capable of efficient clearance. This also suggests that possibly several find-me signals may be released by one cell and loss of one may be compensated sufficiently enough by others.

The key channel involved with nucleotide find-me signals is Panx1. Under homeostatic conditions, Panx1 deficient mice have no overt phenotype (Bond and Naus, 2014), however this may be a consequence of compensation from other pannexin family members (Panx2/Panx3) (Bargiotas et al., 2011; Lohman and Isakson, 2014), or other nucleotide release channels. Alternatively, Panx1 deficient mice may need to be stressed to increase apoptotic load, as these mediators may be more readily compensated at basal levels of apoptosis. Studies have suggested that Panx1 is involved in several pathological scenarios (**Table 1.1**), but whether this is dependent on nucleotide release from apoptotic cells awaits further clarification. This is because, in addition to their role in nucleotide release from apoptotic cells, the pannexin channels are also involved in regulating the integrity of the dying cells (Poon et al., 2014a), regulation of vascular constriction via nucleotides released by non-apoptotic mechanisms (Billaud et al., 2015), and cancer cell migration (Furlow et al., 2015). Due to the ubiquitous expression (Baranova et al., 2004) and vast regulatory mechanisms of Panx1 activation (Chiu et al., 2014; Taylor et al., 2015), novel cell-type specific knockout and transgenic mice affecting apoptosis specific activation may be necessary to understand its involvement during cell clearance *in vivo*.

Numerous knockout studies have been performed on other proteins involved in different aspects of these attraction signals. **Table 1.1** lists some of the phenotypes of knockout mice relevant for find-me signal release or recognition. It is important to keep in mind that these proteins and soluble mediators are also known to play other roles; therefore, the participation of these signals *in vivo* requires greater clarification.

Another major issue with several find-me signals is *in vivo* concentration. As shown through investigations on LPC, apoptotic cell supernatants contained a concentration of 200nM LPC, but the authors had to use 20-30 μ M of purified LPC to detect cell migration (Lauber et al., 2003; Peter et al., 2008). Although plasma levels of LPC are known to be considerably high (100 μ M-150 μ M) (Okita et al., 1997; Riederer et al., 2010), extracellular actions of LPC have been reported (Huang et al., 1999); an observation likely in part due to the availability of free LPC, as the modified lipid is thought to be bound to albumin and other carrier proteins (Croset et al., 2000; Ojala et al., 2006). Without detailed knowledge of the receptor for LPC during phagocyte migration, it is difficult to determine if physiological LPC is pertinent. Similarly, there is a discrepancy in the physiological S1P concentrations (>200nM) (Okajima, 2002) compared to the S1P concentrations needed to stimulate phagocyte migration (1-1000nM) and the much lower S1P levels measured in the supernatants of apoptotic cells (12-16pmol) (Gude et al., 2008). S1P is also bound in blood to albumin and lipoproteins (mostly HDL) (Murata et al., 2000). Therefore, how these signals are able to mediate migration *in vivo* requires elucidation, as phagocyte recruitment was not studied *in vivo*. Release of these components may be restricted to a small local area, where higher concentrations could be achieved and thereby have an effect on nearby phagocytes. Alternatively, whether LPC or S1P bound to serum proteins or other extracellular components can affect their migratory capabilities during engulfment is another possible factor in determining their ability to attract phagocytes.

Unlike lipid find-me signals, work on the nucleotides, using an air pouch model of phagocyte migration could show that these mediators were indeed able to induce monocyte chemotaxis *in vivo*. Supernatants of apoptotic cells released concentrations of 100-200nM

ATP and UTP during cell death (Chekeni et al., 2010; Elliott et al., 2009; Poon et al., 2014a). Studies have shown that resting ATP plasma levels are ~28nM (Gorman et al., 2007), indicating that the release of ATP from apoptotic cells is significant compared to physiological concentrations. Not surprisingly, the EC₅₀ for many purinergic P2Y receptors are below 1μM, including P2Y₂, which recognizes ATP and UTP at concentration of 100nM and 200nM, respectively (Junger, 2011). On the other hand, the extracellular ATP can be easily degraded by nucleotidases (Zimmermann et al., 2012) making nucleotides available only over a short range. These observations indicate that nucleotides do have the capacity to serve as proper find-me signals *in vivo*, but certain features of this nucleotide-mediated phagocyte attraction require further characterization.

Table 1.1: Efforts to define function of ‘find-me’ signals *in vivo*.

A list of knockout mice of proteins linked to specific find-me signal release or recognition. Some of phenotypes associated with these knockout mice should be cautiously interpreted as the linkage between these phenotypes, the specific find-me signals, or apoptotic cell clearance is not detailed. This demonstrates the necessity to develop novel methodologies to truly understand the impact of find-me signals via combination of genetic and pharmacological methods *in vivo*.

'Find-me Signal'	KO mice	Phenotype	Mechanism	Ref
LPC	iPLA ₂	Neuronal dystrophy/neurodegeneration Male reduced fertility Increased neonatal death	Insufficient membrane remodeling Impaired spermatozoa motility Placenta malformation	(Bao et al., 2004b; Beck et al., 2011; Shinzawa et al., 2008)
	ABCA1	Decreased circulating HDL/ Congestive heart failure/kidney glomerulonephritis	Improper cholesterol efflux/lipid laden macrophages in areas of high turnover/immune complex deposition	(Aiello et al., 2002; Christiansen-Weber et al., 2000; Timmins et al., 2005)
	G2A	Increased Atherosclerosis Autoimmune syndrome	Macrophage specific ABCA1-/- in ApoE-/- LDLR-/- mice T cell hyperresponsiveness	(Le et al., 2001)
S1P	SphK1	Attenuated colon cancer Attenuate DSS induced colitis	Plays a role in tumor proliferation Decrease pro-inflammatory factors	(Kohno et al., 2006; Snider et al., 2009)
	SphK2	Enhanced colitis associated cancer	Increase SphK1/S1P which leads to inflammation Increased pro-inflammatory mediators	(Lai et al., 2009; Liang et al., 2013)
	SphK1/2	Exacerbated collagen-induced arthritis Embryonic lethal	Defects in neural and vascular development Increased numbers of apoptotic cells in fetal embryos	(Mizugishi et al., 2005)
FKN	CX3CL1	Attenuated atherosclerotic lesions Decreased macrophages in B cell germinal centers	Fewer macrophages in lesions Impaired phagocyte migration	(Teupser et al., 2004; Truman et al., 2008)
	CX3CR1	Attenuated atherosclerotic lesions	Impaired monocyte recruitment to atherosclerotic lesions (ApoE-/-)	(Combadiere et al., 2003)
ATP/UTP	Panx1	Increased inflammation during peritonitis Delayed onset of disease in EAE Blood pressure regulation dysfunction	Decrease release of anti-inflammatory mediator AMP Increased P ₂ X ₇ expression Defective smooth muscle cell vasoconstriction	(Billaud et al., 2015; Bond and Naus, 2014; Lutz et al., 2013; Penuela et al., 2014; Yamaguchi et al., 2014)
	P2Y2	Decreased allergic airway inflammation	Reduced eosinophil and dendritic cell migration	(Müller et al., 2010)

1.2.7. Additional functions of find-me signals

Find-me signals were first discovered to affect apoptotic cell clearance based on their ability to promote migration. However, continued studies on these factors has brought about interesting observations, suggesting other roles important for engulfment. As cell clearance is an overall anti-inflammatory process, find-me signals may also contribute to the suppression of inflammation during cell clearance. Additionally, the factors may stimulate the 'appetite' of a phagocyte or increase their capacity to engulf. This section will cover some of the auxiliary functions of these apoptotic-released signals and how it may regulate cell clearance (**Table 1.2**).

Nucleotides are well known to have extracellular signaling capabilities. Although ATP was first considered a pro-inflammatory stimulus, it is now appreciated that the signaling is more complex (Idzko et al., 2014; la Sala et al., 2003). Low levels of ATP can actually have anti-inflammatory properties such as decreasing the secretion of pro-inflammatory cytokines from macrophages and dendritic cells (Haskó et al., 2000; la Sala et al., 2001). Many of the inflammatory properties of ATP are linked to their stimulation of the P2X₇R; however, the activation of P2X₇R requires high concentrations of ATP (50-100µM) (Junger, 2011), indicating that 100-200nM ATP released during cell death is unlikely to activate the P2X₇R. In fact, this has been supported by studies that showed pannexin mediated ATP release does not activate P2X₇R and the inflammasome (Qu et al., 2011). P2X receptors only engage ATP, while the P2Y receptor family, many of which are implicated in migration, can recognize ATP, UTP, and their metabolic breakdown components (Honda et al., 2001; Kronlage et al., 2010). This recognition repertoire can play an important function in cell clearance, as apoptotic cells also release UTP.

Furthermore, ATP and UTP can also elicit monocyte migration indirectly by affecting adhesion molecule expression on vascular endothelial cells. Outside of migration, nucleotides have also been shown to have effects on phagocytosis. UDP acting through P2Y₆ has been reported to increase microglial phagocytosis although the mechanism is not known (Koizumi et al., 2007). Stimulation of P2 purinergic receptors with nucleotides can increase the phagocytic capacity of macrophages, which is thought to be dependent on an increase of apoptotic cell receptor expression, such as $\alpha_v\beta_3$. Nucleotide effects on increased phagocytosis and receptor expression could be seen as early as 30 minutes, indicating the swift communication that can occur between find-me signals and the phagocyte (Marques-da-Silva et al., 2011). Although ATP and UTP are released from apoptotic cells, their degradation products may be able to further substantiate their extracellular actions during clearance. Adenosine is a potent anti-inflammatory molecule and can suppress both innate and adaptive components of the immune system. It was recently suggested that apoptotic cells can also release substantial amounts of AMP (also through Panx1), which can contribute to the anti-inflammatory effects associated with apoptotic cell clearance (Yamaguchi et al., 2014). Therefore, nucleotides provide an exciting new avenue for cell clearance, both in migration and subsequent consequences, with many avenues for future investigation.

Fractalkine has been shown to enhance phagocytosis by macrophages via its ability to enhance MFG-E8 induction, however, this upregulation was seen after 24 hours of fractalkine treatment (Leonardi-Essmann et al., 2005; Miksa et al., 2007). In addition to increasing phagocytosis, FKN has also been associated with anti-inflammatory actions such as providing neuroprotection during glutamate toxicity to promote neuronal survival

(Mizuno et al., 2003; Noda et al., 2011), modulating TNF- α secretion by microglia (Zujovic et al., 2000), and promoting proliferative effects (White and Greaves, 2012; White et al., 2010), which may all play important roles in different settings of cell clearance. However, clarification is needed as to which processed or cleaved form of FKN affects these processes (90kDa or 60kDa).

LPC may also play an indirect role in migration by upregulating the expression of different chemokines responsible for monocyte, T cell, and neutrophil recruitment on vascular endothelial cells (Quinn et al., 1988; Tibes et al., 1999). LPC has been shown to both increase production of pro-inflammatory cytokines (Huang et al., 1999; Taniuchi et al., 1999), and have anti-inflammatory effects such as inhibiting high mobility group protein B1 (HMGB1) secretion (Chen et al., 2005). These differential effects are dependent on different receptors as well as cell types, but not yet fully understood. LPC can also act as an indirect eat-me signal, wherein the apoptotic induction of iPLA₂ activity promotes the LPC-dependent binding of IgM to apoptotic (Kim et al., 2002), late apoptotic (Fu et al., 2007; Zwart et al., 2004) and necrotic cells (Ciurana et al., 2004), leading to complement activation and clearance. LPC-IgM dependent binding to different apoptotic and necrotic states may serve as a backup to normal recognition in situations where large numbers of cells are undergoing apoptosis.

While the receptor mediating S1P recognition during cell death is not known, S1P has been shown to have both anti-inflammatory and anti-apoptotic effects on macrophages (Weigert et al., 2006). S1P release during apoptosis can cause M2 polarization, leading to lower pro-inflammatory cytokines. Interestingly these actions are thought to be a consequence of S1P generation by SphK2 (Weigert et al., 2007), and not SphK1 (suggested

to be responsible in the generation of the S1P find-me signal). Further detailed analysis of these different sphingosine kinase isoforms and their activity during cell death will be important for the understanding of S1P. Lastly, while the death of circulating cells does not generally disrupt any tissues, epithelial death is more complex as it can affect integrity of barrier surfaces. A recent study has shown that S1P released from apoptotic cells can act on neighboring cells through S1P₂R to facilitate apical extrusion of the dying cell (Gu et al., 2011; 2015).

Apart from these well-studied mediators, other components released during apoptosis have been implicated in stimulating functions outside of chemotaxis. Apoptotic blebs can regulate migration indirectly by enhancing monocyte-endothelial interactions in the vasculature, an event that is driven by oxidized phospholipids on the vesicles (Huber et al., 2002). Although apoptotic bleb-induced migration may be important for efficient clearance, unlike apoptotic bodies, phagocytosis of such blebs stimulates dendritic cell maturation. This can lead to dendritic cell-mediated T cell activation, which can predispose to autoimmune disease (Fransen et al., 2009a; 2009b). Ribosomal protein S19 has been reported to antagonize neutrophil chemotaxis and induce their apoptosis, while still attracting monocyte/macrophages, indicating its anti-inflammatory properties (Yamamoto, 2007). Finally, independent of the ability to induce phagocyte migration, EMAPII and TyrRS have both been shown to elicit pro-inflammatory actions such as increased peroxidase activity in neutrophils and production of TNF α , respectively (Kao et al., 1994; Wakasugi and Schimmel, 1999). These observations do not coincide with the generally anti-inflammatory nature of apoptotic cell clearance; therefore, a deeper understanding of these mediators is needed.

Table 1.2: ‘Find-me signals’ and possible supplementary actions they can play during apoptotic cell clearance.

The contexts in which these signals were discovered and the different cell types that are known to release them are indicated. The table also describes a list of some of the additional signaling capabilities that these mediators are capable of eliciting as well as additional information that is not known or debated in the field.

'Find-me' Signal	Discovery Context (Cell-types)	<i>In vivo</i>	Supplementary Actions	Comments
LPC	MCF7 _{caspase 3}	-	DC maturation, affect MIP-2, TNF α , IFN γ release; H ₂ O ₂ , superoxide release from neutrophils, HMGB1 release, T cell and NK cell chemotaxis, and affect B cell Ab release	LPC species and receptors may be important for specific functions during cell clearance
S1P	Jurkat Cells	-	Anti-apoptotic, lymphocyte migration, decrease TNF α , IL-6 and IL-12 production, polarization to M2 macrophage, increase IL-10 and PGE ₂ , suppress T cell proliferation and activation responses	Unknown receptor, (SIP ₁ /SIP ₃ have been implicated in migration) ABCA1 regulates lysophospholipid release during apoptosis (maybe S1P)
FKN	Burkitt lymphoma cells Activated CD19-lymphocytes	✓	Chemoattractant for NK cells, T cells, B cells, protective effects in CNS, increase phagocytosis	Unknown protease for 60kDa fragment generation Many auxiliary effects are a consequence of 90 kDa form
ATP/UTP	Thymocytes Jurkat Cells MCF7 _{caspase3}	✓	Inflammatory at high concentrations and anti-inflammatory at low concentrations, increase phagocytosis of microglia and macrophages through P ₂ Y ₆ and P ₂ X _{1/3} , respectively	Effects of ATP metabolites on phagocytes are unclear Other factors released by Panx1 is also not known
RP S19	AsPC-1 HL-60 NIH3T3 RA synovial tissue	✓	Inhibit neutrophil chemotaxis, responsible for adaptive immune response toward apoptotic cells, pro-apoptotic effects on non-macrophages	Chemotactic factor was not released until 24 hours after apoptosis induction Release during physiological apoptotic death not examined
EMAPII	32D Meth A cells MEFs	-	Increase myeloperoxidase activity in neutrophils, neutrophil chemotaxis, upregulation of TNF-R1, pro-apoptotic effects on endothelial cells and lymphocytes, activation of monocytes	Released 10-12 hours after apoptosis Unknown receptor on monocytes Pro-EMAPII (p43) can also be secreted (non-apoptotic) and has pro-inflammatory properties
TryRS	U-937	-	Pro-angiogenic, C-terminal product stimulated pro-inflammatory and chemotactic effects similar to EMAPII, N-terminal fragment only induced migration in neutrophils	C-terminal fragment shares homology with EMAPII Released 12 hours after apoptosis

1.2.8. Open questions in the field

Apoptotic cells are capable of the controlled release of different soluble and/or membrane-bound mediators. These released factors can have several effects during physiology and pathology, including the ability of find-me signals to attract phagocytes toward apoptotic cells (Ravichandran, 2003). It has become evident that not only are the find-me signals involved in chemotaxis, but they may also play additional roles that promote efficient and anti-inflammatory engulfment of dying cells. While our understanding of find-me signals has moved rapidly, a number of questions remain to be addressed. First, defining how the many different find-me signals are released by a given apoptotic cell *in vivo* is not known; perhaps this depends on the type of apoptotic cells and the type of apoptosis induction. Second, what is the distance/attraction radius for a released find-me signal before its original properties are altered, such as metabolic conversion? This is a rather challenging question; as sensitive probes are needed to determine the low levels of find-me signals that might be released from a few dying cells *in vivo* (rather than in tissue culture contexts where a large number of cells can be induced to undergo death more or less synchronously). Third, what is the effect of metabolites that are derived from the original find-me signals; for example, is there a positive or negative feedback from neighboring cells, and how do the metabolites affect the neighboring tissue milieu? Fourth, another substantial layer of complexity arises when one considers different settings such as inflammation, tumors, or wound healing. In these states, different cell types may simultaneously and continually undergo death, and also different phagocytes (recruited and tissue-resident macrophages, neutrophils, as well as non-professional phagocytes) may be simultaneously responding to the find-me signals released. This heterogeneity of

phagocytes can differentially react to or release additional factors in response to sensing of the find-me signal factors; also, the kinetics of their response has been shown to range from minutes to hours, a phenomenon that may depend on the find-me signal or reaction elicited. This type of complexity is both beautiful and daunting, but further understanding of these different signals *in vivo* will help determine their roles in apoptotic cell clearance and in turn many physiological and pathological conditions.

1.3. Pannexin 1

Panx1 is one of three members in the pannexin family that comprises PANX1, PANX2, PANX3, discovered recently (2000) due to their homology to invertebrate gap junction forming proteins, innexins (Baranova et al., 2004). Panx1 has been characterized as a 47.5 kDa cell surface protein with four transmembrane domains and cytoplasmic N and C terminal regions (Hua et al., 2003). Elegant work has highlighted important N-glycosylation residues on all three pannexin family members important for their intracellular trafficking and intermixing (Penuela et al., 2009). Initial reports suggested that, unlike Panx2 and Panx3 expression, which is mostly restricted to the brain and bone respectively, Panx1 expression is more widespread, being found in a variety of different cells types (Baranova et al., 2004). The ubiquitous expression of Panx1 implies its diverse function, however, additional work is needed to better understand its biological relevance. More recent evidence has begun to uncover that Panx2 expression may not be restricted to the central nervous system (Le Vasseur et al., 2014). This is an interesting finding as some reports detail that pannexin family members may be able to functionally compensate for one another (Lohman and Isakson, 2014), however, limited tools exist for the study of Panx2 and Panx3. As a result, Panx1 will be the focus of this introduction and work. Additionally, given the recent discovery of Panx1, new research is constantly changing the way we study Panx1. Therefore, I will explain what is currently known about Panx1, but also other aspects of the channel that were initially proposed.

1.3.1. Panx1 channel properties

Although Panx1 is homologous in protein sequence to the invertebrate gap junction forming proteins innexins, evidence strongly suggests that they do not form gap junctions

(Dahl and Locovei, 2006). Instead, Panx1 proteins are thought to oligomerize at the plasma membrane to form hemi channels (Ambrosi et al., 2010), which allow the passage of ions and small molecules (Wang et al., 2007) to and from the extracellular space. Initial reports, using amino acid sequence homology and computational mapping of the protein extrapolated that Panx1 would form hexamers at the plasma membrane, much like connexins or other tetra-spanning proteins like LRRC8 channels (Abascal and Zardoya, 2012). Additionally, ectopic expression of concatenated Panx1 constructs also indicated that these channels were able to form functional hexameric proteins. With the use of tools such as TIRF, cryo-EM, electrophysiology, and ATP/dye uptake, we were able to demonstrate that a hexameric concatemer of Panx1 could function within cells (Chiu et al., 2017). However, these studies were performed in cells that have endogenous Panx1 expression making it possible for these proteins to insert themselves into the ectopically expressed hexameric concatemer. Revisiting these studies in a Panx1 knockout background could give us a better understanding of the channel's properties. In fact, just this year several protein structures for Panx1 have been determined! These data indicate that Panx1 most likely forms a heptameric channel (seven Panx1 subunits) at the plasma membrane (Michalski et al., 2020). This exciting research changes the long-held dogma of hexameric Panx1, causing us to revisit the structural make-up of the channel. As we continue to discover the structural properties of Panx1, it will lead to further insight into other aspects of this hemichannel function.

Regulation of the channel has been studied extensively with several different models proposed for its activation. Panx1 channels are thought to be closed at the normal resting potential of a cell, however this may depend on the specific species of Panx1 and

the overexpression system used (unpublished data) (Bruzzone et al., 2003). Upon activation, Panx1 demonstrated a unitary conductance of ~ 75 pS (Chiu et al., 2014; Ma et al., 2012). However, other reports suggest higher recordings of ~ 500 pS (Bao et al., 2004a). These contradicting results could be a consequence of the difference systems used, such as the specific Panx1 ortholog, the cell over-expression system (xenopus or human), experimental approach (electrophysiology recording setup), and possibly even the duration of stimulation. As a result, the extent of activation remains a debated topic, but possibly through standardized practices on Panx1 channel measurements, a consensus can be reached. Furthermore, the selectivity of the channel has also been debated. While the majority of reports indicate non-selective ion transport, recent studies have proposed that the channel is anion selective (Chiu et al., 2014). Again, without a standardized practice in the field, it becomes difficult to uncover the true properties of the channel as different experimental practices can affect outcomes. Therefore, as we continue to study Panx1, we will undoubtedly overcome these hurdles.

In addition to ion selectivity, studies on the channel pore size revealed that small solutes of less than 1 kDa can pass through Panx1 (Wang and Dahl, 2010; Wang et al., 2007). The only molecules accepted to be released in a Panx1-dependent manner upon activation are ATP/UTP, however given the large predicted pore size, it is exciting to speculate that other molecules may also be released. Several different mechanisms for Panx1 regulation have been proposed, those that are intrinsic to the channel and cell signaling events that can lead to Panx1 activation. Intrinsic properties of activation include membrane depolarization (Locovei et al., 2006a), mechanical stimulation (Penuela et al., 2007), and increases in extracellular potassium (Silverman et al., 2009). Activation can

also be receptor-mediated through Gαq-coupled receptors (Billaud et al., 2015) and purinergic receptors (P2X and P2Y) (Locovei et al., 2006b). It is worth noting that as with other studies characterizing relatively newly detailed Panx1, our continued investigation could change our understanding of the mechanisms that activate the channel. Additionally, our lab and collaborators have comprehensively studied a novel, cleavage-based activation of Panx1. One of the best-described means of Panx1 activation is the C terminal cleavage of the protein by executioner caspases-3 and-7, which was shown to be essential for channel activation during apoptosis (Chekeni et al., 2010). Consequently, a C-terminal truncation mutant results in a constitutively active channel, while mutation of the caspase-cleavage site renders the pore incapable of nucleotide release. Further studies showed that the C-terminal portion of the protein serves to block the channel pore in a “ball and chain” fashion (Sandilos et al., 2012). Overall, given the infant state of Panx1 research, continued studies on the channel will be needed to better characterize its different properties.

Figure 1.3: Pannexin 1 channels.

a, Panx1(blue) tertiary (left image) and quaternary structure(right image). C-term, C terminus. N-term, N-terminus. C, Cysteine. **b**, A non-exhaustive schematic of different activation mechanisms for Panx1 mediated ATP release. Panx1 has been proposed to be activated by extracellular potassium (K^+), changes in membrane potential ($\Delta\psi$), caspase-3 and -7, ionotropic receptors; purinoreceptors-2X(P2X), N-methyl-D-aspartic acid receptor(NMDA), and G-protein coupled receptors (GPCR); alpha-1D adrenergic receptor(α_{1D}), purinoreceptors-2Y(P2Y).

1.3.2. Panx1 in disease pathogenesis

Pharmacological data on Panx1 has implicated its involvement in different biological processes (Bargiotas et al., 2011; Thompson et al., 2008; Wang et al., 2013). Although Panx1 KO mice had no obvious phenotype under homeostatic conditions (Anselmi et al., 2008; Bargiotas et al., 2011; Qu et al., 2011; Seminario-Vidal et al., 2011), the channel does play more prominent roles when tissues are under stress. For example, there is accumulating evidence that emphasizes the importance of Panx1 in ischemia reperfusion injury. Panx1 deletion protects and attenuates disease severity during reperfusion injury, whether it be in the kidney, lung, or brain (Bargiotas et al., 2011; Jankowski et al., 2018; Sharma et al., 2018). Additional studies have implicated Panx1 involvement in the induction and resolution of inflammation (Adamson and Leitinger, 2014) and in the control of blood pressure homeostasis by α_1D -regulated activation through modulation of the intracellular loop of Panx1 (Billaud et al., 2015). New evidence is also beginning to highlight the importance of Panx1 in memory. However, due to its non-homogeneous expression patterns (Hanstein et al., 2013), activation mechanisms and biological interactions (Bond and Naus, 2014), the different means by which the channel may be involved in disease pathogenesis is only now being clarified.

Lastly, and most recently, the importance of Panx1 in humans is highlighting the necessity to fully understand this channel in different disease settings. A report in 2016 identified the first known human Panx1 homozygous mutation, which results in several severe abnormalities (Shao et al., 2016). Additionally, another more recent and mechanistic paper described an important role for Panx1 in the human reproductive system (Sang et al., 2019). These studies reiterate the fact that it is important to fully understand how Panx1

may be involved in different disease pathologies. And while the Panx1 KO mice do not have any severe abnormalities that we have found, it may also suggest the need to develop new tools to study this protein, such as the generation of transgenic mice. Given our interest in airway pathologies, the involvement of Panx1 in these settings have not been explored. However, differential expression profiles of Panx1 in diseased tissues including the lung (Cho et al., 2011) imply that it may be relevant during airway disease. Therefore, it remains important to investigate Panx1 in airway inflammation, both with the use of the current Panx1 tools and novel approaches.

1.4. Focus of this work and key hypothesis.

In this dissertation, I detail my work on two different biological processes; how apoptotic cells can communicate with the surrounding tissue and how Panx1 may be involved during allergic airway inflammation. In Chapter II, I discuss in detail how apoptotic cells could communicate with their neighboring cells via metabolic signals. These ‘good-bye’ signals uncover a novel mechanism through which metabolites can function as extracellular signaling molecules and play important roles in physiology and pathology. Furthermore, we demonstrate that the beneficial effect of specific apoptotic metabolites can be harnessed in pre-clinical models of inflammatory diseases. In Chapter III, I uncover a Panx1-dependent communication axis that is important for proper control of inflammation during airway disease. More specifically, I demonstrate how extracellular ATP released via Panx1 is important for the optimal suppressive capacity of T_{reg} cells on T_{eff} cells. Overall this work expands on the understanding of apoptotic cells and pannexin 1 channels during allergic airway inflammation.

1.4.1. Publications arising from my work under Dr. Ravichandran

[Christopher B. Medina](#), Parul Mehrotra*, Sanja Arandjelovic*, Justin S.A. Perry*, Yizhan Guo, Sho Morioka, Brady Barron, Scott F. Walk, Bart Ghesquière, Alexander S. Krupnick, Ulrike Lorenz, and Kodi S. Ravichandran. Metabolites released from apoptotic cells act as tissue messengers. *Nature* 580, 130-153. 2020.

Justin S. A. Perry*, Sho Morioka*, [Christopher B. Medina](#), J. Iker Etchegaray, Brady Barron, Michael H. Raymond, Christopher D. Lucas, Suna Onengut-Gumuscu, Eric

Delpire, and Kodi S. Ravichandran. Interpreting an apoptotic corpse as anti-inflammatory involves a chloride sensing pathway. ***Nature Cell Biology*** 21, 1532-1543. 2019.

Sho Morioka*, Justin SA Perry*, Michael H Raymond, [Christopher B. Medina](#), Yunlu Zhu, Liyang Zhao, Vlad Serbulea, Suna Onengut-Gumuscu, Norbert Leitinger, Sarah Kucenas, Jeffrey C Rathmell, Liza Makowski, Kodi S Ravichandran. Efferocytosis induces a novel SLC program to promote glucose uptake and lactate release. ***Nature*** 563, 714-718. 2018.

Jakub Jankowski, Heather M Perry, [Christopher B. Medina](#), Liping Huang, Junlan Yao, Amandeep Bajwa, Ulrike M Lorenz, Diane L Rosin, Kodi S Ravichandran, Brant E Isakson, Mark D Okusa. Epithelial and Endothelial Pannexin1 Channels Mediate AKI. ***Journal of American Society of Nephrology*** 29(7), 1887-1899. 2018.

Yu-Hsin Chiu, Xueyao Jin*, [Christopher B. Medina*](#), Susan A. Leonhardt, Volker Kiessling, Bradley C. Bennett, Shaofang Shu, Lukas K. Tamm, Mark Yeager, Kodi S. Ravichandran and Douglas A. Bayliss. A quantized mechanism for activation of pannexin channels. ***Nature Communications*** 8, 14324. 2017.

Miranda E. Good*, Yu-Hsin Chiu*, Ivan K. H. Poon*, [Christopher B. Medina](#), Joshua T. Butcher, Suresh K. Mendu, Leon J. DeLalio, Alexandar W. Lohman, Norbert Leitinger, Eugene Barrett, Ulrike M. Lorenz, Bimal N. Desai, Iris Z. Jaffe, Douglas A. Bayliss, Brant E. Isakson, and Kodi S. Ravichandran. Pannexin 1 channels as an unexpected new target of the anti-hypertensive drug spironolactone. ***Circulation Research*** 122(4), 606-615. 2017.

[Christopher B. Medina](#) and Kodi S. Ravichandran. Do not let death do us part: ‘find-me’ signals in communication between dying cells and the phagocytes. ***Cell Death and Differentiation*** 23(6), 979-89. 2016.

Yu-Hsin Chiu, Elizabeth C. Gonye, [Christopher B. Medina](#), Catherine A. Doyle, Joanna K. Sandilos, Ming Zhou, Thomas P. Conrads, Bimal N. Desai, Kodi S. Ravichandran and Douglas A. Bayliss. Deacetylation as a receptor-regulated direct activation switch for Pannexin channels. ***Nature Communications*** (2nd revision).

[Christopher B. Medina](#), Christopher D. Lucas, Kenneth S. Tung, Ulrike Lorenz, and Kodi S. Ravichandran. A pannexin channel axis controls communication between T_{reg} and T_{eff} cells and the severity of airway inflammation. ***Science*** (under submission). 2020.

Christopher D. Lucas, [Christopher B. Medina](#), David A. Dorward, Michael H. Raymond, Brady Barron, J. Iker Etchegaray, Sanja Arandjelovic, Emily Farber, Suna Onengut-Gumuscu, Eugene Ke, Moira KB Whyte, Adriano G. Rossi, Kodi S. Ravichandran. Pannexin1 drives efficient injury-induced epithelial proliferation and tissue repair. (Manuscript under preparation for submission to ***Immunity***). 2020.

Chapter II

Metabolites released from apoptotic cells function as novel tissue messengers

This work was recently published in Nature (March 18, 2020): Christopher B. Medina, Parul Mehrotra, Sanja Arandjelovic*, Justin S.A. Perry*, Yizhan Guo, Sho Morioka, Brady Barron, Scott F. Walk, Bart Ghesquière, Alexander S. Krupnick, Ulrike Lorenz, and Kodi S. Ravichandran*

2.1. Abstract

Caspase-dependent apoptosis accounts for ~90% of homeostatic cell turnover in the body (Nagata et al., 2010), and regulates inflammation, cell proliferation, and tissue regeneration (Bergmann and Steller, 2010; Fuchs and Steller, 2011; Rothlin et al., 2015). How apoptotic cells mediate such diverse effects is not fully understood. Here, we profiled the apoptotic ‘metabolite secretome’ and addressed their effects on the tissue neighborhood. Apoptotic lymphocytes and macrophages release specific metabolites, while retaining their membrane integrity. A subset of these metabolites is also shared across different primary cells and cell lines after apoptosis induction by different stimuli. Mechanistically, apoptotic metabolite secretome was not due to passive emptying of contents, rather orchestrated. First, caspase-mediated opening of the plasma membrane Pannexin 1 channels facilitated release of a select subset of the metabolite secretome. Second, certain metabolic pathways continue to remain active during apoptosis, with release of select metabolites from a given pathway. Functionally, the apoptotic metabolite secretome induced specific gene programs in healthy neighboring cells, including suppression of inflammation, cell proliferation, and wound healing. Further, a cocktail of

select apoptotic metabolites reduced disease severity in mouse models of inflammatory arthritis and lung graft rejection. These data advance the concept that apoptotic cells are not 'inert corpses' waiting for removal, rather release metabolites as 'good-bye' signals that actively modulate tissue outcomes.

2.2. Introduction

Apoptosis is an essential and evolutionarily conserved process that occurs in the body both under physiological conditions such as development (Lindsten et al., 2000) and homeostatic tissue turnover (Fuchs and Steller, 2011), as well as pathological settings such as inflammation and wound healing (Tseng et al., 2007). Several lines of evidence suggest that the apoptotic form of cell death is anti-inflammatory (Gregory and Paterson, 2018). For example, clearance of apoptotic cells (efferocytosis) elicits anti-inflammatory mediators from phagocytes and dampens the inflammatory tone within tissues (Birge et al., 2016; Voll et al., 1997). Interestingly, the process of apoptosis itself, independent of phagocytosis, has also been shown to modulate physiological events, such as embryogenesis (Hardy et al., 1989) and tissue regeneration (Bergmann and Steller, 2010; Ryoo et al., 2004), with pathologies arising when apoptosis is inhibited (Ke et al., 2018). However, the mechanisms by which apoptotic cells themselves mediate these functions are incompletely understood. As it is known that apoptotic cells remain intact for a period of time before they are engulfed, one potential mechanism through which these cells could signal is via the release of molecules that diffuse within a tissue to influence neighboring cells. In fact, a few soluble factors released from apoptotic cells have been detailed in the context of ‘find-me’ phagocyte recruitment signals (Medina and Ravichandran) (Gude et al., 2008; Lauber et al., 2003; Truman et al., 2008), yet the full apoptotic secretome and its effects on neighboring cells are unclear. Thus, we investigated the release of smaller molecules (metabolites <1kDa) from the apoptotic cells.

2.3. Materials and methods

2.3.1. Reagents

Trovaflloxacin, spironolactone, dexamethasone, spermidine, fructose 1,6-bisphosphate, dihydroxyacetone phosphate, inosine 5'-monophosphate, and guanosine 5'-monophosphate were obtained from Sigma. UDP-glucose was obtained from Abcam and Annexin V-Pacific Blue was from BioLegend. 7AAD, TO-PRO-3, anti-CD11b-PE (clone M1/70), anti-CD11c-PE (clone N418), and anti-CD16/CD32 (clone 93) were obtained from Invitrogen. Antibodies specific for mouse CD95 were obtained from BD. Human anti-Fas (clone CH11) was obtained from Millipore. Other reagents were obtained as follows: ABT-737 (abcam), TRAIL (Sigma), and zVAD-FMK (Enzo).

2.3.2. Mice

C57BL/10 and C57BL/6J wild-type mice were acquired from Jackson Laboratories. $Panx1^{fl/fl}$ and $Panx1^{-/-}$ mice have been described previously (Poon et al., 2014a). To generate mice with deletion of $Panx1$ in thymocytes, $Panx1^{fl/fl}$ mice were crossed to Cd4-Cre mice (Taconic). KRN TCR transgenic mice were a gift from Dr. Diane Mathis at the Harvard Medical School, and were bred to NOD mice (Jackson Laboratories) to obtain the K/BxN mice, which develop progressive spontaneous arthritis (Kouskoff et al., 1996). K/BxN serum was collected from 9-week old K/BxN mice by cardiac puncture. Animal procedures were approved and performed according to the Institutional Animal Care and Use Committee (IACUC) at the University of Virginia.

2.3.3. Apoptosis induction

Wild type Jurkat E6.1 (ATCC) or dominant negative Pannexin1-expressing ($Panx1$ -DN) (Chekeni et al., 2010) cells were resuspended in RPMI-1640 containing 1%

BSA, 1% PSQ, and 10mM HEPES and treated with 250 ng ml⁻¹ anti-Fas (clone CH11), 10μM ABT-737, or exposed to 150mJ cm⁻² ultraviolet C irradiation for 1-2 min (Stratalinker). Jurkat cells were incubated for 4 hours after apoptosis induction. For apoptosis induction in the presence of Panx1 inhibitors, Jurkat cells were treated with spironolactone (50μM) or trovafloxacin (25μM) in RPMI containing 1% BSA and 1% PSQ.

Primary thymocytes isolated from 4 to 6-week old wild-type or Panx1^{-/-} mice were treated with 5 μg ml⁻¹ anti-Fas (clone Jo2), that was subsequently crosslinked with 2 μg ml⁻¹ protein G. Primary thymocytes were incubated for 1.5 hours after apoptosis induction.

B6^{Nlrp1b⁺C1^{-/-}C11^{-/-}} were a gift from Dr. Mohamed Lamkanfi's lab (VIB/UGent, Belgium). BMDMs were generated by culturing mouse bone marrow cells in RPMI media conditioned with 10% dialyzed serum and 1% Pen-strep. The medium was supplemented with 20ng/ml of purified mouse M-CSF. Cells were incubated in a humidified atmosphere containing 5% CO₂ for 6 days. WT B6 or B6^{Nlrp1b⁺C1^{-/-}C11^{-/-}} BMDMs were seeded in 6-well plates and, the next day, either left untreated or stimulated with 500 ng/mL with anthrax PA (500 ng/mL, Quadratech) and LF (250 ng/mL, Quadratech). Supernatants from either untreated or treated BMDMs was collected. Cellular debris was removed via centrifugation step and the clarified supernatant was used for metabolic profiling.

A549 cells were treated with 10μM ABT-737 or exposed 600mJ cm⁻² and incubated for twenty-four hours. HCT-116 cells were treated with 10μM ABT-737 or 100ng ml⁻¹ TRAIL and incubated for 24 hours. All cells were pre-treated for 10 min with 50uM zVAD prior to apoptosis induction in indicated experiments. All cells were incubated at 37 °C with 5% CO₂ for indicated times.

2.3.4. Metabolite detection

Spermidine detection was measured using a colorimetric kit (Cloud-Clone Corp.) via manufacturers' protocol. Briefly, supernatants taken from cells under specified conditions were centrifuged at 1000 x g for twenty minutes. All reagents were brought to room temperature prior to use. 50µl of sample were added to each well followed by equal volume of Detection Reagent A and the plate was mixed. Samples were incubated, covered, for one hour at 37 °C. Wells were washed with 1x Wash solution three times before addition of Detection Reagent B, after which samples were incubated for another thirty minutes at 37 °C. Samples were washed again five times. 90µl of substrate solution was added to each well and incubated for 10 minutes at 37 °C after which 50µl of stop solution was added, the plate was mixed and immediately measure at 450nm on a plate reader (Flex station 3). Analysis was performed by back calculation to the standard curve, background subtraction and normalization to live cell controls.

ATP was measure using a luciferase-based kit (Promega) via manufactures' protocol. All reagents were equilibrated to room temperature before use. Briefly, supernatants taken from cells under specified conditions, were immediately moved to ice, and centrifuged at 500 x g for 5 minutes. Samples were placed back on ice and 50ul of samples and 50 ul of luciferase reagent were mixed in a 96 well opaque plate. Luminescence was immediately measure on the Flex Station 3. Analysis was performed by back calculation to the standard curve, background subtraction and normalization to live cell controls.

Glycerol-3-phosphate and creatine were measured based on manufacturers' protocols (Abcam). Briefly, supernatants were taken from specified culture conditions and

spun at 500 x g. 50 µl of supernatant was added to a 96 well plate. Detection reagents were prepared as indicated in protocol and added to respective wells. Samples were incubated for 40 minutes or 1 hr. for glycerol-3-phosphate and creatine, respectively. OD at 450nm or fluorescence at Ex/Em 535/587 was measured for glycerol-3-phosphate and creatine, respectively.

2.3.5. Flow cytometry of apoptosis and Panx1 activation

Apoptotic cells were stained with Annexin V-Pacific Blue, 7AAD, and TO-PRO-3 for 15 minutes at room temperature in the Annexin V binding buffer (140 mM NaCl, 2.5 µM CaCl, 10 mM HEPES) and subjected to flow cytometry on Attune NxT (Invitrogen). Data were analyzed using FlowJo V10 Software.

2.3.6. Metabolomics analysis of apoptotic supernatant and cell pellet

Sample extraction, processing, compound identification, curation and metabolomic analyses were carried out at Metabolon Inc. (Durham, NC) and Human Metabolome Technologies America (HMT) (Boston, MA) (Evans et al., 2009). Briefly, supernatants were separated from cell pellets via sequential centrifugation and frozen before shipment for metabolomic analysis. For HMT; supernatant samples were spiked with 10ul of water with internal standards, then filtered through a 5-kDa cut-off filter to remove macromolecules and small vesicles. Cationic compounds were diluted and measured using positive ion mode ESI via CE-TOFMS. Anionic compounds were measured in the positive or negative ion mode ESI using CE-MS/MS. Samples were diluted to improve the CE-QqMS analysis. Peak identification and metabolite quantification were determined using migration time, mass to charge ratio, and the peak area normalized to the internal standard

and standard curves. Concentrations reported are on a per million cell basis which was derived by back calculations on the cell number that was used in the experimental set-up.

For untargeted metabolomics analysis through Metabolon, recovery standards were added to samples in order to monitor QC of the analysis. Samples were methanol precipitated under shaking for 2 minutes. After, samples were placed on the TurboVap to remove organic solvent and the samples were stored O/N under nitrogen. Samples were analyzed under 4 different conditions; two for analysis by two separate reverse phase (RP)/UPLC-MS/MS methods with positive ion mode ESI, one for analysis by RP/UPLC-MS/MS with negative ion mode ESI, and one for analysis by HILIC/UPLC-MS/MS with negative ion mode ESI. Using a library based on authenticated standards that contains the retention time/index (RI), mass to charge ratio (m/z), and chromatographic data (including MS/MS spectral data) on all molecules in the library (Metabolon), the metabolite identification could be performed with reverse scores between the experimental data and authenticated standards. While there may be similarities based on one of these factors, the use of all three data points can be used to identify biochemicals. R code used for heatmap generation and volcano plots is available upon request.

2.3.7. Metabolite flux experiments with ^{13}C -arginine labeling

Cells were re-suspended in arginine free RPMI media containing 10% dialyzed serum, supplemented with 1mM $^{13}\text{C}_6$ L-Arginine HCl (Thermo Fischer Scientific). Cells were either exposed to UV or left untreated. This step was performed within a minute of adding the media containing ^{13}C -arginine to cells. The cells were then incubated at 37 °C. Samples were collected every hour to trace the incorporation of the label from arginine into

the polyamine pathway for both UV exposed and live cells. Where indicated, the cells were pre-treated with zVAD-FMK to inhibit caspases.

Metabolite extraction from the pellet or supernatant was performed by adding 300ul of 6%TCA to a pellet of 4 million cells on ice. The samples were then vortexed thoroughly at 4°C, followed by centrifugation to remove cell debris. 100ul of the supernatant and 900ul of Na₂CO₃ (0.1M, pH 9.3) were mixed, followed by the addition of 25ul of isobutyl chloroformate. The mixture was incubated at 37 °C for 30 minutes and then centrifuged for 10 minutes at 20000g. 800ul of the supernatant was transferred to a fresh tube, followed by the addition of 1000µl of diethyl ether and vortexing. The mixture was allowed to sit at RT for 10 minutes for phase separation after which, 900µl sample was collected in a fresh Eppendorf tube. The samples were dried via Speedvac. For LC-MS runs, 150ul of 1:1 mixture of 0.2% acetic acid in water and 0.2% of acetic acid in acetonitrile was added to the dried sample.

2.3.8. RNA-sequencing

LR73 cells (ATCC) were plated at (100x10³) per well in 24-well tissue culture plates and cultured for 16 hours at 37 °C with 5% CO₂. The cells were then rinsed with phosphate buffered saline (PBS), and fresh supernatants taken from live Jurkat, apoptotic Jurkat (UV), or Panx1-DN apoptotic Jurkat (UV) cells were added for 4 hours (as described above). Total RNA was harvested using the Nucleospin RNA kit (Macherey-Nagal) and an mRNA library was constructed with Illumina TruSeq platform. Transcriptome sequencing using an Illumina NextSeq 500 cartridge was then performed on samples from four independent experiments. RNAseq data was analyzed using Rv1.0.136 and the R package DeSeq2 for differential gene expression, graphical representation, and statistical

analysis. R code used for bioinformatic analysis and heatmap generation is available upon request.

2.3.9. Quantitative RT-PCR analysis

RNA was extracted from cells treated with different live or apoptotic supernatants. Where indicated, supernatants were filtered through a 3kDa filter as suggested by manufacturers' protocol. Briefly, supernatants were separated from cells and large vesicles via sequential centrifugations. Supernatants were then added to 3kDA filters (Millipore) and centrifuged for one hour at 3000 x g prior to adding supernatant to live LR73 cells. Nucleospin RNA kit (Macherey-Nagel) was used for RNA extraction and cDNA was synthesized using QuantiTect Reverse Transcription Kit (Qiagen). Gene expression of indicated genes was performed using Taqman probes (Applied Biosystems) and the StepOnePlus Real Time PCR System (Applied Biosystems).

In-vivo thymocyte death induction

Six- to eight-week old Panx1^{fl/fl} or Panx1^{fl/fl}Cd4-Cre mice were injected intraperitoneally with dexamethasone (250 µg). Thymus was harvested 6 hours post-injection and single cell suspension was prepared using 70-µm strainers (Fisher). An aliquot of digested tissue was taken to measure the extent of thymocyte cell death and Pannexin1 activation using Annexin V-Pacific Blue, 7AAD, and TO-PRO-3, as described above. Samples were acquired on Attune NxT (Invitrogen) and analyzed using FlowJo v10 Software.

2.3.10. Thymic myeloid cell isolation and gene expression

Six- to eight-week old Panx1^{fl/fl} or Panx1^{fl/fl}Cd4-Cre mice were injected with dexamethasone and single cell suspensions of thymus were prepared as described above.

Following isolation, cells were incubated with anti-CD16/CD32 (Fc-Block, Invitrogen) for 20 minutes at 4°C. Cells were then stained with anti-CD3-PE and run through a MACS kit using anti-PE microbeads to ‘de-bulk’ the cell suspension and remove a majority of thymocytes. Cell flow through (CD3neg population) was collected and then stained with anti-CD11b-PE and anti-CD11c-PE antibodies 30 minutes at 4°C. Stained cells were purified using the anti-PE MicroBeads MACS kit (Miltenyi Biotec), following manufacturers protocol. Sample aliquots were run on the Attune NxT (Invitrogen) and analyzed using FlowJo v10 Software. Total RNA from purified cells was isolated Nucleospin RNA kit (Macherey-Nagel) for cDNA synthesis and qRT-PCR, as described above.

2.3.11. Memix preparation and *in vivo* treatment

The metabolite mixture MeMix⁶ was composed of these six metabolites: spermidine, fructose 1,6-bisphosphate (FBP), dihydroxyacetone phosphate (DHAP), guanosine 5'-monophosphate (GMP), inosine 5'-monophosphate (IMP), and UDP-glucose. MeMix³ was composed of spermidine, GMP and IMP. Concentrations of metabolites used for *in vitro* LR73 phagocyte treatment were as follows (based on targeted metabolomics): IMP (3.3µM), DHAP (36µM), FBP (0.5µM), GMP (2.1µM), UDP-Glucose (2µM), Spermidine (0.3µM). Concentration of metabolites used for *in vivo* mice treatment were as follows: IMP (100mg/kg), DHAP (50mg/kg), FBP (500mg/kg), GMP (100mg/kg), UDP-Glucose (100mg/kg), Spermidine (100mg/kg).

2.3.12. K/BxN induced arthritis

C57BL/6J mice were given intraperitoneal injections of 150 µl of serum from K/BxN mice on day 0 and paw swelling was measured at indicated time points using a

caliper (Fisher). Measurements are presented as percent change from day 0. On day 1, mice were randomly assigned into three groups and given daily intraperitoneal injections of either MeMix^(3or6) or vehicle through day 5. In separate experiments, mice on day 1 were randomly assigned and given daily injections of either live or apoptotic supernatants through day 5. Clinical scores were assigned for each paw as follows: 0 – no paw swelling or redness observed, 1 – redness of the paw or a single digit swollen, normal V shape of the hind foot (the foot at the base of the toes is wider than the heel and ankle) 2 – two or more digits swollen or visible swelling of the paw, U shape of the hind foot (the ankle and the midfoot are equal in thickness), 3 – reversal of the V shape of the hind foot into an hourglass shape (the foot is wider at the heel than at the base of the toes). A combined clinical score of all paws is presented. Paw measurements and clinical score assignments were performed by an investigator blinded to the treatment groups.

2.3.13. Lung Transplant Rejection Model

Orthotopic left lung transplantation was carried out according to previous reports. To study the alteration of allo-immune response by a minor antigen-mismatched combination, C57BL/10 donor and C57BL/6 recipients were used. The recipient mice were administrated with MeMix³ or vehicle intraperitoneally on post-operative Day 1 and Day 3. On Day 7, the recipient mice were sacrificed and left lung allografts were harvest and processed for histology.

2.3.14. Histology

Lungs were fixed in formalin, sectioned, and stained with hematoxylin and eosin (H&E). The acute rejections were graded according to the International Society for Heart and Lung Transplantation (ISHLT) A Grade criteria by a lung pathologist who is blinded

to the experimental settings (Stewart et al., 2007). For arthritis mice were euthanized at day 8 of K/BxN serum induced arthritis and the hind paws were fixed in 10% formalin (Fisher). Decalcification, sectioning, paraffin embedding, hematoxylin and eosin (H&E) staining and Safranin O staining was performed by HistoTox Labs (Boulder, CO). Images of ankle sections were taken on an EVOS FL Auto (Fisher) and analyzed using the accompanying software. Histology scoring was performed by an investigator blinded to the mouse treatment. For inflammation and cartilage erosion scoring, the following criteria were used - 0, none; 1, mild; 2, moderate; 3, severe. For bone erosion scoring, the following criteria were used: 0, no bone erosions observed; 1, mild cortical bone erosion; 2, severe cortical bone erosion without the loss of bone integrity; 3, severe cortical bone erosion with the loss of cortical bone integrity and trabecular bone erosion.

2.3.15. Statistical analysis

Statistical significance was determined using GraphPad Prism 7, using unpaired Student's two-tailed t-test (paired and unpaired), one-way ANOVA, or two-way ANOVA according to test requirements. Grubbs' Outlier Test was used to determine outliers, which were excluded from final analysis. A p value of <.05 (indicated by one asterisk), <.01 (indicated by two asterisks), <.001 (indicated by three asterisks), or <.0001 (indicated by four asterisks) were considered significant.

2.4. Results

2.4.1. Apoptotic cell secretome

To profile the metabolite secretome of apoptotic cells, we used human Jurkat T cells, primary murine thymocytes, or primary bone-marrow derived macrophages (BMDM), all of which are known to undergo inducible, caspase-dependent apoptosis (UV treatment, anti-Fas antibody crosslinking, or anthrax lethal toxin-induced apoptosis) (Elliott et al., 2009; Van Opdenbosch et al., 2017) (**Figure 2.1a**). As untargeted metabolomics experiments require large numbers of cells, we initially optimized the parameters for this untargeted metabolomics analysis using Jurkat cells (such as cell density, volume of culture medium, duration after apoptosis induction), such that ~80% of the cells were apoptotic, while maintaining cell membrane integrity (Annexin V⁺7AAD⁻) (**Figure 2.2a, b**). After collecting cell supernatants and cell pellets from apoptotic and live cell controls, we performed untargeted metabolomic profiling against a library of >3000 biochemical features/compounds. Supernatants of Jurkat cells after UV-induced apoptosis revealed an enrichment of 123 metabolites relative to live cell supernatant controls, indicative of their release (**Figure 2.1b, Figure 2.2c, d**). About two thirds of the metabolites enriched in the apoptotic cell secretome (85 out of the 123) were reciprocally reduced in the apoptotic cell pellets (**Figure 2.3a-f**), again suggestive of their release.

We also performed similar untargeted metabolomics on supernatants from apoptotic macrophages, induced to undergo apoptosis after incubation with purified anthrax lethal toxin (Van Opdenbosch et al., 2017). Interestingly, compared to apoptotic Jurkat cells, the metabolite secretome of primary macrophages had much fewer metabolites, perhaps due to differences in cell types, modality of death and/or quantities

released (i.e. below detection limits). Regardless, relative to control supernatants from live macrophages, we noted 20 released metabolites from apoptotic macrophages. Strikingly, 16 out of these 20 released metabolites (i.e. 80%) were shared with those released by apoptotic Jurkat cells (**Figure 2.1b**).

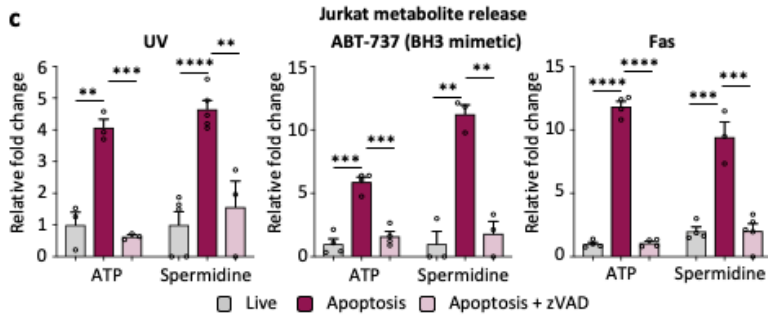
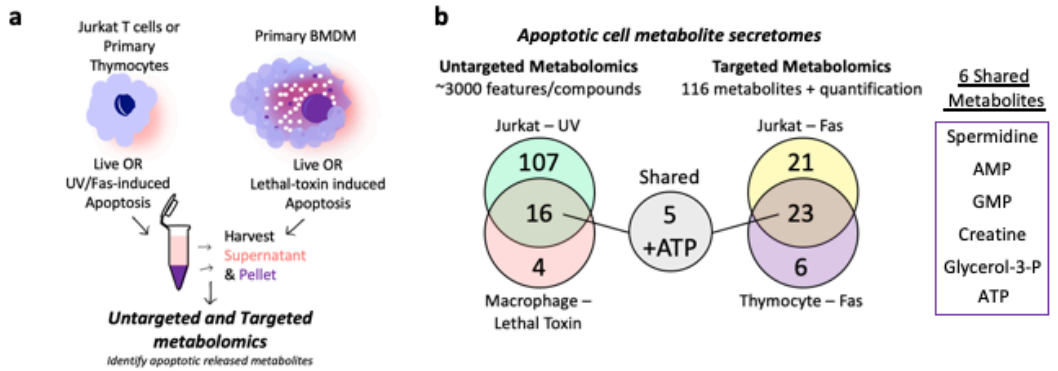
For further validation and to obtain quantitative data on some of the metabolites released, we performed additional ‘targeted metabolomics’ of apoptotic cell supernatants. We analyzed 116 specific metabolites (see methods) and compared Jurkat cells undergoing apoptosis after Fas-crosslinking (‘extrinsic’ cue for apoptosis); in this experiment, we also included primary murine thymocytes for comparison. The specific targeted metabolomics platform was chosen in an attempt to best match the 123 metabolites released from apoptotic Jurkat cells in our primary screen (43 matched metabolites). This targeted approach also included a 5kDa filtering of the supernatant to remove larger molecules (e.g. proteins). Supernatants of Jurkat cells after Fas-induced apoptosis showed an enrichment of many metabolites, most of which were similar to those seen in the supernatants after UV-induced apoptosis (**Figure 2.1b**). Furthermore, supernatants of primary thymocytes undergoing Fas-induced apoptosis also showed release of metabolites from dying cells that overlapped with Jurkat cells undergoing apoptosis (**Figure 2.1b**). Comparison of metabolites that were enriched/released in the apoptotic supernatant of Jurkat cells, thymocytes, and macrophages undergoing apoptosis (via Fas, UV, or toxin-mediated apoptosis) identified five ‘conserved’ metabolites (**Figure 2.1b**). These include: AMP, GMP, creatine, spermidine, and glycerol 3-phosphate (**Figure 2.4a**). ATP represents the 6th shared metabolite. For technical reasons, ATP was not profiled in the metabolomics

platforms, although we could readily measure ATP release by apoptotic Jurkat cells, thymocytes, and macrophages via luciferase assay (**Figure 2.4b**) (Elliott et al., 2009).

To test whether the release of specific metabolites was caspase-dependent and to test other cell types and modalities of apoptosis induction, we used analytical kits to directly assess the presence of 4 of the 6 ‘conserved metabolites’. Jurkat cells, A549 lung epithelial cells and HCT116 colonic epithelial cells were induced to undergo death via different apoptotic cues, such as UV, BH3-mimetic (ABT-737, which directly induces mitochondrial outer membrane permeabilization), and/or TRAIL (an extrinsic mode of apoptosis induction) (**Figure 2.1c-e**). In all of these conditions, we could detect apoptosis-dependent release of the tested metabolites and importantly, this release was attenuated by the pan-caspase inhibitor zVAD (**Figure 2.1c-e**). Besides ATP and AMP (previously known to be released from dying cells) (Yamaguchi et al., 2014), we identify apoptotic cells as a novel ‘natural source’ of several metabolites with active biological functions such as spermidine, creatine, glycerol-3 phosphate, and GMP. It is important to note that the detection of the metabolites in the supernatants was not due to a simple emptying of cellular contents during apoptosis, as comparison of the metabolites present in the supernatants versus cell pellets revealed that many metabolites known to be at high intracellular concentrations, were not released (e.g. alanine, pyruvate, and creatinine) (**Figure 2.1f**). Overall, these data suggest that primary cells and cell lines undergoing caspase-dependent apoptosis (**Figure 2.4c**) release specific metabolites while still maintaining their plasma membrane integrity.

Figure 2.1: Conserved metabolite secretome from apoptotic cells.

a, Schematic for assessing apoptotic metabolite secretomes. **b**, Venn diagrams illustrating the ‘shared’ apoptotic metabolites identified across cell types, modalities of apoptosis induction, and the two metabolomic platforms tested, and the list of five shared metabolites plus ATP. **c, d, e**, Metabolite release from Jurkat T cells (n=3 for ATP-UV, Spermidine-UV+zVAD, Spermidine-ABT, and Spermidine-Fas. n=4 for ATP-ABT, ATP-Fas, and Spermidine-Fas-live. n=5 for Spermidine-UV-live and Spermidine-Fas+zVAD), A549 lung epithelial cells (n=3), and HCT-116 colonic epithelial cells (n=3) across different apoptotic stimulus with or without caspase inhibition with zVAD. **f**, Several abundant metabolites such as (i) alanine, (ii) pyruvate, and (iii) creatinine were not released in the Jurkat T cell supernatants (n=4) (* p < .05, ** p < .01, *** p < .001, **** p < .0001). Data are mean ± s.e.m (c-e), Data are mean ± s.d (e). Unpaired Student’s t-test with Holm-Sidak method for multiple t-tests.



f Jurkat (metabolites not released by apoptotic cells)

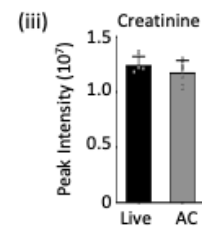
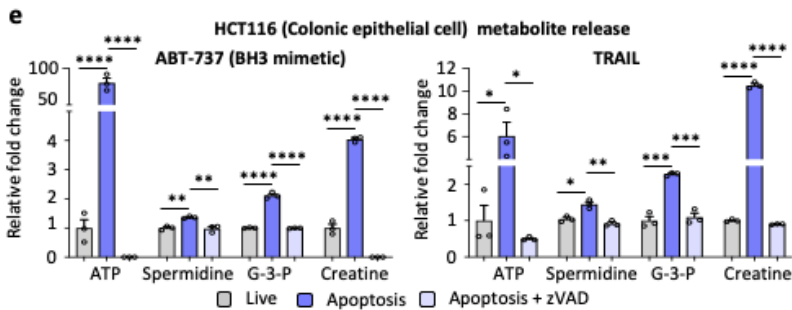
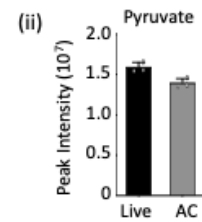
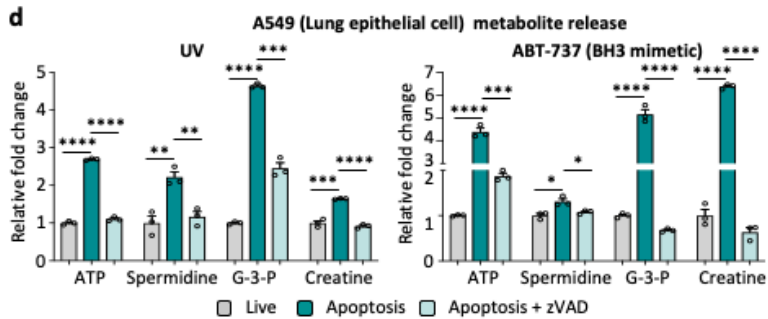
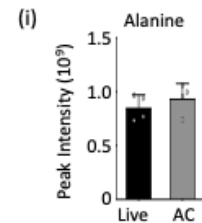
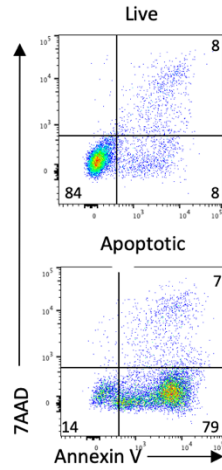


Figure 2.2: Metabolite release from apoptotic Jurkat cells.

A, Jurkat cells were induced to undergo apoptosis after UV irradiation. Staining with 7AAD and Annexin V (AV) were used to determine the percentage of live (AV⁻7AAD⁻), apoptotic (AV⁺7AAD⁻), or necrotic (AV⁺7AAD⁺) cells after 4 hours. **B**, Quantitative analysis of apoptosis (top) and secondary necrosis (bottom) (n=4). Data are mean \pm s.d. Unpaired two-tailed Student's t-test. **** p < .0001. **c**, Volcano Plot produced from untargeted metabolomics of Jurkat T cell supernatants representing statistically enriched or reduced (p < .05) metabolites in the apoptotic supernatants relative to live supernatant. Data are representative of four biological replicates. Two-sided Welch's two-sample t-test. **D**, Heatmap produced from untargeted metabolomics of Jurkat T cell supernatants representing statistically enriched or reduced (p < .05) metabolites in the apoptotic supernatants relative to live supernatants. Data are representative of four biological replicates. Two-sided Welch's two-sample t-test.

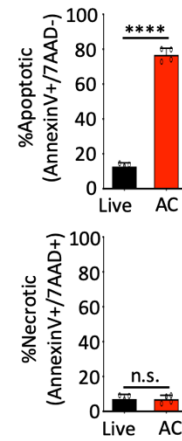
a

Jurkat cells – 4 hours UV treatment

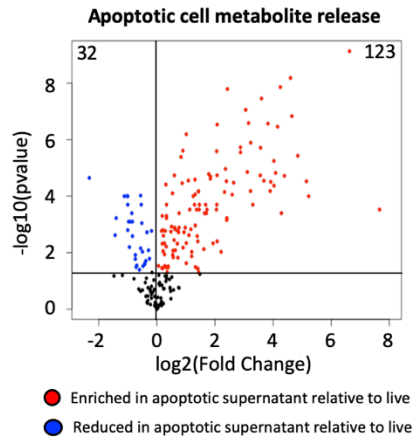


b

Jurkat cells – 4 hours UV treatment



c



d

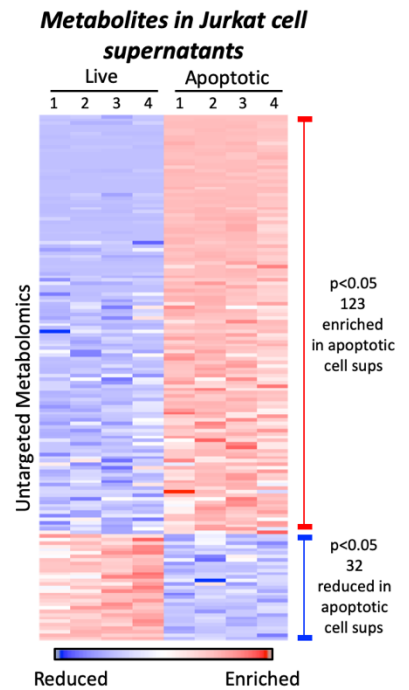


Figure 2.3: Reciprocal metabolite changes between apoptotic supernatant and pellet.

a, Heatmap produced from untargeted metabolomics of Jurkat T cell pellets representing statistically enriched or reduced ($p < .05$) metabolites in the apoptotic pellet relative to live cell pellet ($n=4$ biologically independent samples). Two-sided Welch's two-sample t-test.

b, Bi-directional plot representing the 85 metabolites that were statistically enriched in the apoptotic supernatant ($p < .05$) and simultaneously reduced in the apoptotic cell pellet relative to live cell conditions. Metabolites were grouped by metabolic pathways ($n=4$ biologically independent samples). Two-sided Welch's two-sample t-test. **c-f**, Mass

spectrometry was used to determine the relative amount of (c) spermidine. (**** $p < .0001$), (d) inosine (**** $p < .0001$), (e) UDP-glucose (supernatant **** $p < .0001$, pellet * $p=0.014$), and (f)AMP (**** $p < .0001$) in Jurkat T cell supernatants and cell pellets in live and apoptotic conditions ($n=4$ biologically independent samples). Data are mean \pm s.d. Unpaired two-tailed Student's t-test.

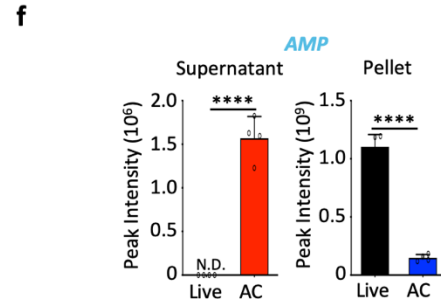
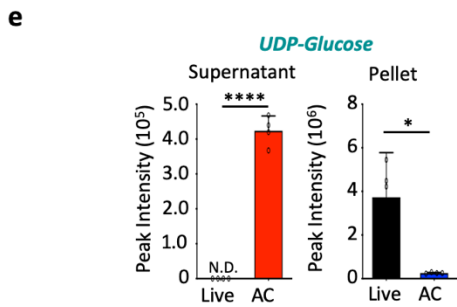
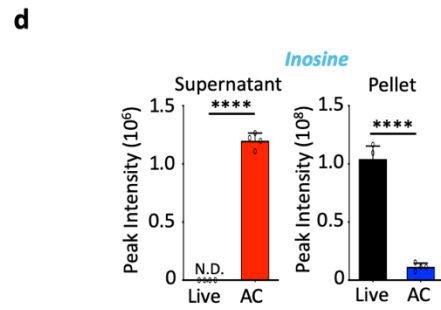
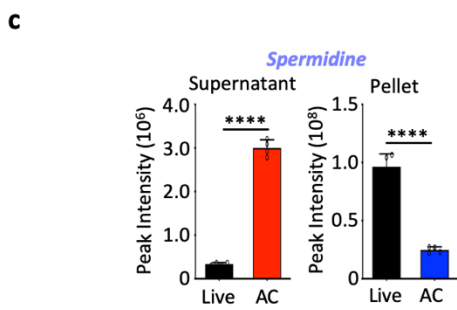
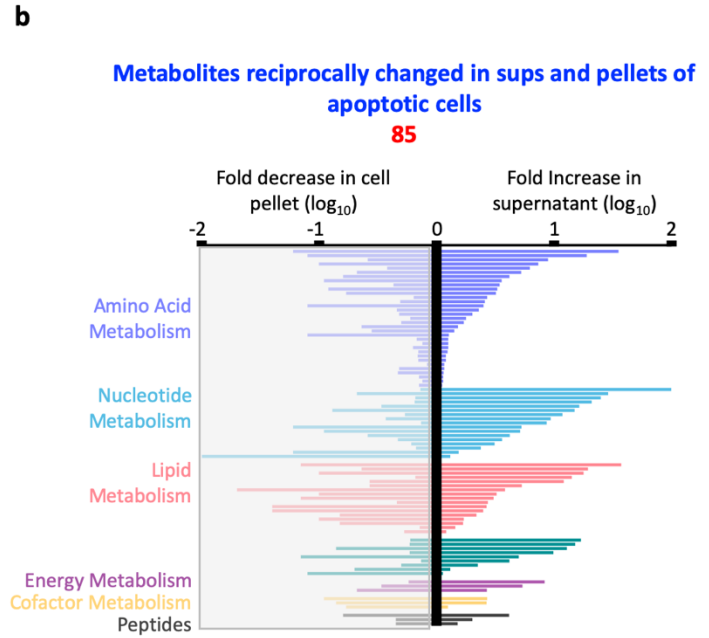
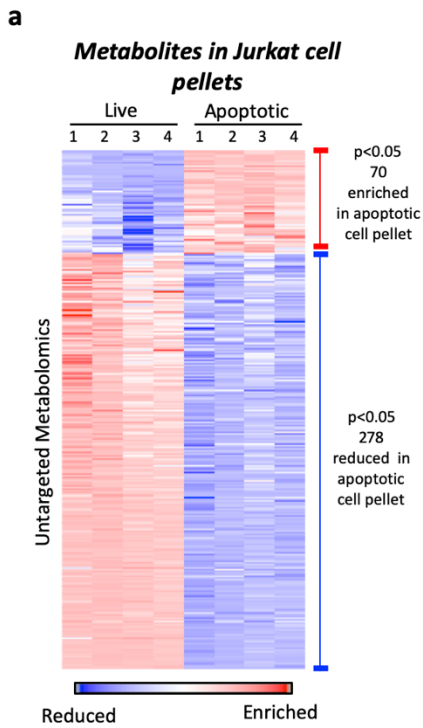
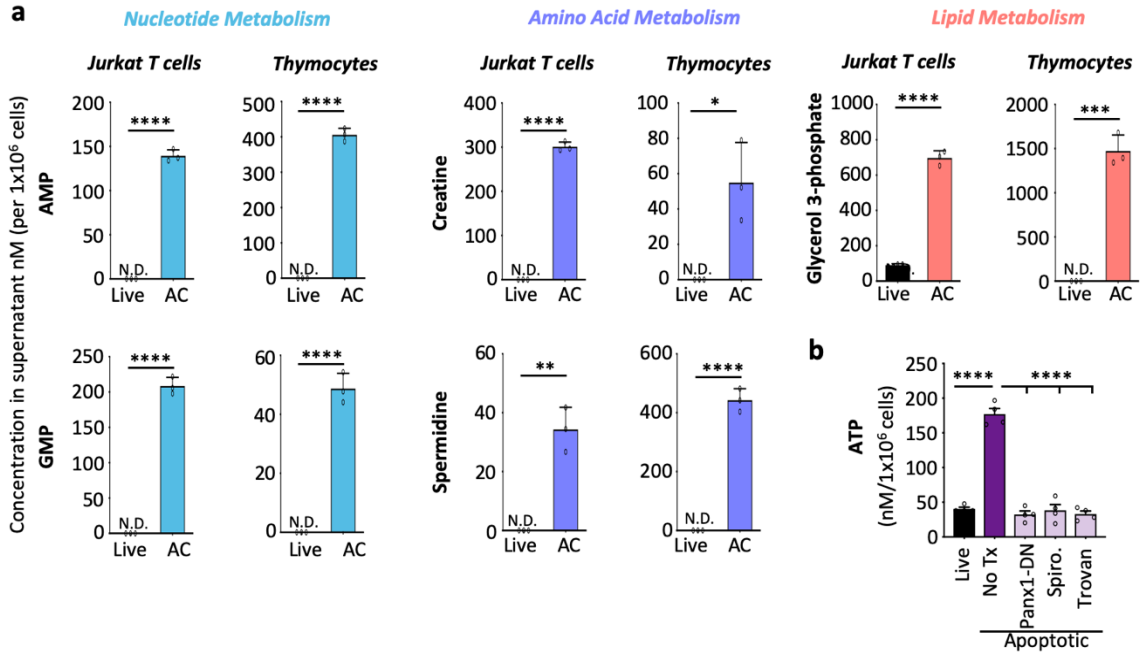


Figure 2.4: Conserved metabolite release during apoptosis.

a, Mass spectrometry was used to measure the concentration of the of the five metabolites that were released across all conditions and platforms tested in live or apoptotic supernatants per million Jurkat T cells (left) or isolated primary thymocytes (right) (back-calculated from total cells used in experimental set-up) (n=3). Metabolites are grouped by pathways to which they have been linked. Data are mean \pm s.d. Unpaired two-tailed Student's t-test. Thymocyte-creatine *p=0.014, Jurkat-spermidine **p=0.0014, Thymocyte-glycerol-3-phosphate ***p=0.0002, ****p < .0001. **b**, Luciferase assay was used to measure the concentration of ATP release in the supernatant across the different apoptotic Jurkat cells (n=4). Data are mean \pm s.e.m. Ordinary One-way ANOVA, Turkey's multiple comparison test. ****p < .0001. **c**, Table outlining the different cell types, apoptotic stimulus, techniques and metabolites screened for Untargeted (>3000 features/compounds) and Targeted (116 metabolites) metabolomics included ATP, Spermidine, Glycerol-3-phosphate (G-3-P) and creatine.



c

Cell Type	Apoptotic Stimulus	Approach	Metabolites Screened
1. Jurkat E6.1 (T cell)	UV	Untargeted Metabolomics	>3000
	Fas	Targeted Metabolomics	116
	ABT-737 (BH3 mimetic)	Colorimetric/Fluorometric Kit	ATP, Spermidine
2. Primary Thymocyte	Fas	Targeted Metabolomics	116
3. Primary BMDM	Anthrax Lethal Toxin	Untargeted Metabolomics	>3000
4. A549 (Lung epithelial cell)	UV	Colorimetric/Fluorometric Kit	ATP, Spermidine, G-3-P, Creatine
	ABT-737 (BH3 mimetic)	Colorimetric/Fluorometric Kit	ATP, Spermidine, G-3-P, Creatine
5. HCT116 (colonic epithelial cell)	ABT-737 (BH3 mimetic)	Colorimetric/Fluorometric Kit	ATP, Spermidine, G-3-P, Creatine
	TRAIL	Colorimetric/Fluorometric Kit	ATP, Spermidine, G-3-P, Creatine

2.4.2. Orchestrated metabolite release

During the various types of analyses of the apoptotic metabolites, two interesting observations stood out. First, despite the many cellular metabolites detectable in the pellet, only a subset is detectable in the apoptotic cell supernatants; second, even within a known metabolic pathway where one compound serves as the precursor for the next, only some but not others were released into the apoptotic supernatants. We hypothesized that this selectivity in metabolite release could arise from at least two scenarios that are not mutually exclusive: first, specific channels might open during apoptosis to permeate certain metabolites, and second, the metabolic activity within the dying cell could also influence the secretome. To test the notion that specific channels activated during apoptosis facilitate the release of select metabolites, we focused on pannexin channels. Pannexin 1 (Panx1) channels can conduct ions and small molecules up to 1kDa in size across the plasma membrane, and are activated during apoptosis by caspase-mediated cleavage of the intracellular C-terminal tail (that blocks the channel pore at steady state) (Chekeni et al., 2010). Apoptotic cells, but not live cells, take up the dye TO-PRO-3 (671 Daltons) in a Panx1-dependent manner (Chekeni et al., 2010), while the larger 7AAD dye (1.27 kDa) is excluded from apoptotic cells (**Figure 2.5a, b**). We tested the relevance of Panx1 in apoptotic metabolite release by genetic and pharmacological approaches. Genetically, we used Jurkat cells expressing a dominant negative Panx1 with a caspase cleavage site mutation (Chekeni et al., 2010) (Panx1-DN,) or primary thymocytes from Panx1-deficient mice (Panx1^{-/-}) (Poon et al., 2014a). For the pharmacological approach, we used two inhibitors, trovafloxacin (Trovan) and spironolactone (Spiro), which we had previously identified in unbiased screens as effective Panx1 inhibitors (Good et al., 2018; Poon et al.,

2014a). After confirming that disrupting Panx1 activity per se did not affect the ability of cells to undergo apoptosis (**Figure 2.6a-e**), we performed metabolomics of the supernatants. Untargeted metabolomics of the supernatants from apoptotic Jurkat cells (UV-induced) with and without Panx1 inhibition revealed that Panx1 contributed to the release of a select subset of the secretome, accounting for 25 out of the 123 apoptotic metabolites (i.e. about one fifth) (**Figure 2.7a** and **Figure 2.8a**). The Panx1-dependent metabolites included nucleotides, nucleotide-sugars, as well as metabolites linked to energy metabolism and amino acid metabolism, and most have not been previously reported to permeate through Panx1. A similar Panx1-dependent metabolite release signature was seen in the supernatants of Jurkat cells during Fas-mediated apoptosis, and when comparing thymocytes from wild type or Panx1^{-/-} mice (**Figure 2.8b, c**). As not all metabolites released from apoptotic cells were dependent on Panx1 activation, this suggests that other mechanisms of metabolite release from apoptotic cells also exist (**Figure 2.8d, e**). From this analysis, we could ascribe eight shared metabolites as Panx1-dependent between apoptotic Jurkat cells and apoptotic primary thymocytes (**Figure 2.7b** and **Figure 2.9**).

To test whether the secretome of an apoptotic cell might also be influenced by the metabolic activity of the dying cell, we chose the polyamine pathway for several reasons. First, the polyamine spermidine was released in significant quantities from apoptotic Jurkat cells, macrophages, thymocytes, as well as epithelial cell lines after different modes of apoptosis induction. Additionally, spermidine release was Panx1-activation dependent (**Figure 2.7c**). Second, among the two metabolites immediately upstream of spermidine, putrescine was not released from either live or apoptotic cells, while ornithine was present

at the same level in both live and apoptotic cell supernatants (**Figure 2.7d**), suggesting selectivity in release within this pathway. Third, exogenous supplementation of spermidine has been documented to reduce inflammation and improve longevity (Guo et al., 2011; Madeo et al., 2018), and our observations of spermidine release from apoptotic cells provides the first natural/physiological extracellular source of this polyamine during apoptosis.

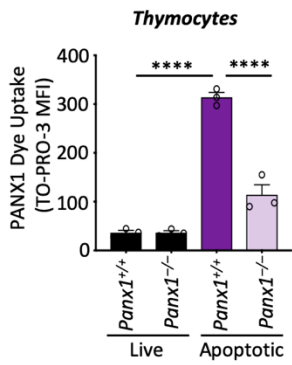
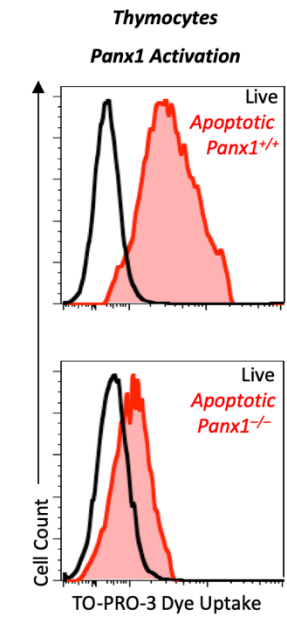
Therefore, we asked whether apoptotic cells simply release the existing (pre-synthesized) polyamine, or whether there might be continued metabolic flux through the polyamine pathway during apoptosis to supplement and coordinate its release. The upstream steps of spermidine generation include the metabolism of arginine → ornithine → putrescine → spermidine, with each conversion regulated by specific enzymes. Interestingly, a recent report (Liu et al., 2018) documented that in HCT-116 cells undergoing apoptosis, the majority of mRNA gets degraded, yet a small fraction of mRNA is ‘retained’ in the dying cell. Re-analysis of the retained mRNA dataset revealed that the polyamine pathway enzyme transcripts were not degraded during apoptosis, including spermidine synthase (SRM) that converts putrescine to spermidine (**Figure 2.10a**) (Liu et al., 2018). We also independently noted that in Jurkat cells the mRNA for spermidine synthase was retained during apoptosis, relative to housekeeping genes (**Figure 2.10b**). To address this more directly, we performed metabolic flux labeling experiments. We added ¹³C-Arginine medium to Jurkat cells immediately prior to apoptosis induction, and traced the label incorporation within cells into putrescine and spermidine for the next few hours (via mass spectrometry) (**Figure 2.7e**). In the first hour after apoptosis induction, apoptotic cells displayed increased ¹³C label incorporation into the polyamine pathway, compared to

live cells. After normalizing for total label incorporation and focusing on the carbons within the polyamine pathway (see methods), apoptotic cells showed 40% greater ^{13}C label/min incorporation into putrescine during the first hour than live cell controls (**Figure 2.7f** left). Although the rate of incorporation of ^{13}C label into putrescine dips during the 2nd hour, it was still comparable to live cells. The apoptotic cells incorporated ~25% more ^{13}C label from arginine into spermidine per minute in the first hour after apoptosis induction relative to live cells (**Figure 2.7f** right). Further, ^{13}C labelled spermidine was detectable in the supernatants of apoptotic cells, and this was partially reduced by inhibition of caspases, suggesting apoptosis-dependent modulation (**Figure 2.10c**). Interestingly, despite its active generation (revealed by the ^{13}C labeling), putrescine was not detectable in apoptotic cell supernatants from Jurkat cells (or in the macrophage or thymocytes data set), while spermidine was generated and released in a Panx1-dependent manner from apoptotic conditions (**Figure 2.7d**). These data advance the concept that apoptotic cells can orchestrate the generation and release of select metabolites into the extracellular milieu in at least two levels – caspase-dependent opening of specific channels (Panx1), and the continued metabolic activity of certain pathways.

Figure 2.5: Panx1 activation and inhibition during cell death.

a, Representative histograms of TO-PRO-3 dye uptake (top) as a readout of Panx1 activation in live and apoptotic thymocytes from wild type (Panx1^{+/+}) and Panx1 knockout (Panx1^{-/-}) mice. Quantification of Panx1 activation across different conditions was assessed via flow cytometry by measuring the mean fluorescent intensity of TO-PRO-3 dye uptake (bottom) (n=3). Data are mean ± s.e.m. Ordinary One-way ANOVA, Turkey's multiple comparison test. **** p <.0001. **b**, Representative histograms of TO-PRO-3 dye uptake as a readout of Panx1 activation in live and apoptotic wild-type Jurkat T cells, Panx1-DN Jurkat T cells, and Jurkat T cells treated with two different Panx1 inhibitors spironolactone (50µM) or trovafloxacin (25µM) (top). Quantification of TO-PRO-3 dye uptake by the apoptotic cells measured as MFI assessed using flow cytometry (bottom) (n=4). Data are mean ± s.e.m. Ordinary One-way ANOVA, Turkey's multiple comparison test. **** p < .0001.

a



b

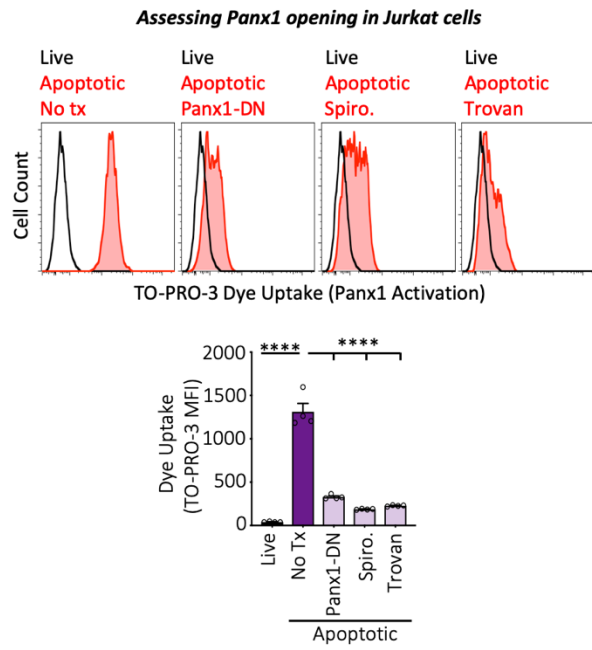


Figure 2.6: Panx1 inhibition does not influence apoptotic cell death.

a, Control or Panx1^{-/-} thymocytes were treated with anti-Fas (5 μg ml⁻¹) for 1.5 hours. Cells were stained with 7AAD and Annexin V to determine the percentage of live (AV⁻7AAD⁻), apoptotic (AV⁺7AAD⁻), or necrotic (AV⁺7AAD⁺) cells. **b**, Quantitation of apoptosis (top) and secondary necrosis (bottom) of control and Panx1 knockout thymocytes (n=3). Data are mean ± s.e.m. Ordinary One-way ANOVA, Turkey's multiple comparison test. ***p=0.0004. **c,d**, Quantification of apoptosis and secondary necrosis from the samples prior to metabolomics analysis (n=4). Data are mean ± s.e.m. Ordinary One-way ANOVA, Turkey's multiple comparison test. ****p < .0001. **e**, Cells were stained with 7AAD and Annexin V to determine the percent of live (AV⁻7AAD⁻), apoptotic (AV⁺7AAD⁻), or necrotic (AV⁺7AAD⁺) cells.

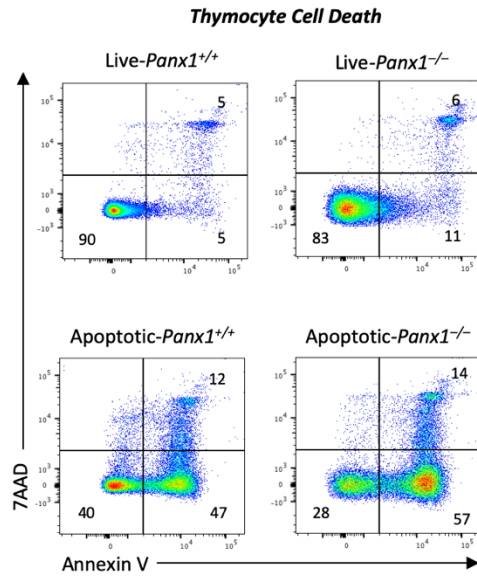
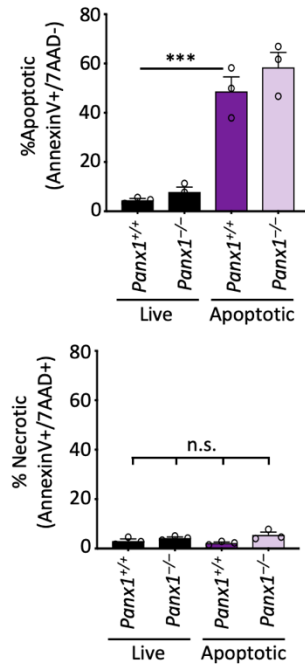
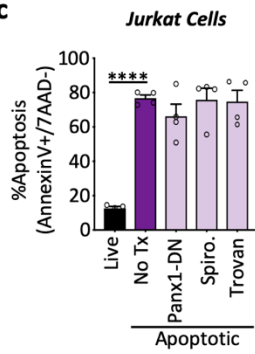
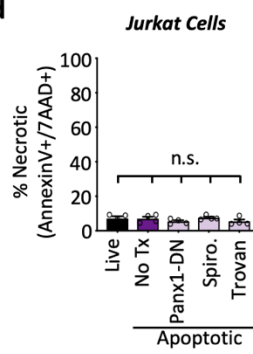
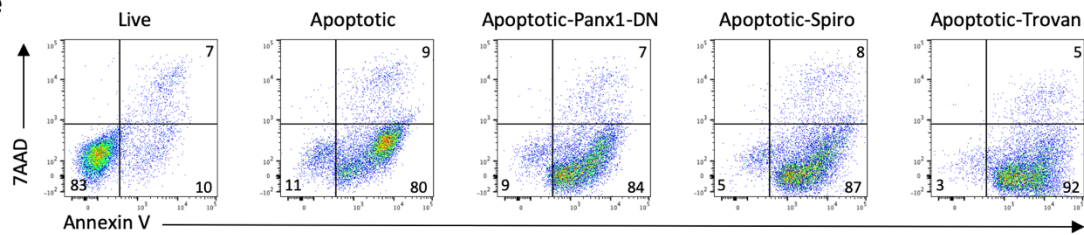
a**b****c****d****e**

Figure 2.7: Panx1 activation and continued metabolic activity of dying cells orchestrates metabolite release.

a, Panx1-dependent metabolite release. Heatmap produced from untargeted metabolomics of Jurkat T cell supernatants representing the metabolites that were statistically enriched in the apoptotic supernatants relative to live supernatant ($p < .05$), and reduced when Panx1 was inhibited via a Panx1-DN (genetic), and two Panx1 inhibitors (Spiro and Trovan) (pharmacologic) ($p < .05$). Metabolites are grouped by pathway. Charge and relative sizes (Da) of the metabolites are also shown ($n=4$). Two-sided Welch's two-sample t-test. **b**, Three-way Venn diagram (left) illustrating the eight Panx1-dependent apoptotic metabolites observed among the cell types and apoptotic modalities tested. ATP (not detected here) represents the 9th metabolite. **c**, Supernatant spermidine concentration per million cells (targeted metabolomics) from Jurkats (Fas crosslinking - 4 hours - left) ($n=3$) ($***p=0.0002$) or primary thymocytes with *Panx1* deletion (Fas - 1.5 hours - right) ($n=3$) ($****p=0.0001$). **d**, (left) Schematic of the polyamine metabolic pathway. (right) Relative amounts of ornithine, putrescine, and spermidine in Jurkat T cell supernatants in live and apoptotic conditions, with or without Panx1 inhibition ($n=4$) ($****p=0.0001$) **e-f**, Active polyamine metabolic activity during apoptosis. Experimental layout for ¹³C-arginine labeling (f), and incorporation of ¹³C-labeled arginine into the polyamine pathway intermediates putrescine (f-left) ($***p=0.0003$) and spermidine (f-right) ($*p=0.025$) after cell death induction ($n=6$). Data are mean \pm s.e.m. Ordinary One-way ANOVA, Turkey's multiple comparison test (c,d). Unpaired Student's t-test with Holm-Sidak method for multiple t-tests (e,f).

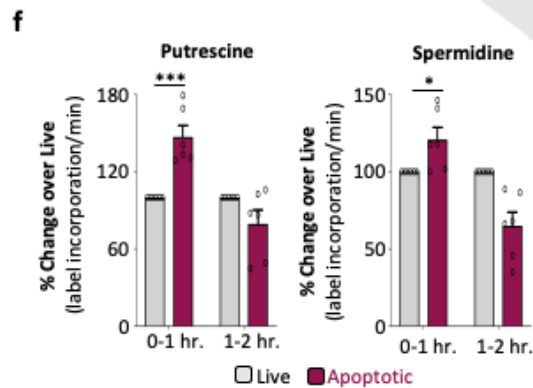
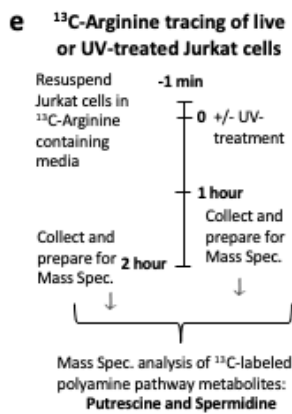
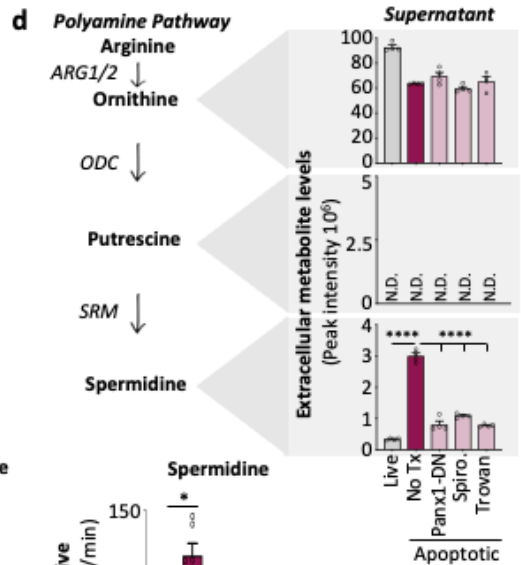
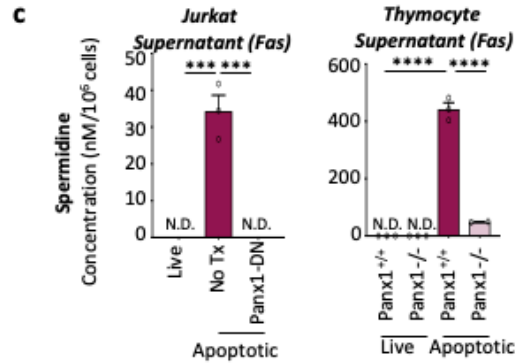
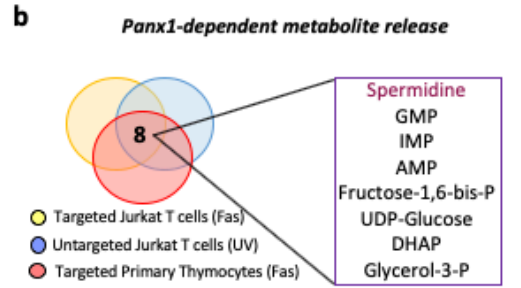
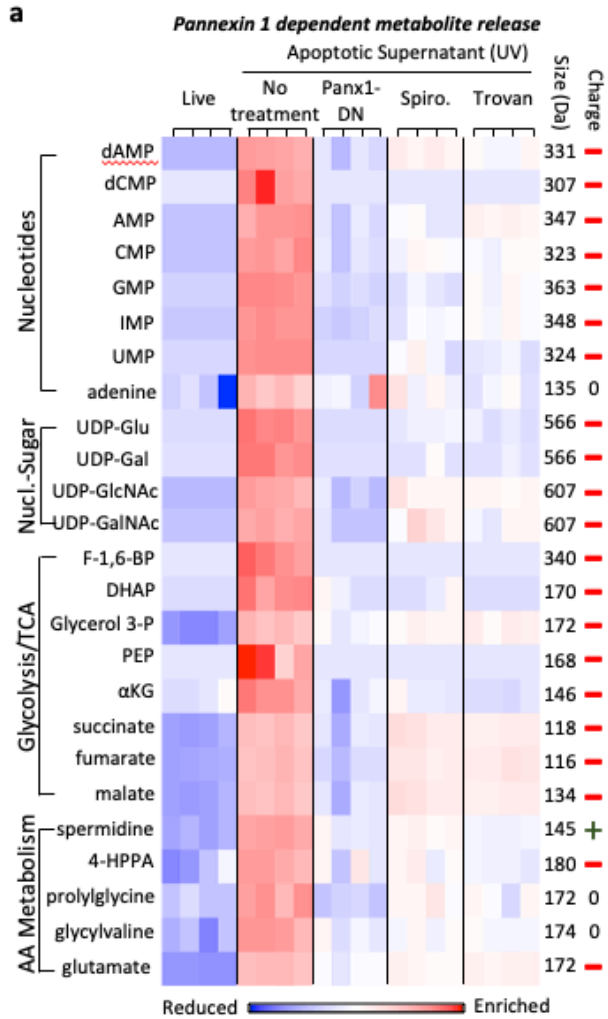


Figure 2.8: Panx1-dependent metabolite release during apoptosis.

a, Mass spectrometry was used to determine the relative amount of AMP, GMP, UDP-Glucose, and fructose 1,6-bisphosphate in Jurkat T cell supernatant across different conditions (n=4). Data are mean \pm s.e.m. Ordinary One-way ANOVA, Turkey's multiple comparison test. **** p < .0001. **b**, Jurkat cells were induced to undergo apoptosis with anti-Fas treatment (250ng ml⁻¹). Mass spectrometry was used to measure the absolute concentration per million cells of (a) AMP, (b) UDP-glucose, and (c) fructose 1,6-bisphosphate in the supernatants of Jurkat T cells across different conditions (back-calculated from total cells used in experimental set-up) (n=3). Data are mean \pm s.e.m. Ordinary One-way ANOVA, Turkey's multiple comparison test. (UDP-Glucose Live vs. No Txn **p=0.0013, No Txn vs. Panx1-DN *p=0.031, **** p< .0001). **c**, Mass spectrometry was used to determine the absolute concentration of AMP, GMP, UDP-Glucose, and fructose 1,6-bisphosphate per million cells (back-calculated from total cells used in experimental set-up) in the supernatant from isolated primary thymocytes across different conditions (n=3). Data are mean \pm s.e.m. Ordinary One-way ANOVA, Turkey's multiple comparison test. **** p< .0001. **d-e**, Relative concentrations were determined by mass spectrometry for inosine (d) and choline (e) in live, apoptotic, or apoptotic supernatants where Panx1 was inhibited (n=4). Data are mean \pm s.e.m. Ordinary One-way ANOVA, Turkey's multiple comparison test. **** p<.0001.

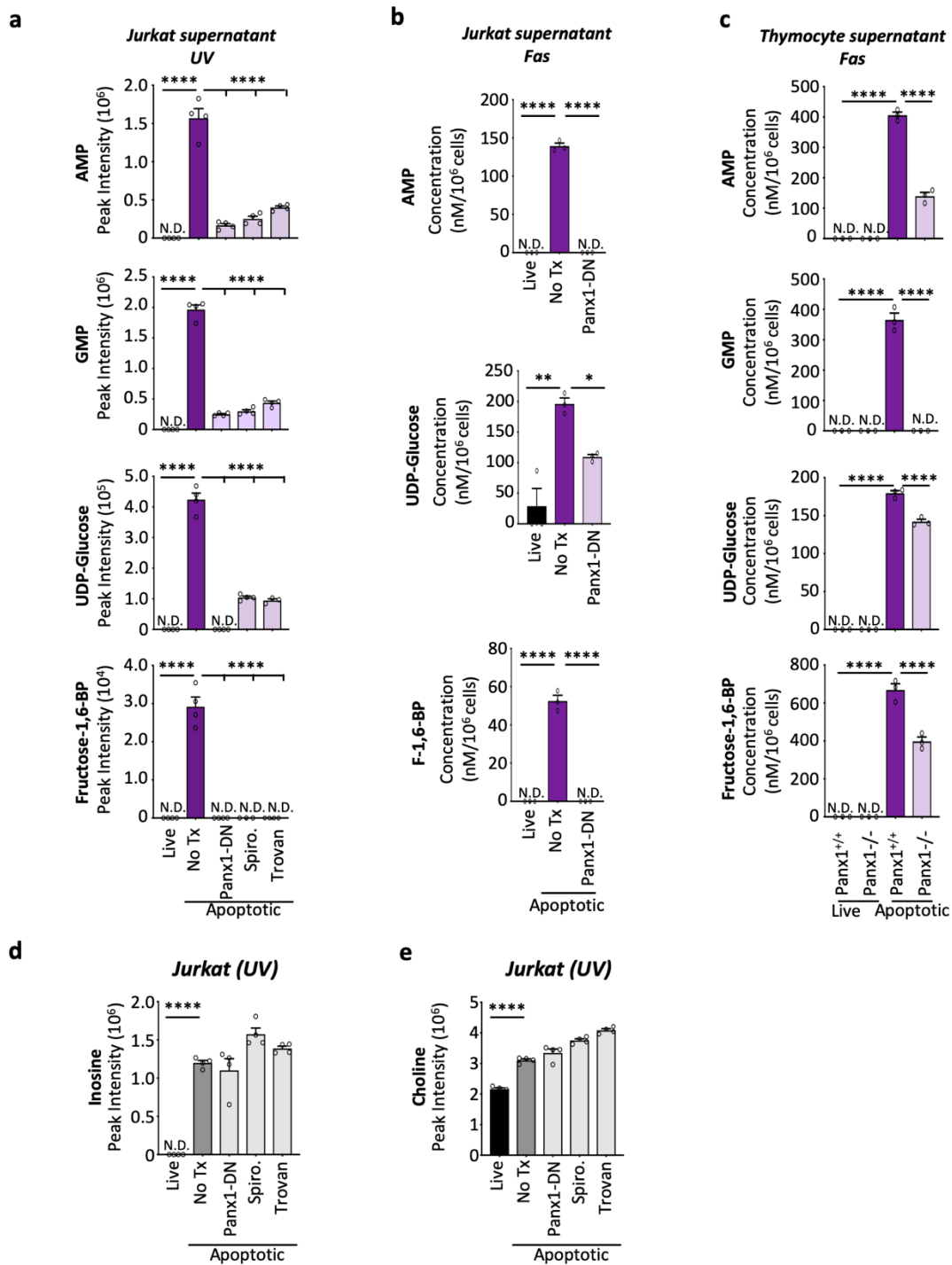
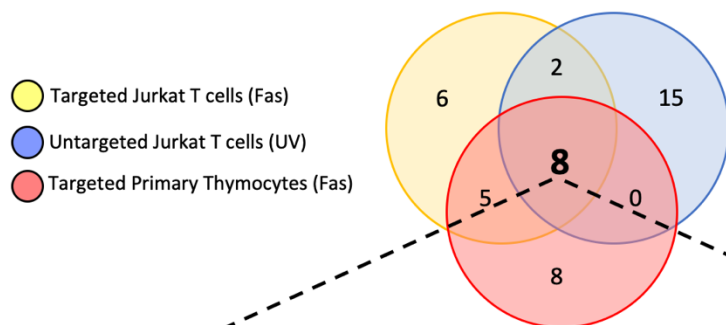


Figure 2.9: Conserved Panx1 secretome.

a, Three-way Venn diagram (top) comparing Panx1-dependent metabolites released from apoptotic cells across different conditions tested. Table (bottom) showing the relative peak intensity (untargeted metabolomics) or absolute concentrations (targeted metabolomics) in the supernatant of the indicated cell treatments and knockout mice.

Panx1 dependent metabolite release



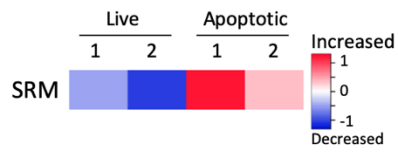
Panx1-depenedent metabolites (Consistent across all platforms/conditions)	Targeted (Jurkat) (nM/10 ⁶ cells)			Untargeted (Jurkat) (Peak Intensity)			Targeted (Thymocytes) (nM/10 ⁶ cells)		
	Live	Apoptotic	Apoptotic Px1DN	Live	Apoptotic	Apoptotic Px1DN	Live	Apoptotic Panx1 ^{+/+}	Apoptotic Panx1 ^{-/-}
spermidine	N.D.	34	N.D.	0.3x10 ⁶	3.0x10 ⁶	0.8x10 ⁶	N.D.	441	49
dihydroxyacetone phosphate (DHAP)	N.D.	3559	650	N.D.	1.2x10 ⁶	0.2x10 ⁶	N.D.	1471	581
Glycerol 3 - phosphate	89	697	359	0.4x10 ⁶	5.4x10 ⁶	1.6x10 ⁶	42	248	166
fructose- 1,6- bisphosphate	N.D.	52	N.D.	N.D.	2.9x10 ⁴	N.D.	N.D.	668	397
adenosine 5'-monophosphate (AMP)	N.D.	139	N.D.	N.D.	1.6x10 ⁶	0.2x10 ⁶	N.D.	406	140
inosine 5'-monophosphate (IMP)	28	330	55	N.D.	2.2x10 ⁶	0.09x10 ⁶	35	140	84
guanosine 5'-monophosphate (GMP)	N.D.	208	7	N.D.	2.0x10 ⁶	0.2x10 ⁶	N.D.	52	N.D.
UDP-glucose	87	196	109	N.D.	4.2x10 ⁵	2.5x10 ⁵	N.D.	182	142

Figure 2.10: Transcriptional and metabolic changes during apoptosis.

a, Re-analyses of RNA-seq data from apoptotic cells (*Lui et. al., 2018*) demonstrating that the SRM mRNA levels are increased/retained during apoptosis. **b**, After induction of apoptosis (n=4), the SRM mRNA expression was assessed over time relative to live controls (n=5). Data are mean \pm s.e.m. Two-way ANOVA (**p=0.007). **c**, Incorporation of ¹³C-labeled arginine into the polyamine pathway intermediate spermidine and release from Jurkat cells after apoptosis, and its partial reduction by the pan-caspase inhibitor zVAD (n=3). Data are mean \pm s.d. Unpaired two-tailed Student's t-test (**p=0.0088).

a

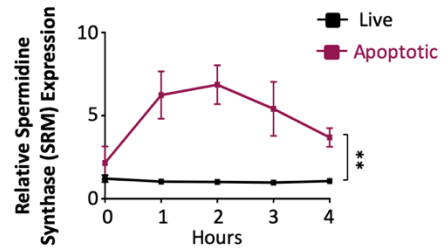
HCT116 – Trail-induced apoptosis



Analyzed by us using data from
Liu, X et. al. Cell. 2018

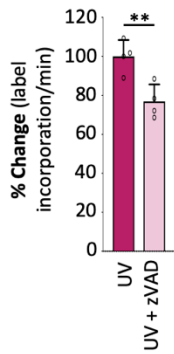
b

Jurkat – UV-induced apoptosis



c

¹³C-Labeled Spermidine release
(Supernatant)



2.4.3. Metabolites as extracellular signaling molecules

Next, we tested the potential functional consequence of these released metabolites on nearby live cells. To determine whether released apoptotic cell-derived metabolites signal to alter gene expression programs in healthy nearby cells such as phagocytes, we collected supernatants from live or apoptotic Jurkat cells (same conditions as for the untargeted metabolomics studies above, with UV-induced apoptosis); we then added these supernatants to LR73 cells, a model phagocyte useful in revealing mechanisms or responses after efferocytosis that have been subsequently confirmed in macrophages and other cell types engulfing apoptotic cells (Juncadella et al., 2013; Morioka et al., 2018; Wang et al., 2017) (**Figure 2.11a**). RNAseq analysis of LR73 cells after a 4hr incubation with apoptotic cell supernatants indicated that metabolites released from apoptotic cells can induce distinct transcriptional changes in phagocytes, compared to controls (live cell supernatants) (**Figure 2.11b** and **Figure 2.12a**). Pathway analysis, by hand-curating each of the hits individually, together with commonly used analysis software, revealed that the apoptotic secretome altered gene programs linked to cytoskeletal rearrangements, inflammation, wound healing/tissue repair, anti-apoptotic functions, metabolism, and regulation of cell size (**Figure 2.11b**), providing, in part, a molecular and metabolic basis for how apoptosis may influence wound healing, inflammation or other essential processes.

By comparing gene programs induced in phagocytes treated with supernatants from apoptotic cells versus conditions where Panx1 function was blocked (via genetic inhibition of Panx1), we identified 110 genes as differentially regulated in live cells by Panx1-dependent apoptotic metabolites (82 up and 28 down) (**Figure 2.11c**). Gene programs in live cells regulated by Panx1-dependent released metabolites from apoptotic cells include

those involved in anti-inflammatory processes, anti-apoptotic pathways, metabolism, and actin rearrangement (**Figure 2.11c**). Secondary validation via qPCR indicates genes linked to anti-inflammatory roles in phagocytes (Nr4a1, Pbx1) (Chung et al., 2007; Ipseiz et al., 2014), wound healing (Areg, Ptgs2) (Goessling et al., 2009; Zaiss et al., 2015), and metabolism (Slc14a1, Sgk1, Uap1) (Morioka et al., 2018; Shayakul et al., 2013) were affected by Panx1-dependent metabolites (**Figure 2.11d** and **Figure 2.12b**). Furthermore, filtration of supernatants through 3kDa filters, prior to phagocyte treatment, resulted in similar gene transcriptional changes (**Figure 2.12c**), supporting the notion of metabolite-mediated signaling from dying cells in this context rather than larger proteins or vesicles from dying cells. Collectively, the above transcriptomics approaches uncovered that metabolites released from apoptotic cells, a subset of which are released in a Panx1-dependent manner, can alter selective gene programs in the surrounding cells that sense these metabolic signals.

To test *in vivo* whether apoptotic Panx1-dependent metabolites can induce gene expression changes in the surrounding tissue phagocytes, we induced apoptosis of immature thymocytes via dexamethasone (Dex) administration into mice (Ahmed and Sriranganathan, 1994). We used Panx1^{fl/fl}Cd4-Cre mice, where Panx1 is targeted for deletion only within the thymocytes (**Figure 2.13a**). After confirming that Panx1 was not deleted in the live macrophages and dendritic cells (see schematic in Fig. 4a and Extended Data 10a right), and that comparable dexamethasone-induced thymocyte apoptosis occurs in control and Panx1^{fl/fl}Cd4-Cre mice (**Figure 2.13b, c**), we isolated CD11b⁺ macrophages and CD11c⁺ dendritic cells from the thymus and analyzed gene expression changes (**Figure 2.13d, e**). In wild-type mice, compared to vehicle-injected control mice, dexamethasone-

induced apoptosis of thymocytes resulted in increased expression in surrounding live myeloid cells of *Uap1*, *Ugdh*, and *Pbx1* (involved in metabolic processes linked to anti-inflammatory macrophage skewing/glycosylation and IL-10 transcription)(Chung et al., 2007; Jha et al., 2015; Zhang et al., 2018) (**Figure 2.14a**). Importantly, this response in the myeloid cells was attenuated in *Panx1^{fl/fl}Cd4-Cre⁺* mice lacking *Panx1* channels in the dying thymocytes (**Figure 2.14a**). Thus, *Panx1*-dependent metabolite release from apoptotic thymocytes can induce gene expression changes in the surrounding tissue myeloid cells *in vivo*.

When we tested a few of the metabolites individually for their ability to induce a set of anti-inflammatory and tissue-repair genes, we found that individual metabolites were quite inefficient (data not shown). Since it appears these metabolites are simultaneously released from dying cells, we hypothesized that a metabolite mixture, rather than single metabolites may mediate stronger extracellular signaling. Out of the 8 *Panx1*-dependent metabolites, we tested 6 of them in two separate metabolite cocktails: i) spermidine, fructose-1,6-bis-phosphate, dihydroxyacetone phosphate, UDP-glucose, guanosine monophosphate, and inosine monophosphate; and ii) spermidine, guanosine monophosphate, and inosine monophosphate (**Figure 2.14b**). All six have been previously administered *in vivo* in mice (or rats) without toxicity (**Table 2.1**). The two metabolites that we chose not to include in our cocktail were AMP, which can be converted into adenosine, a known anti-inflammatory and vasodilatory metabolite (Dubyak and el-Moatassim, 1993), and glycerol-3-phosphate, for which it was difficult to determine the optimal *in vivo* dose. Importantly, while the individual metabolites were quite inefficient or lacking the ability to activate specific gene expression patterns, the metabolite mixtures

were quite potent in inducing gene expression in LR73 cells *in vitro*, including genes linked to anti-inflammatory macrophage skewing/glycosylation (Uap1, Ugdh) (Jha et al., 2015), IL-10 transcription and inflammation resolution (Pbx1 (Chung et al., 2007), Ptgs2 (Scher and Pillinger, 2009)), and metabolic processes (Slc14a1, Sgk1), some of which have also been shown to be involved in phagocytosis (Morioka et al., 2018) (**Figure 2.14c**). For simplicity, we have denoted the metabolite mixtures as MeMix⁶ and MeMix³ (**Figure 2.14b**).

2.4.4. Therapeutic potential of apoptotic cell released metabolites

We next tested whether the MeMix⁶ and/or MeMix³ might have a beneficial effect in attenuating inflammation given the anti-inflammatory gene signatures they were able to induce. For this we first used a mouse model of serum-transfer induced arthritis. Here, a single injection of the arthritic serum from K/BxN mice into C57BL/6J mice results in inflammation of the joints with progressive arthritic symptoms, followed by disease resolution (Korganow et al., 1999). Further, relevant to our question, this model is dependent on activation of the innate immune system components such as myeloid cells (Korganow et al., 1999), with apoptosis known to occur during disease (see schematic in **Figure 2.14d**). Prior to testing MeMix⁶ and MeMix³, we first asked whether the ‘full’ apoptotic secretome could alleviate inflammation in this arthritis model, and this was the case (**Figure 2.13f**). When we tested MeMix⁶ or MeMix³ administration after arthritis induction when the disease symptoms are already noticeable, it resulted in significant attenuation of paw swelling and other arthritic parameters, compared to vehicle controls (**Figure 2.14d**). Since it has been shown that fructose 1,6-bisphosphate alone can have ameliorative roles in arthritis (Veras et al., 2015), we narrowed our subsequent

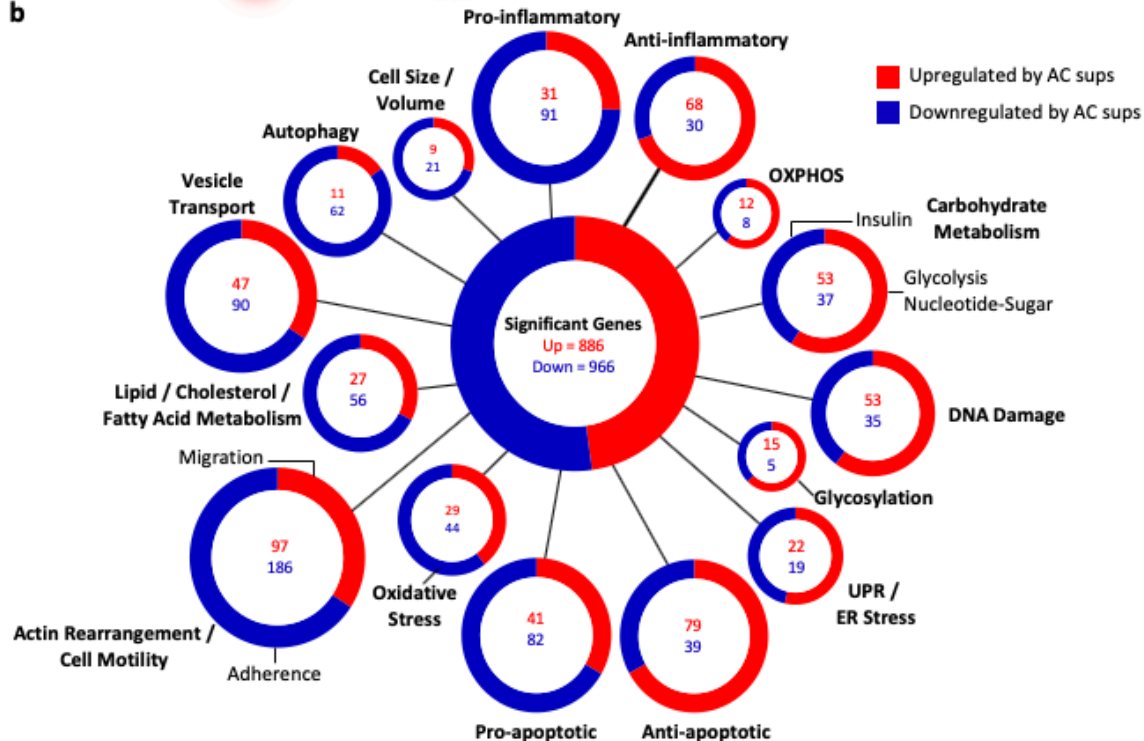
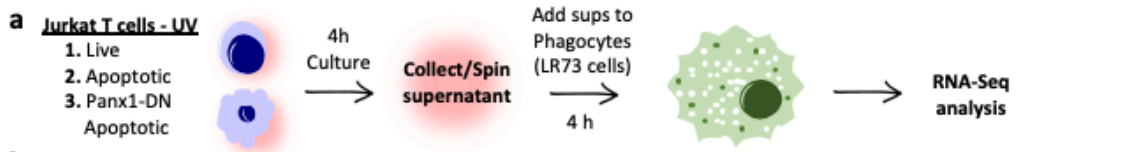
investigations to MeMix³, which does not contain fructose 1,6-bisphosphate, and instead contains spermidine, GMP, and IMP. MeMix³ not only alleviated paw swelling and external clinical arthritis parameters in mice, but also significantly protected the arthritic mouse joints from inflammation, bone erosion, and cartilage erosion (**Figure 2.14e, f**). These data suggest that a mixture of just three naturally released, Panx1-dependent, apoptotic cell metabolites (originating from an unbiased metabolomics screen) can be harnessed for beneficial anti-inflammatory effects *in vivo*.

We also tested Memix³ in a lung transplant rejection model, where myeloid cell-dependent inflammation plays an important role in the outcome of this solid organ transplant. Local immune responses in the lung, specifically the innate and adaptive immune responses orchestrated by graft-resident antigen presenting myeloid cells, dictate graft acceptance or rejection (Gelman et al., 2009). Interestingly, administration of apoptotic cells in the form of extracorporeal photopheresis (ECP) can ameliorate graft rejection and is currently in clinical use (Isenring et al., 2017), although whether this benefit is due to metabolites released from apoptotic cells is not known. To examine the anti-inflammatory effects of apoptotic metabolites in this model, we transplanted C57BL/10 left lung allografts to a minor antigen mismatched C57BL/6 recipient (**Figure 2.14g**) (Krupnick et al., 2009), treating the graft recipients with Memix³ or saline vehicle control on post-operative days 1 and 3. On day 7 post-engraftment, saline-treated control mice showed severe acute rejection of allografts (as per the International Society for Heart and Lung Transplantation A grade (Stewart et al., 2007)). Remarkably, grafts in the Memix³ treated mice had only minimal inflammation in the transplanted lungs (**Figure 2.14h**), suggestive of amelioration of lung rejection. Further, complementary flow cytometric

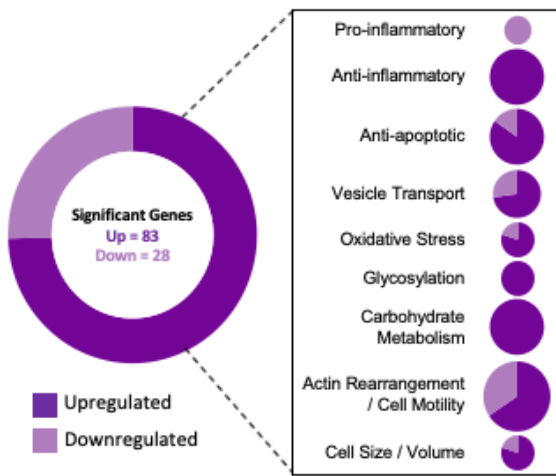
analysis of the lung showed reduced CD4 and CD8 cells in the transplanted lung of mice treated with Memix³. Thus, a subset of apoptotic Panx1-dependent derived metabolites can be harnessed for beneficial effects in two different inflammatory settings *in vivo*.

Figure 2.11: Metabolites from apoptotic cells influence gene programs in live cells.

a, Schematic for assessing gene induction by apoptotic cell supernatants in LR73 cells. **b**, Gene expression programs induced in phagocytes by the apoptotic secretome. Display shows the differentially regulated genes (1852 total, 886 upregulated, 966 downregulated), categorized per known or predicted function(s), literature, and sequence similarity. Circle size is proportional to the number of differentially expressed genes (n=4) (Significance <0.05). **c**, Differentially regulated genes in phagocytes in response to apoptotic cell supernatants with or without pannexin channel inhibition (82 upregulated, 28 downregulated) (n=4). **d**, Validation of genes regulated by Panx1-dependent metabolites. LR73 cells were incubated with indicated supernatants for 4hr, gene expression of *Areg* (n=7) (****p=0.0001), *Nr4a1*(n=7) (Live-AC ****p=0.0001, AC-AC Panx1-DN ***p=0.0008), *Uap1*(n=4) (****p=0.0001), and *Pbx1* (n=5) (Live-AC **p=0.009, AC-AC Panx1-DN *p=0.014) expression in phagocytes. Data are mean \pm s.e.m. Ordinary One-way ANOVA, Turkey's multiple comparison test.



c Gene programs altered in response to PANX1-dep. metabolites



d Validation of genes regulated by PANX1 metabolites

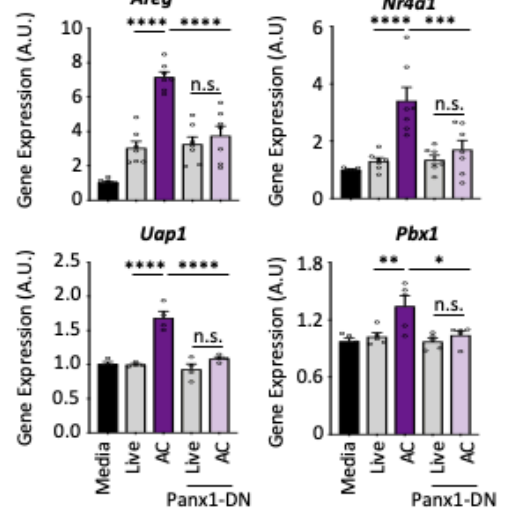
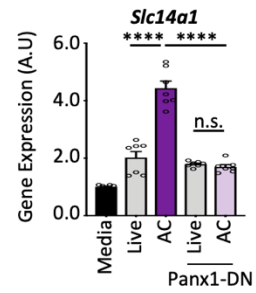
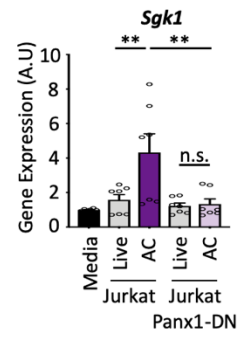
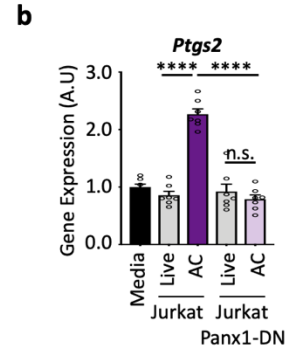
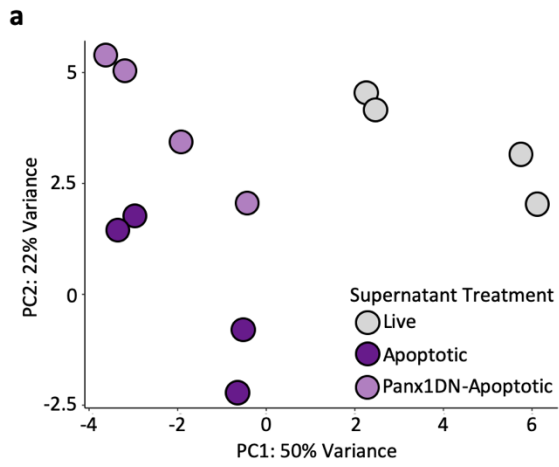


Figure 2.12: Transcriptional changes on surrounding phagocytes induced by Panx1-dependent metabolite release during apoptosis.

a, Principle component analysis (PCA) on the RNAseq data as a quality control statistic (n=4 biological replicates). **b**, Experimental procedure was as described in Figure 3d. qPCR was used to assess gene expression changes in *Ptgs2* (top) (****p<0.0001) and *Sgk1* (middle) (Live-AC **p=0.0074, AC-AC-Panx1DN **p=0.0031) (and *Slc14a1* (bottom) (****p<0.0001) in phagocytes after treatment with supernatants from Jurkat cells or Jurkat cells expressing dominant negative Panx1 (n=7). Data are mean \pm s.e.m. Ordinary One-way ANOVA, Turkey's multiple comparison test. **c**, Experimental procedure was as described in Figure 3d, however before treatment of LR73 cells with supernatant, the supernatant was filtered through a 3kDa filter to remove large molecules. qPCR was used to assess gene expression changes in and *Sgk1* (top) (**p=0.0001) and *Slc14a1* (bottom) (****p<0.0001) in phagocytes after treatment with supernatants under specified conditions (n=3). Data are mean \pm s.e.m. Ordinary One-way ANOVA, Turkey's multiple comparison test.



c 3kDa filtered supernatant

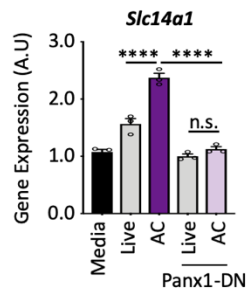
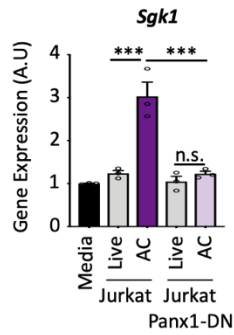


Figure 2.13: In-vivo thymic cell death analysis and supernatant effects during arthritis.

a, Analysis of thymic populations used for experimental data presented in Figure 4a. After thymus isolation, the CD11b⁻CD11c⁻ population which contained thymocytes was used for mRNA isolation to test the efficiency of deletion *Panx1* allele. qPCR analysis of *Panx1* mRNA in wild-type (*Panx1^{fl/fl}* CD4-Cre⁻) (n=6) or mice in which *Panx1* has been knocked out in thymocytes (*Panx1^{fl/fl}* CD4-Cre⁺) (n=7) (left) (**p=0.0015). CD11b^{+/c+} myeloid cells harvested from the thymus of *Panx1^{fl/fl}*CD4-Cre^{-/+} were analyzed for *Panx1* expression to demonstrate that *Panx1* not deleted. *Panx1* deletion was only deleted from thymocytes and not the myeloid cells which do not express CD4. Data are mean ± s.d. Unpaired two-tailed Student's t-test. **b**, Representative flow cytometric plots showing the extent of apoptosis induced by dexamethasone in control and *Panx1^{fl/fl}* CD4-Cre⁺ mice. After thymus isolation, an aliquot of cells was stained with 7AAD and Annexin V to determine the % of live, apoptotic, or necrotic (AV⁺7AAD⁺) cells. **c**, Quantitative analysis of apoptosis (left) and secondary necrosis (right) of CD11b⁻CD11c⁻ thymic populations from *Panx1^{fl/fl}* CD4-Cre⁻ (PBS n=4, Dex n=10) or *Panx1^{fl/fl}* CD4-Cre⁺ (PBS n=3, Dex n=9) mice treated with PBS or dexamethasone. Data are mean ± s.e.m. Ordinary One-way ANOVA, Turkey's multiple comparison test (****p<0.0001). **d**, Representative flow cytometry plots demonstrating the purity of CD11b⁺CD11c⁺ population after magnetic separation from the different mice and treatment conditions. **e**, Comparison of the CD11b⁺CD11c⁺ cells isolated from the different conditions. *Panx1^{fl/fl}* CD4-Cre⁻ (PBS n=4, Dex n=7) or *Panx1^{fl/fl}* CD4-Cre⁺ (PBS n=3, Dex n=6). Data are mean ± s.e.m. Ordinary One-way ANOVA, Turkey's multiple comparison test. **f**, Apoptotic supernatants alleviate

KBx/N induced arthritic disease. C57Bl/6J mice were injected with K/BxN serum to induce arthritis. Live (n=4) or apoptotic (n=5) supernatant was given for five days after arthritis induction. Paw swelling was measured using a caliper and reported as % change compared to day 0. Data are mean \pm s.e.m. Two-way ANOVA (*p=0.0131).

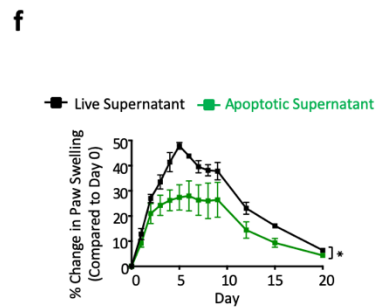
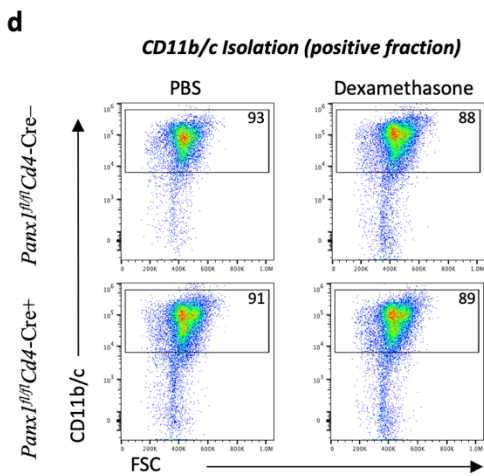
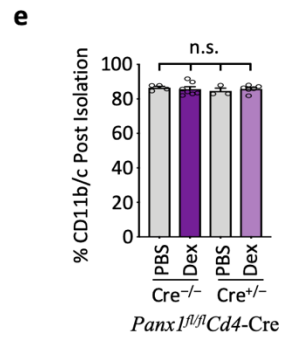
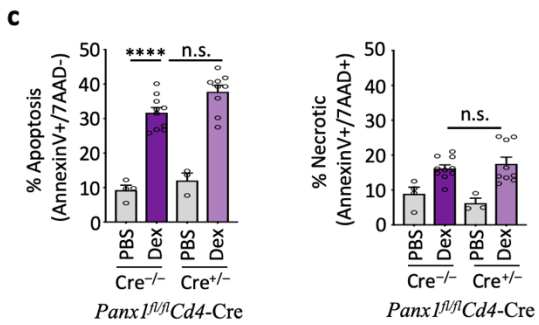
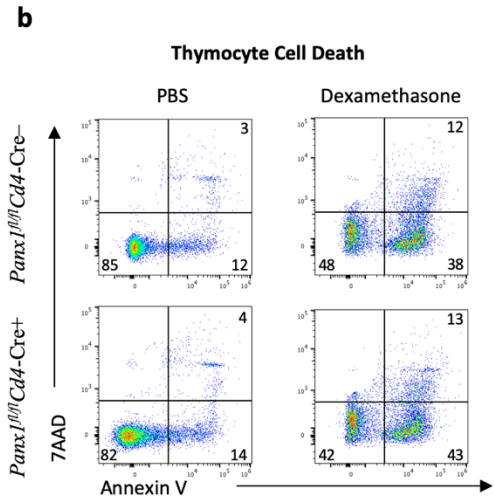
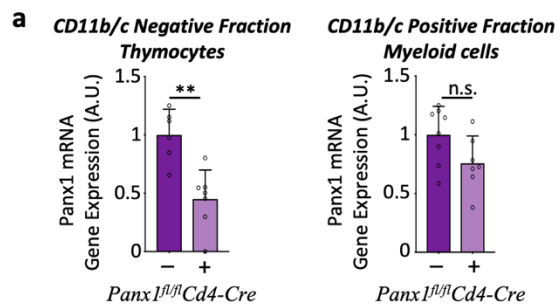


Figure 2.14: Panx1-dependent metabolite release during apoptosis modulates phagocyte gene expression *in vivo* and can alleviate inflammation.

a, Panx1 expression in apoptotic thymocytes influences gene expression in myeloid cells *in vivo*. Control mice (Panx1^{fl/fl}, no Cre) or mice lacking Panx1 in thymocytes (Panx1^{fl/fl} Cd4-Cre) were injected with dexamethasone to induce apoptosis in thymocytes (Panx1^{fl/fl} Cd4-Cre- PBS n=3, Panx1^{fl/fl} Cd4-Cre- Dex n=6, Panx1^{fl/fl} Cd4-Cre+ PBS n=4, Panx1^{fl/fl} Cd4-Cre+ Dex n=4). After 6hr, CD11b⁺ CD11c⁺ phagocytes were purified for mRNA. qPCR analysis of *Uap1* (WT PBS-WT Dex *p=0.032, WT Dex-KO Dex ****p<0.0001), *Pbx1* (WT PBS-WT Dex ****p=0.0001, WT Dex-KO Dex *p=0.0103), and *Ugdh* (****p<0.0001) in CD11b⁺CD11c⁺ phagocytes. **b**, Panx1-dependent metabolites released from apoptotic cells were compared across cell types and apoptotic conditions to design different metabolite mixtures, *Memix*⁶ (blue) and *Memix*³ (purple). **c**, *MeMix*⁶ (n=6) and *MeMix*³ (n=4) solutions mimic gene expression changes in phagocytes induced by apoptotic supernatants (*p<0.05, **p<0.01, ****p<0.0001). **d**, Schematic of arthritis induction and treatments (top). Paw swelling was measured using a caliper and reported as % change compared to day 0 (*MeMix*⁶ **p=0.0028, *MeMix*³ ***p=0.0003). Scores were assessed on a scale of 1-4 per paw (*MeMix*⁶ ***p=0.0004, *MeMix*³ ****p=0.0001) (Vehicle n=16, *MeMix*⁶ n=11, *MeMix*³ n=12). **e**, Ankle inflammation and bone erosion were scored via H&E staining (left) and Safranin O (right), respectively, from arthritic mouse paws. Increased magnifications of affected areas are also shown. **f**, Clinical analysis of inflammation, bone erosion, and cartilage erosion was scored by an investigator blinded to treatments (Vehicle n=6, *MeMix*³ n=7) (****p<0.0001). **g**, *MeMix*³ metabolite solution alleviates inflammation in a minor antigen-mismatch lung transplant model. Orthotopic

left lung transplantation from C57BL/10 mice into C57BL/6 recipient mice, with *Memix*³ administered on post-operation day 1 and 3. Lungs were harvested for histological scoring on day 7. **h**, H&E staining (left) and ISHLT Rejection score (right) (Vehicle n=6, *MeMix*³ n=6) (*p=0.024). Data are mean \pm s.e.m. (a,c,d). Data are mean \pm s.d. (f,h). Ordinary One-way ANOVA, Turkey's multiple comparison test (a). Unpaired two-tailed Student's t-test (c,f,h). Two-Way ANOVA (d).

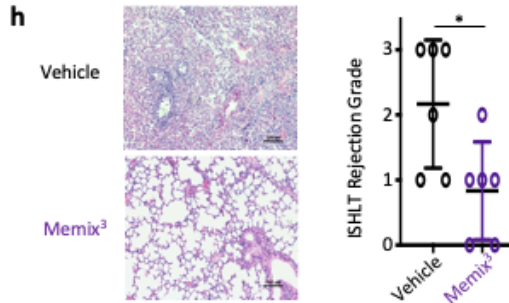
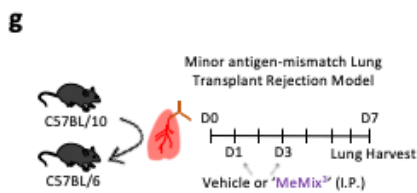
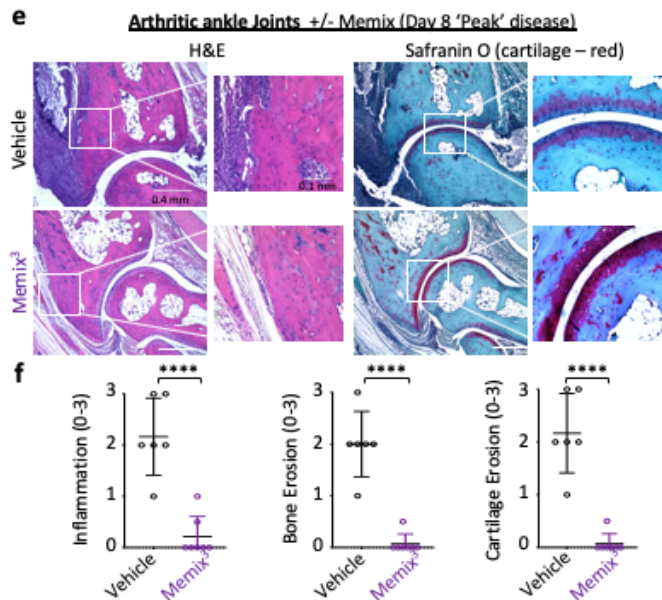
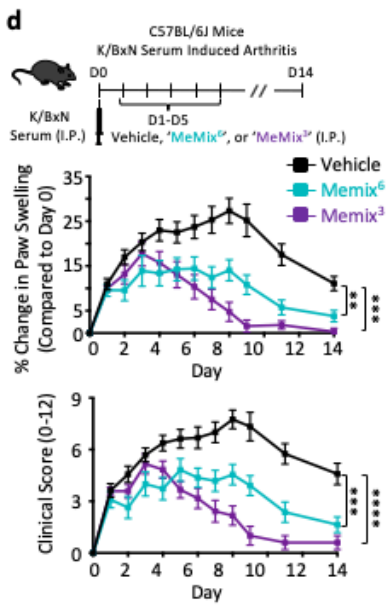
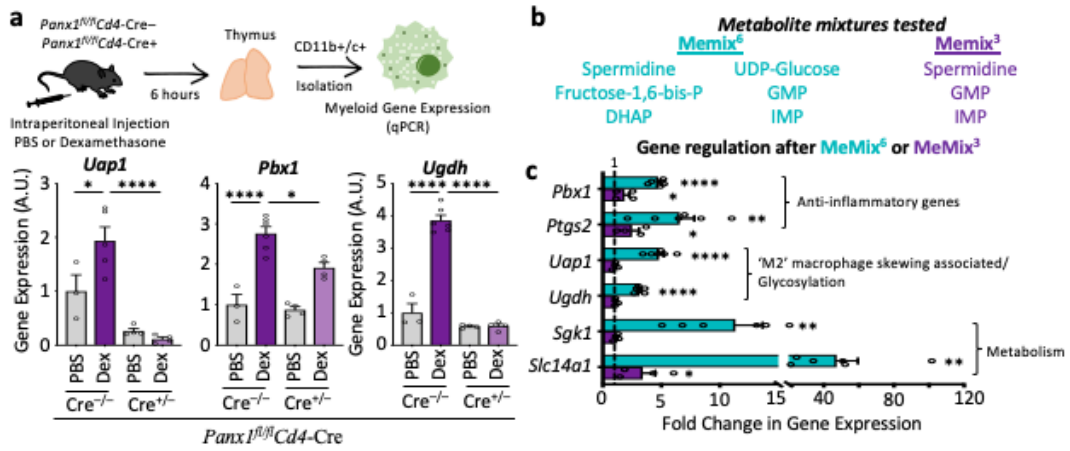


Table 2.1: Reported extracellular function of metabolites.

a, Table of metabolites that were released in a Panx1-dependent manner from untargeted metabolomics of Jurkat T cells. Along with metabolite name, charge, size and reported literature using extracellular treatment of the specific metabolite and their effects are also included.

Untargeted Metabolomics

Panx1-dependent metabolites released from apoptotic cells	Size (Da)	Charge	Extracellular Function
fumarate	116	-	Anti-inflammatory immunomodulator*
succinate	118	-	Inflammatory macrophage activation PGE2 production
malate	134	-	Unknown
adenine	135	Neutral (o)	Unknown
spermidine	145	+	Anti-inflammatory, Anti-aging, Autophagy inducer
alpha-ketoglutarate	146	-	Bone Development
glutamate	147	-	Neurotoxic, Convulsive
phosphoenolpyruvate (PEP)	168	-	Unknown
dihydroxyacetone phosphate (DHAP)	170	-	Anti-inflammatory**, Athero-protective**
Glycerol 3 - phosphate	172	-	Unknown
prolylglycine	172	Neutral(o)	Memory, Neuroprotective
glycylvaline	174	Neutral(o)	Unknown
4-hydroxyphenylpyruvate	180	-	Unknown
2'-deoxycytidine 5'-monophosphate	307	-	Unknown
cytidine 5'-monophosphate (5'-CMP)	323	-	Unknown
uridine 5'-monophosphate (UMP)	324	-	Increase acetylcholine levels Increase CDP-choline levels Memory, Neurite outgrowth
2'-deoxyadenosine 5'-monophosphate	331	-	Sperm motility****
fructose- 1,6- biphosphate	340	-	Neuroprotective, anti-inflammatory
adenosine 5'-monophosphate (AMP)	347	-	Anti-inflammatory*****, Vasodilator*****
inosine 5'-monophosphate (IMP)	348	-	Anti-Inflammatory*****, Proliferation*****, Neuroprotective*****
guanosine 5'- monophosphate (5'-GMP)	363	-	Anti-convulsant*****
UDP-glucose	566	-	Inflammatory, Proliferation, Repair
UDP-galactose	566	-	Unknown
UDP-N-acetylglucosamine	607	-	Unknown
UDP-N-acetylgalactosamine	607	-	Unknown

*Dimethyl fumarate

**3,4-DHAP

****2-deoxyadenosine

*****Adenosine

*****Inosine

*****Guanosine

2.5. Discussion

Collectively, the data presented here advance several concepts. First, by taking an unbiased approach to better understand the metabolite secretome of apoptotic cells, we identify specific metabolites that are released from apoptotic cells (different cell types and different modes of apoptosis induction). While we focus on the metabolites that were ‘shared’ across the cell types tested, it is likely that different cells types may release additional unique metabolites dependent on their metabolic state and tissue environment. These data also demonstrate that apoptotic cells are not inert, rather can actively generate and release a select set of metabolites. The specificity of metabolite release could arise from a combination of metabolic changes that occur during apoptosis (e.g. sustained spermidine production), and/or the opening of specific channels that release subsets of metabolites (e.g. Panx1). Second, these released metabolites form part of a metabolite-based communication from apoptotic cells within the tissue, and serve as a potent signaling modality to modulate multiple gene programs in the neighboring cells. This was best evidenced by caspase-mediated and Panx1-dependent release of specific metabolites from apoptotic thymocytes that communicated with myeloid cells of the thymus *in vivo*. Although Pannexin channels have recently been implicated in a variety of physiological processes including hypertension (Billaud et al., 2015), cancer metastasis (Furlow et al., 2015), and neuropathic pain (Weaver et al., 2017), these studies have predominantly focused on one type of nucleotide release (ATP) and the subsequent purinergic signaling. The data presented here significantly expand the repertoire of molecules released through pannexin channels, with implications for both physiological and pathological processes. While, apoptotic metabolites are capable of influencing the tissue environment both during

homeostasis and in situations where apoptosis may be heightened, such as under inflammatory insults, it must be understood that tissue specific death (or tumor specific death) may also play unique roles in controlling different microenvironments. While the use of small kDa filters in these studies helped focus on ‘free’ metabolites, whether apoptotic cell-derived small vesicles potentially carrying metabolites may also play a role in intercellular signaling remains to be defined. Third, we could administer a selected cocktail of apoptotic metabolites to attenuate arthritic symptoms and to improve lung transplantation outcomes across minor-histocompatibility mismatch. This provides a proof-of-concept that it is possible to harness the beneficial therapeutic properties of apoptosis in specific inflammatory conditions.

2.6. Author Contributions

C.B.M. and K.S.R designed the experiments. C.B.M. performed majority of the experiments. P.M.M. performed the macrophage apoptosis and polyamine tracing experiments. S.A. and C.B.M performed the arthritis experiments. J.S.A.P. assisted with the bioinformatic analyses. Y.G. and A.S.K. assisted with the lung transplant experiments. S.M., B.B., and S.W. provided experimental expertise on few specific experiments. B.G. assisted with the polyamine mass-spectrometry and U.L. provided mice and conceptual advice. C.B.M. and K.S.R wrote the manuscript with input from coauthors.

Chapter III

A pannexin channel axis controls communication between T_{reg} and T_{eff} cells and the severity of airway inflammation

This work is under submission: Christopher B. Medina, Christopher D. Lucas, Kenneth S. Tung, Ulrike M. Lorenz, and Kodi S. Ravichandran

3.1. Abstract

Allergic airway inflammation (AAI) affects millions of people all over the world. While different genetic and environmental factors can pre-dispose to airway inflammation, Type 2 inflammatory responses coordinated by CD4⁺ T cells remain central to disease progression (Lambrecht and Hammad, 2015). Extracellular nucleotides, such as ATP, have been implicated in both airway inflammation and T cell activation, yet the modalities of ATP release and how this might influence Th2 dependent airway inflammation is unclear. Pannexin 1 (Panx1) channels are large pore channels that are known to release ATP into the extracellular milieu in different contexts. Here, we identify an immunoregulatory axis wherein the Panx1-dependent communication between T_{reg} and T_{eff} cells via extracellular ATP contribute to the severity of airway inflammation. First, we identify a correlation between decreased Panx1 expression on the peripheral blood mononuclear cells and asthmatic patients implicating the channel in AAI pathology (Raedler et al., 2015). Experimentally, we noted that mice with a global deletion of *Panx1* have more severe airway inflammatory response to house dust mite (HDM) allergen. Cell-type-specific knockout mice studies revealed a specific requirement for Panx1 expression on T cells for dampening airway inflammation. Further, through generation of Panx1 transgenic mice and re-expression of Panx1 specifically in T cells, where the rest of the mouse is null for

Panx1, revealed that T cell Panx1 is necessary and sufficient to control airway inflammation. Mechanistically, T_{reg}-mediated suppression of T_{eff} cells depended on Panx1 expression: as loss of Panx1 in both T_{reg} and T_{eff} cells blunted the suppression, Panx1 expression in either population was sufficient for Treg-mediated suppression. Supplementation of exogenous ATP to *Panx1*^{-/-} cultures rescued T_{reg} mediated suppression, and this depended on CD39/CD73 and adenosine generation. Collectively, these data suggest that a Panx1-dependent immunoregulator axis facilitates optimal communication/control between T_{reg} and T_{eff} cells, and for dampening the severity of airway inflammation.

3.2. Introduction

Allergic airway inflammation (AAI), also known as allergic asthma, affects ~1 in 20 people or about 300 million worldwide (Lambrecht and Hammad, 2015). While treatments such as inhaled corticosteroids can alleviate the inflammatory symptoms of disease, many patients are still refractory to such therapeutics (Umetsu and Dekruyff, 2006). For that reason, a better understanding of the molecular details that govern this disease is needed for the development of better treatments. AAI is dominated by a T_H2 inflammatory response in which $CD4^+$ T cells infiltrate the lungs where they produce IL-4 and IL-5 to mediate eosinophilia, IgE accumulation via B-cell class switching, mast cell degranulation, and eventually bronchial hyperreactivity (Agrawal and Shao, 2010; Walker et al., 1991). Interestingly, extracellular ATP (eATP) has been found in the bronchoalveolar lavage (BAL) of asthmatic patients; however, the roles that eATP might play during disease is unclear (Lázár et al., 2010). In fact, reports have identified both inflammatory and immunosuppressive roles for eATP during AAI, which could be dependent on the specific microenvironments of eATP release, the duration and concentration of ATP, the conversion of ATP to immunosuppressive molecules such as adenosine, or even the specific cell types exposed to the extracellular nucleotides (Idzko et al., 2013; 2007; Li et al., 2015). Therefore, further elucidating how eATP is regulated during AAI and the specific molecules involved in coordinating and controlling eATP may help better understand disease progression and impact future therapeutic options.

Initial observations regarding extracellular nucleotides (such as ATP) highlighted a pro-inflammatory effect of these molecules; however, recent evidence suggests a more complicated paradigm based on several levels of extracellular nucleotide regulation

(Antonioli et al., 2013; Eltzschig et al., 2013). First, different cell surface ectonucleotidases, such as CD39 and CD73, are known to break down ATP/ADP/AMP to the immunosuppressive molecule adenosine (Antonioli et al., 2013; Haskó and Cronstein, 2004). As a result, expression of these ectonucleotidases can control whether extracellular nucleotides will have a dominantly immune-stimulatory effect through ATP or a suppressive one through adenosine. Secondly, the differential expression of purinergic receptors and adenosine receptors which recognize and respond to the extracellular nucleotides (ATP, ADP, AMP, and adenosine) can regulate diverse outcomes (Junger, 2011; Rayah et al., 2012). Lastly, the relative instability of these extracellular nucleotides suggests that these molecules act in a more local environment and do not signal across long ranges. Therefore, the specific microdomains of extracellular nucleotides may be more important in dictating their function under certain pathological and physiological settings.

Regardless, the source of extracellular nucleotides in different disease settings including allergic airway inflammation are relatively unknown. Although many reports indicate uncontrolled tissue damage as the main mechanism of ATP release, whether cells can coordinate microenvironmental extracellular ATP levels in a controlled manner to influence their function during inflammatory settings remains an interesting question. One mechanism by which cells may be able to control extracellular nucleotide levels is through specific channels on their cell surface. Pannexin 1 (Panx1) is a recently discovered protein that has been shown to form heptameric channels at the plasma membrane capable of releasing ATP into the extracellular space (Ransford et al., 2009). Panx1 activation and ATP release can occur during several different cellular processes, including cell death, receptor mediated activation of the channel, mechano-stimulation, and even increases in

intracellular calcium (Chiu et al., 2018). Further, contrary to the release of ATP from complete lysis of a cell (which can be pro-inflammatory), even during caspase-mediated apoptosis, the amount of ATP released is less than 0.1% of the cellular ATP content. Therefore, whether through small amounts ATP release in a local context, Panx1 might mediate intercellular communication and what effects this has during disease settings such as allergic airway inflammation remains to be determined.

In this study, we first highlight the observation that peripheral blood mononuclear cells of asthmatic patients have decreased Panx1 expression relative to healthy controls. Consistent with this, global Panx1 deletion in mice resulted in an increased inflammatory response during allergic airway inflammation, suggesting a protective or immunosuppressive role for Panx1 during disease. Panx1 requirement is independent of its role during cell death, and independent of its expression on myeloid cells. However, Panx1 expression on T cells was both necessary and sufficient to control inflammation during airway disease. Mechanistically, we demonstrate that Panx1 is playing a non-cell autonomous role important for T_{reg} -mediated suppression of T_{eff} cell proliferation both *in vitro* and *in vivo*. The defective suppression that results when Panx1 is absent from the T_{reg} - T_{eff} cell interface was due to a lack of extracellular ATP as T_{reg} -mediated suppression could be rescued by supplementing back ATP. Overall, we describe a niche-specific role for Panx1-dependent eATP in mediating the optimal suppressive capacity during the T_{reg} - T_{eff} cell communication axis, which in turn is important for the proper control of inflammation during allergic airway inflammation.

3.3. Materials and methods

3.3.1. Mice

C57BL/6J mice were ordered from Jackson Laboratories. $Panx1^{fl/fl}$ and $Panx1^{-/-}$ mice have been described previously (Poon et al., 2014a). $Panx1^{fl/fl}$ mice were crossed to Cd4-Cre (Taconic), Foxp3-Cre (provided by Dr. Ulrike Lorenz), or Cx3cr1-Cre (Jackson) mice to generate knockout of Panx1 specifically in all T cells, T regulatory cells, or the myeloid lineage, respectively. Panx1-transgenic ($Panx1^{Tg}$) mice were generated as described below. For *in vivo* experiments, female and male mice aged 8 weeks to 12 weeks were used. All procedures and protocols were approved by the Institutional Animal Care and Use Committee (IACUC) at the University of Virginia.

3.3.2. Generation of Panx1-transgenic mice

Flag-tagged Panx1cDNA were cloned into previously characterized CAG-STOP-eGFP-ROSA26TV (CTV) vector containing a chicken actin promoter, a floxed NEO-STOP cassette, and an IRES-eGFP (Xiao et al., 2007). CTV-Panx1Tg vector (25 μ g) was linearized using the restriction enzyme SgfI (Promega) prior to transfection into C57BL/6 embryonic stem cells (JM8A3, KOMP) via electroporation (BTX ElectroSquarePorator). Electroporated cells were plated on mitomycin-treated MEF (Millipore) cells and incubated for 48 hours after which ES cells were selected using Geneticin (G418)(Gibco) at 200mg ml⁻¹. Resistant clones were picked and expanded before being harvested for analysis and storage. Southern Blot analysis and qPCR was used to determine homologous recombination in the *Rosa26* locus. Panx1Tg and eGFP expression were confirmed after transfection of Cre recombinase using an aliquot of the selected ES cells. Selected clones were injected into blastocysts and implanted into pseudopregnant females for generation

of chimeric mice. The chimeric mice were then bred to C57BL/6J to determine germline transition and were subsequently backcrossed several generations to obtain a pure C57BL/6J background. $Panx1^{Tg}$ mice (which do not express the $Panx1$ transgene until crossed to a Cre mouse line) were further bred to global $Panx1^{-/-}$ mice in order to be able to re-express $Panx1$ on a knockout background. $Panx1^{-/-} Panx1^{Tg}$ mice were then bred to $Panx1^{-/-} Cd4-Cre$ mice to specifically express $Panx1$ only in CD4 expressing cells within the mouse.

3.3.3. HDM-induced allergic airway inflammation

Mice were primed intranasally with 10 μ g of low endotoxin house dust mite extracts (HDM)(Indoor Biotechnologies) on days 0, 2, and 4 and then challenged intranasally on days 10, 12, and 14 (Juncadella et al., 2013). Mice were harvested and analyzed for allergic airway inflammation 24-36 hours after the last challenge. Bronchoalveolar lavage (BAL) was performed via delivery of 1.0 ml of PBS intratracheally through a canula. BAL fluid was centrifuged and supernatants were frozen at -80°C for subsequent cytokine analysis via Luminex MAGPIX at the University of Virginia Flow Cytometry Facility. Collected cells were treated with RBC lysis (Sigma-Aldrich), washed, and stained for surface markers to distinguish cell populations. For immunophenotyping, harvested lungs were placed in HBSS media containing Ca^{2+}/Mg^{2+} (Gibco) and type 2 collagenase (Worthington Biochemicals Corporation). Lungs were then minced and incubated at 37°C for an hour with intermittent pipetting every 15 minutes to create a single cell suspension. Homogenates were passed through a 70 μ m filter, treated with RBC lysis buffer, washed and resuspended in PBS with 1% BSA for surface immunostaining.

3.3.4. Immunostaining and cell count

Collected BAL cells and lung single cell suspension were stained for macrophages, T cells, neutrophils, eosinophils, and monocytes using: CD11c, CD11b, Ly6G, F4/80, CD3, CD4, CD8, CD44, CD69, Foxp3. For intracellular Foxp3 staining cells were fixed and permeabilized using the eBioscience Foxp3 Transcription Factor Staining Buffer Set according to manufacturers' protocol.

3.3.5. Lung histology and immunohistochemical staining

For lung hematoxylin and eosin staining, mice were perfused through the heart with PBS. A canula was then inserted into the trachea and the lungs were gently inflated with 10% formalin at a constant fluid pressure of 25cm. The trachea was then tied, cut, and the lungs were removed and placed in 10% formalin for overnight fixation. After 24 hours the lungs were placed into 70% ethanol. Paraffin embedding, sectioning, and H&E staining was performed by the Histology Core at the University of Virginia. Immunohistochemical staining for cleaved caspase 3 was performed by the University of Virginia Biorepository and Tissue Research Facility (BTRF). Full imaging of the entire lung was performed using the Leica SCN400 at the UVA BTRF. Cleaved caspase 3 quantification was performed by counting all positive stained cells in the left lobe of the mouse lung by a blinded experimentalist. H&E clinical scoring was performed by Dr. Kenneth Tung who was blinded to all experimental conditions and genotypes.

3.3.6. Quantitative RT-PCR

Total RNA was extracted from isolated tissues or cells using NucleoSpin RNA (Macherey-Nagel) and cDNA was generated using Quantitect Reverse Transcriptase kit (Qiagen) according to manufacturers' protocols. Quantitative expression of Panx1, Panx2,

Panx3, and GAPDH was performed using Taqman probes (Applied Biosystems) and the StepOnePlus Real Time PCR system (ABI).

3.3.7. Western Blotting

Total protein extracts were prepared from specified isolated tissue or cells using RIPA lysis buffer supplemented with protease inhibitors (Calbiochem). Equal amounts of protein were loaded onto TGX-precast gels (Bio-Rad), subjected to SDS-PAGE, and transferred to PVDF membrane blots using the Transblot Turbo Transfer System (Bio-Rad). Panx1 (clone : D9M1C, Cell Signaling Technologies), p-ERK, and ERK was used for immunoblotting at 1:1000 at 4°C overnight. Actin-HRP (clone : AC15, Sigma) was used as a loading control. PVDF blots were then exposed using Western Lightning Plus ECL kit (Perkin-Elmer) and chemiluminescence was detected using the ChemiDoc Touch imaging system (Bio-Rad).

3.3.8. CD4 T cell Isolation

Spleens were harvested from 8-12-week-old mice, homogenized, and run through 70µm filters, and treated with RBC lysis buffer. Single cells suspensions were resuspended in MACS buffer and CD4 T_{eff} and T_{reg} cells were isolated using the CD4⁺ CD25⁺ Regulatory T cell Isolation kit (Miltenyi Biotech), according to manufacturers' protocol. Briefly, splenocytes were incubated with an antibody cocktail to negatively select via magnetic separation CD4 T cells, followed by an additional positive selection to separate CD4⁺CD25⁻ T_{eff} from CD4⁺CD25⁺ T_{reg} cells. Isolation efficiency and purity was analyzed via flow cytometry on the Attune Nxt Flow Cytometry.

3.3.9. Apoptosis measurement

BALF was harvested as indicated above and cells were stained with annexin V-Pacific blue and 7AAD in annexin V binding buffer for 15 minutes at room temperature. Samples were then diluted two-fold with binding buffer, put on ice and analyzed on the Canto I. Apoptotic cells were characterized as AV+7AAD- and secondary necrotic cells were characterized as AV+7AAD+ cells.

3.3.10. T cell Activation and Suppression Assays

Isolated T_{eff} cells were incubated with 2.5µg/ml of α-CD3 and 1.25µg/ml α-CD28 to induce T cell activation. For downstream TCR analysis T cells were incubated for indicated amount of time at 37°C. Cells were then spun down, flash frozen and lysed for western blot analysis of downstream TCR signaling proteins. Upregulation of T cell activation markers CD69, CD44, CD25, and CD62L were measured after T cells were incubated with α-CD3 and α-CD28 for indicated amount of time. Cells were then stained for respective markers on ice and run for flow cytometric analysis on the BD FACS Canto. To measure T cell proliferation, T_{eff} cells were stained with 5µM CFSE (Invitrogen) according to manufacturers' protocol prior to activation and CFSE dilution was measured via flow cytometry. For suppression assays different ratios of T_{eff}: T_{reg} cells were incubated for 4 days after α-CD3 and α-CD28 treatment and extent of CFSE dilution was measured. Where indicated ATP was added to cultures at 10µM on Day 0.

3.3.11. Statistical analysis

Statistical significance was determined using GraphPad Prism 7, using unpaired Student's two-tailed t-test (paired and unpaired), one-way ANOVA, or two-way ANOVA according to test requirements. Grubbs' Outlier Test was used to determine outliers, which were excluded from final analysis. A p value of <.05 (indicated by one asterisk), <.01

(indicated by two asterisks), $<.001$ (indicated by three asterisks), or $<.0001$ (indicated by four asterisks) were considered significant.

3.4. Results

3.4.1. Global *Panx1* knockout mice exhibit increased airway inflammation

When we queried human datasets to examine expression of the channel in healthy and asthmatic patients, we discovered that *Panx1* expression was reduced in the peripheral blood mononuclear cells (PBMCs) of allergic asthmatic children relative to healthy controls (**Figure 3.1a**), potentially suggesting the involvement of the channel during disease (Raedler et al., 2015). In order to investigate the importance of *Panx1* in AAI, we used a mouse model of house-dust mite (HDM)-induced allergic airway inflammation, a pathologically relevant allergen, with sensitization in developed countries of 20-40% frequently reported (Calderón et al., 2015; Gandhi et al., 2013; Gold et al., 2015). After two weeks of HDM treatment (a priming and a challenge phase) (**Figure 3.1b**), wild-type mice (*Panx1*^{+/+}) developed the typical T_H2-mediated inflammatory response characterized by eosinophils and CD4⁺ T cell recruitment into the lungs (**Figures 3.1c, d**). Of note, alveolar macrophage numbers did not change in this model (**Figure 3.1e**). Interestingly, global *Panx1* deficient mice (*Panx1*^{-/-}) exhibited exacerbated disease severity as measured by increased immune cell infiltration into the lungs (**Figures 3.1c, d**), including increased activated T cell numbers (**Figure 3.1f**), and greater disease pathology assessed by H&E (**Figures 3.1g, h and Figure 3.2a**). These data suggest a regulatory role for *Panx1* during airway inflammation as loss of the channel results in exacerbated inflammation.

Panx1 has been shown to be involved in a variety of cellular process such as mediating macrophage recruitment to the site of cell death via the release of ATP (Chekeni et al., 2010). Prompt removal of apoptotic cells is essential as uncleared dying cells can undergo secondary necrosis and cause excessive inflammation (Juncadella et al., 2013;

Morioka et al., 2019). To determine whether loss of Panx1 resulted in increased numbers of uncleared dying cells, we examined cleaved caspase-3 staining in lung tissue sections and Annexin-V/7AAD staining in the bronchoalveolar lavage fluid (BALF) from wild-type or *Panx1*^{-/-} mice. While HDM treatment did increase the number of apoptotic cells relative to healthy controls, *Panx1*^{-/-} mice did not have any further increase in the number of apoptotic or necrotic cells present in the airways (**Figure 3.3a-d**). This suggested that the role of Panx1 during AAI may be independent of cell death and clearance.

Figure 3.1: *Panx1*^{-/-} mice exhibit increased inflammation during HDM-induced AAI.

a, Panx1 expression on PBMC of healthy or allergic asthmatic children (ctrl $n=13$, a.asthmatics $n=14$) (* $p=0.015$). **b**, Schematic representation for the mouse model of house dust mice induced allergic airway inflammation. **c**, Representative flow plots showing the extent of eosinophil and CD4 T cell infiltration into the bronchoalveolar space (PBS-*Panx1*^{+/+} $n=4$, PBS-*Panx1*^{-/-} $n=5$, HDM-*Panx1*^{+/+} $n=19$, HDM-*Panx1*^{-/-} $n=21$) and lung (PBS-*Panx1*^{+/+} $n=3$, PBS-*Panx1*^{-/-} $n=3$, HDM-*Panx1*^{+/+} $n=22$, HDM-*Panx1*^{-/-} $n=20$), respectively, in wild-type (*Panx1*^{+/+}) and global *Panx1*^{-/-}. **d-f**, Absolute cellularity of eosinophils (**d**, left) (* $p=0.017$), CD4 T cells (**d**, right) (** $p=0.008$), alveolar macrophages (**e**), and activated CD69+ CD4 T cells (**f**) (* $p=0.033$). **g**, Representative H&E lung histology images of wild-type ($n=13$) and global *Panx1*^{-/-} ($n=8$) mice during HDM challenge. **h**, Disease severity score as assessed by a pathologist blinded to genotypes (* $p=0.05$). Unpaired student's t-test.

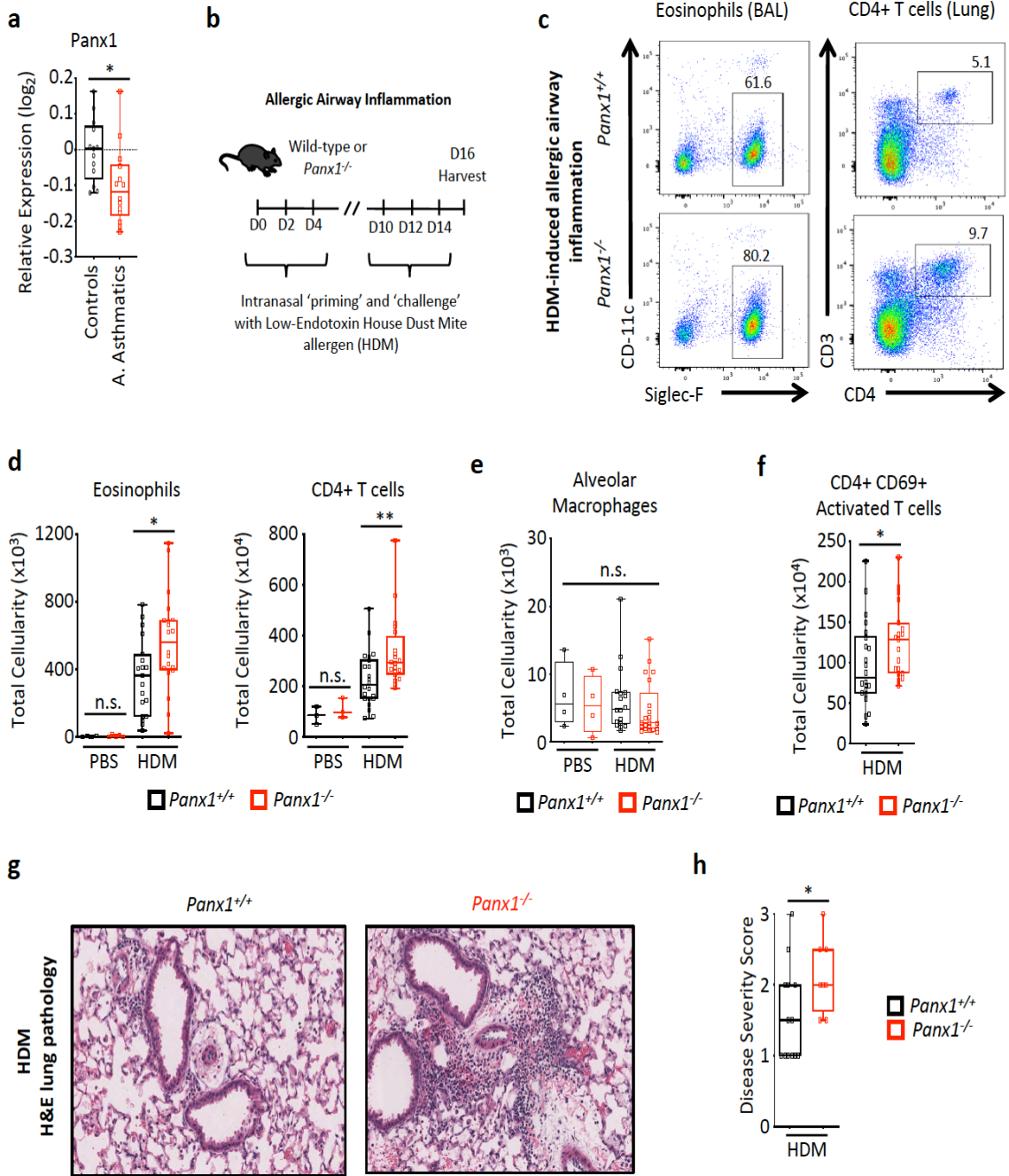


Figure 3.2: *Panx1*^{-/-} mice exhibit increased histological disease severity.

a, Representative H&E lung histology images of wild-type and global *Panx1*^{-/-} mice during HDM challenge or control PBS treatment.

a

H&E lung pathology

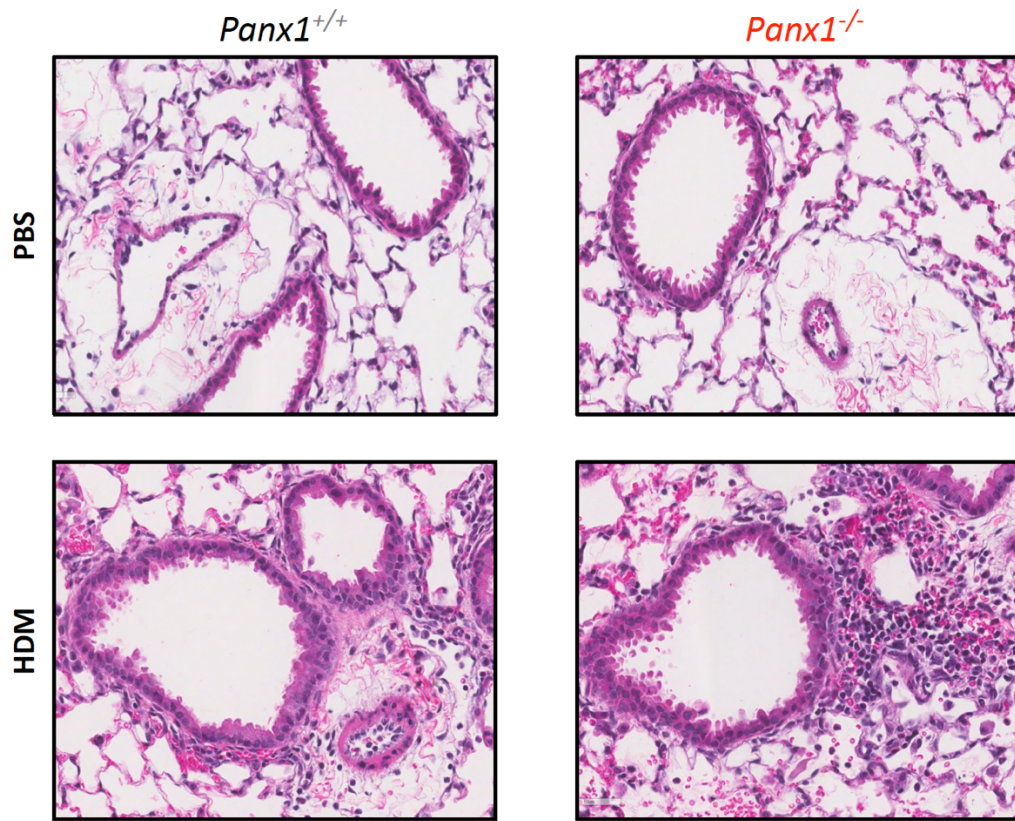
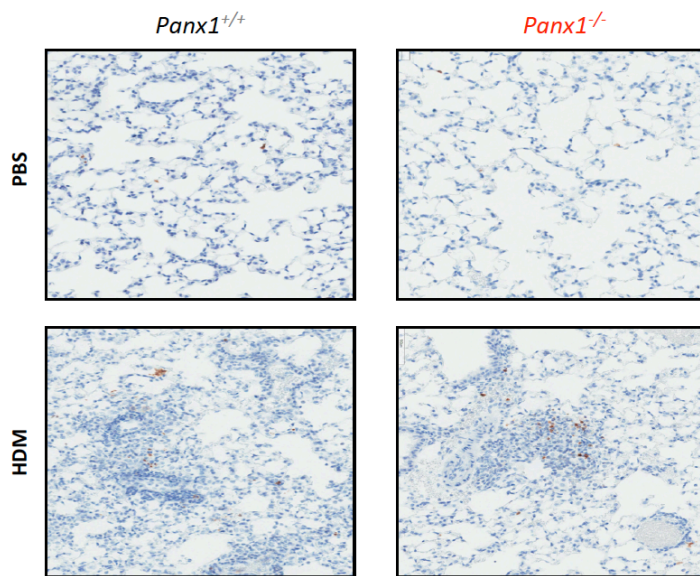
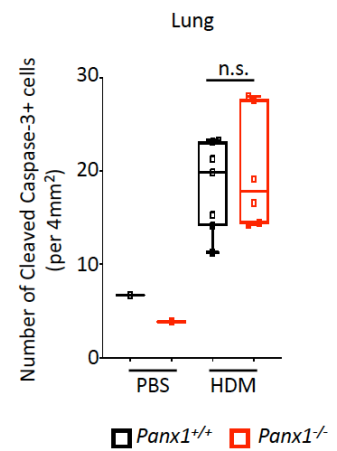
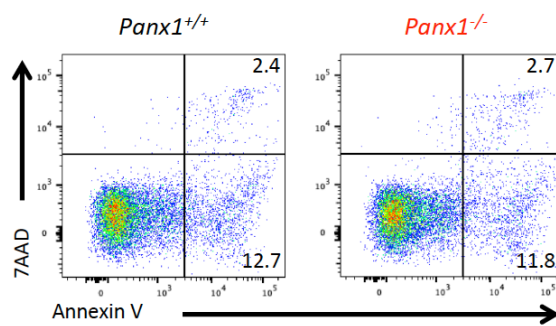
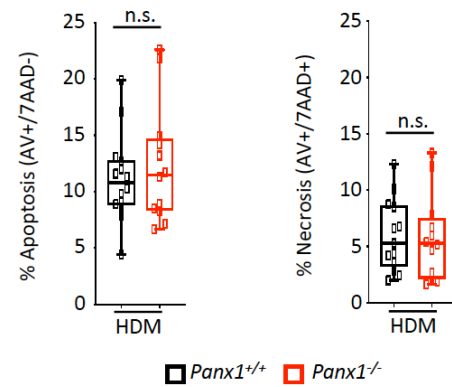


Figure 3.3: *Panx1*^{-/-} mice do not contain increased number of apoptotic cells.

a, Representative cleaved caspase-3 staining in lungs of wild-type and global *Panx1*^{-/-} mice during HDM challenge or control PBS treatment. **b**, Quantitative analysis of the number of cleaved caspase-3 positive cells in wild-type and global *Panx1*^{-/-} lungs (PBS-*Panx1*^{+/+} *n*=1, PBS-*Panx1*^{-/-} *n*=1, HDM-*Panx1*^{+/+} *n*=8, HDM-*Panx1*^{-/-} *n*=6). **c**, Representative flow cytometry plots assessing the extend of cell death (Annexin V and 7AAD) in the BALF from wild-type and global *Panx1*^{-/-} mice. **d**, Quantitative analysis of apoptosis (left) and necrosis (right) in wild-type and global *Panx1*^{-/-} BALF (HDM-*Panx1*^{+/+} *n*=14, HDM-*Panx1*^{-/-} *n*=12). Unpaired student's t-test.

a**Cleaved caspase-3 staining****b****c****Bronchoalveolar Lavage****d****Bronchoalveolar Lavage**

3.4.2. Panx1 expression on T cells is necessary to control inflammation during AAI

We subsequently focused on immune cells to further investigate the role of Panx1 as the human data (**Figure 3.1a**) demonstrated decreased Panx1 expression in the PBMCs of asthmatic patients. Gene expression analysis using the Immgen database across multiple immune cell types identified T cells as the highest expressers of Panx1 (**Figure 3.4a**). We confirmed that primary splenic naïve T cell Panx1 expression was >100 fold higher than macrophages. Furthermore, T cells only express Panx1, while macrophages express both Panx2 and Panx3 (**Figure 3.5a**). Although expression of Panx2 or Panx3 did not change upon global Panx1 deletion, these isoforms have been shown to functionally compensate for loss of Panx1 under certain settings (Lohman and Isakson, 2014). Additionally, Panx1 expression analysis of total lung tissue demonstrated that lung tissue also expressed high levels of Panx2 in addition to Panx1 (**Figure 3.4b**). In view of the high expression of Panx1 on T cells, their inability to express other pannexin family proteins that could possibly compensate for loss of Panx1, and the central role of CD4 T cells in mediating allergic airway inflammation (Agrawal and Shao, 2010; Muehling et al., 2017), we examined whether loss of Panx1 specifically on T cells was responsible for the increased disease severity seen in the global *Panx1*^{-/-} mice.

In order to test the role of Panx1 on T cells during allergic airway inflammation, we crossed *Panx1*^{fl/fl} mice to *Cd4-Cre* mice (*Panx1*^{fl/fl} *Cd4-Cre*⁺) to delete Panx1 on most (if not all) T cells (**Figure 3.5b**). The severity of HDM-induced airway inflammation in *Panx1*^{fl/fl} *Cd4-Cre*⁺ mice phenocopied the global *Panx1*^{-/-} mice, as these mice exhibited increased eosinophil and CD4⁺ T cell infiltration into the lungs relative to *Panx1*^{fl/fl} *Cd4-Cre*⁻ littermate controls (**Figures 3.5c, d**). Increased inflammation was not dependent on

Cre expression/toxicity (**Figure 3.6a**). *Panx1^{fl/fl} Cd4-Cre⁺* mice also displayed greater numbers of activated T cells and higher levels of IL-4 in the bronchoalveolar lavage fluid, a critical cytokine dictating the T_H2 response during allergic inflammation (Steinke and Borish, 2001)(**Figures 3.5e, f**). In accordance with increased inflammation in the lungs, *Panx1^{fl/fl} Cd4-Cre⁺* exhibited worse lung pathology than wild-type littermate controls as measured by disease severity score (**Figure 3.5g**). As an additional control, we specifically deleted Panx1 in the mononuclear phagocyte population using *Cx3cr1-Cre* (**Figure 3.6b**). We were unable to detect any difference in the extent of inflammation between *Panx1^{fl/fl} Cx3cr1-Cre⁺* and *Panx1^{fl/fl} Cx3cr1-Cre⁻* mice, therefore, excluding a role for Panx1 expressed in macrophages during allergic airway inflammation (**Figures 3.6c, d**). These data highlight the necessity and specificity of Panx1 on T cells to limit disease severity during AAI.

Figure 3.4: Panx1 gene expression in different cell types.

a, Gene expression data from the Immgen database assessing the relative expression of Panx1 across several immune cell types. **b**, qPCR analysis of Panx1, Panx2, and Panx3, expression in wild-type and global *Panx1*^{-/-} mice in total lung tissue. (*Panx1*^{+/+} *n*=4, *Panx1*^{-/-} *n*=3).

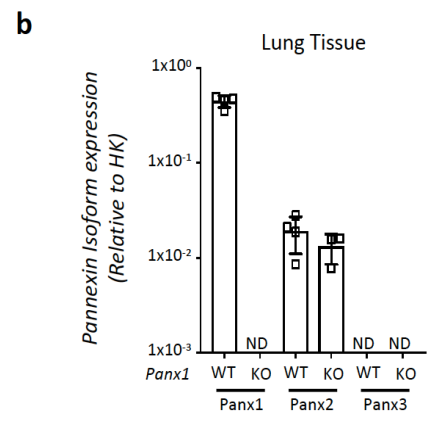
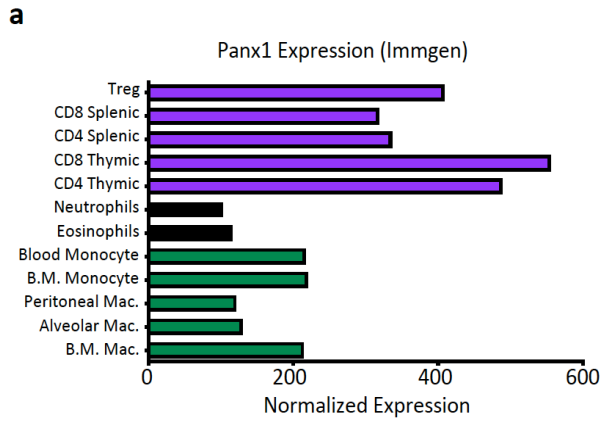


Figure 3.5: Panx1 expression on T cells limits inflammation during disease.

a, Panx1 expression on mouse CD4 T cells and mouse bone-marrow derived macrophages in wildtype ($n=4$) or $Panx1^{-/-}$ ($n=3$) mice. **b**, Schematic representation of $Cd4-cre$ mediated Panx1 deletion and efficiency of knockout. **c**, Representative flow plots showing the extent of eosinophil and CD4 T cell infiltration into the bronchoalveolar space (PBS– $Panx1^{fl/fl}Cd4-cre^{-}$ $n=2$, PBS– $Panx1^{fl/fl}Cd4-cre^{+}$ $n=3$, HDM– $Panx1^{fl/fl}Cd4-cre^{-}$ $n=13$, HDM– $Panx1^{fl/fl}Cd4-cre^{+}$ $n=11$) and lung (PBS– $Panx1^{fl/fl}Cd4-cre^{-}$ $n=3$, PBS– $Panx1^{fl/fl}Cd4-cre^{+}$ $n=4$, HDM– $Panx1^{fl/fl}Cd4-cre^{-}$ $n=15$, HDM– $Panx1^{fl/fl}Cd4-cre^{+}$ $n=13$), respectively. **d-f**, Absolute cellularity of eosinophils (**d**, left) (** $p=0.009$), CD4 T cells (**d**, right) ($*p=0.012$), activated CD69+ CD4 T cells (**e**) ($*p=0.032$), and BALF IL-4 cytokine levels (**f**) ($*p=0.034$). **g**, Representative H&E lung histology images of $Panx1^{fl/fl}Cd4-cre^{-}$ ($n=12$) and $Panx1^{fl/fl}Cd4-cre^{+}$ ($n=14$) mice during HDM challenge. Disease severity score as assessed by a pathologist blinded to genotypes ($*p=0.029$). Unpaired student's t-test.

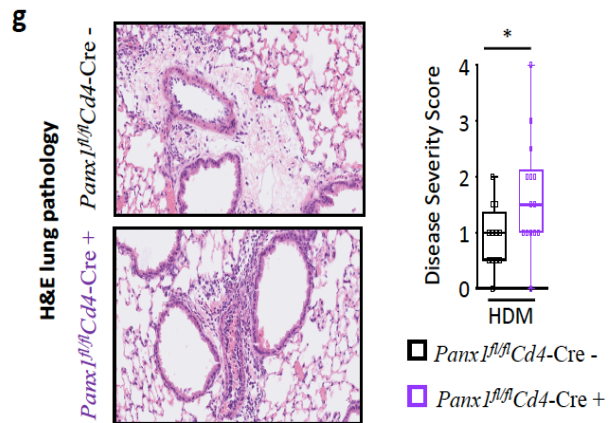
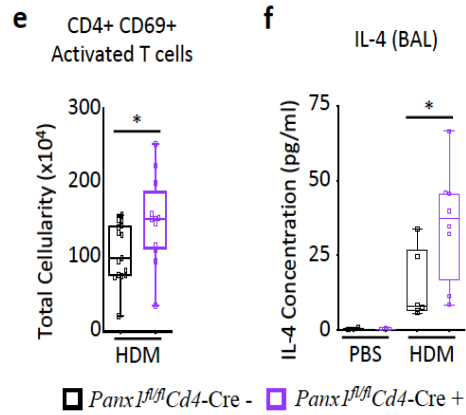
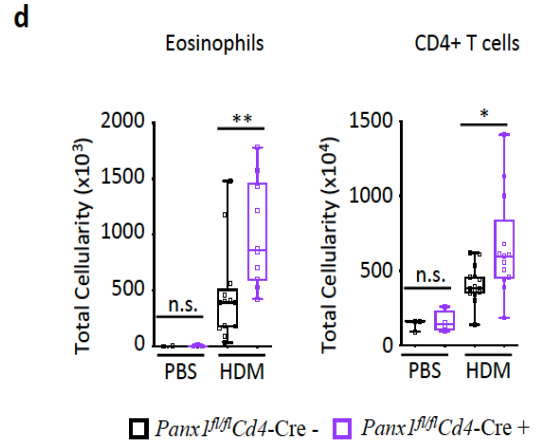
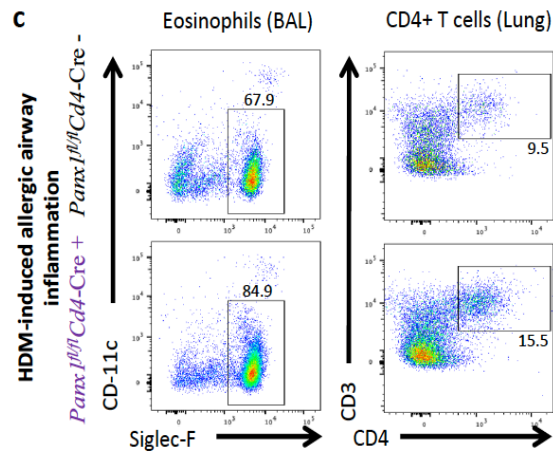
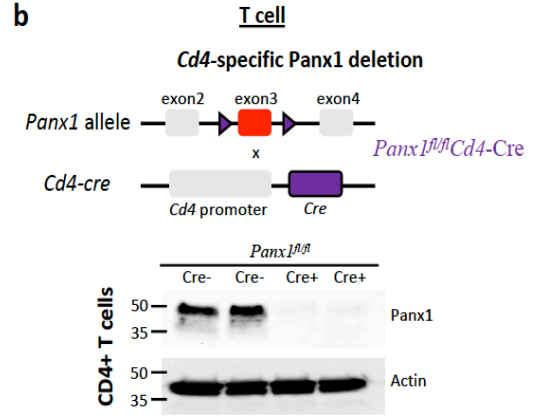
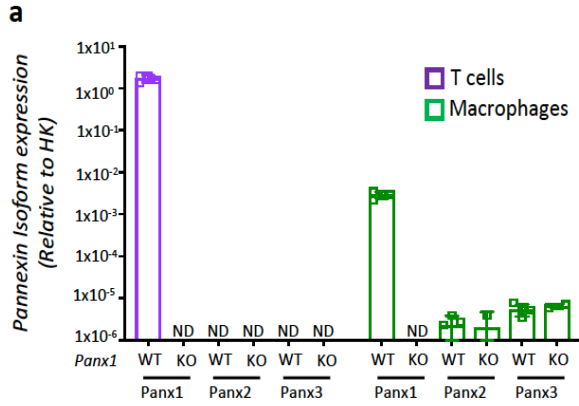
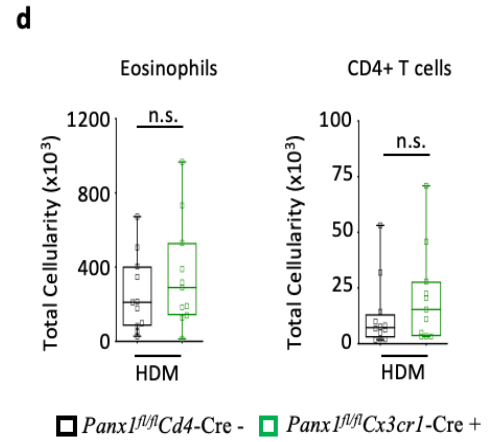
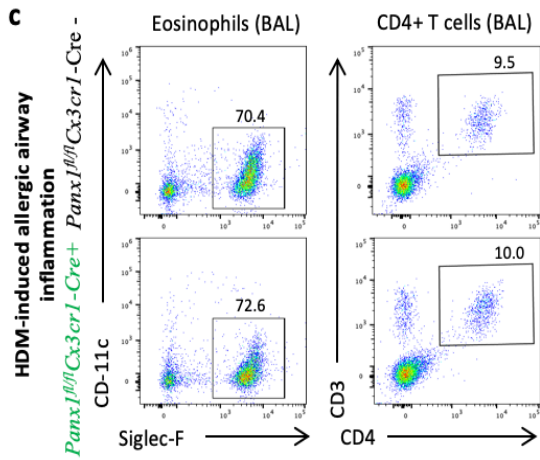
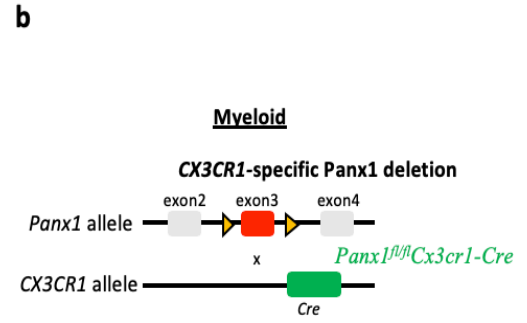
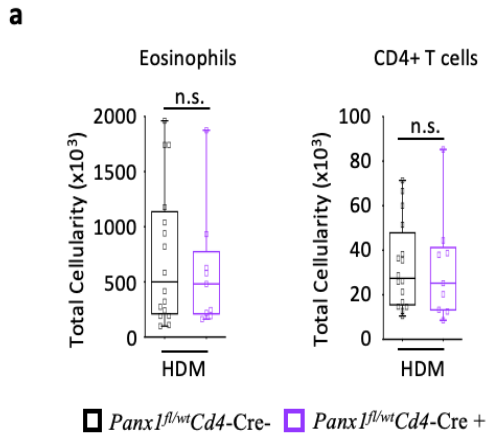


Figure 3.6: Cre expression or Panx1 deletion using *Cx3cr1-cre* does not affect inflammation during AAI.

a, Absolute cellularity of eosinophils (left) and CD4 T cells (right) in wildtype mice with or without *Cd4-cre* expression after HDM challenge (*Panx1^{fl/wt}Cd4-cre⁻* *n*=16, *Panx1^{fl/wt}Cd4-cre⁺* *n*=9). **b**, Schematic representation of *Cx3cr1-cre* mediated Panx1 deletion and efficiency of knockout. **c**, Representative flow plots showing the extent of eosinophil and CD4 T cell infiltration into the bronchoalveolar space after HDM challenge (*Panx1^{fl/fl}Cx3cr1-cre⁻* *n*=12, *Panx1^{fl/fl}Cx3cr1-cre⁺* *n*=11). **d**, Absolute cellularity of eosinophils (left) and CD4 T cells (right). Unpaired student's t-test.



3.4.3. Panx1 does not play a cell intrinsic role during T cell activation or on T_{reg} cells

Panx1 has been reported to play a role in T cell activation (Schenk et al., 2008), however, previous work used non-specific inhibitors instead of genetic mice models, as *Panx1*^{-/-} mice were only subsequently developed (Qu et al., 2011). To more directly address the cell intrinsic role of Panx1 during T cell activation, we isolated naïve CD4⁺ T effector cells (T_{eff}) (CD4⁺CD25⁻) from wild-type and *Panx1*^{-/-} mice and treated them with anti-CD3 and anti-CD28 to track their activation across several parameters. We analyzed expression of the activation markers CD69, CD44, and CD25 and the downregulation of CD62L over a 48-hour period and were unable to detect any differences between wild-type and *Panx1*^{-/-} T_{eff} cells (**Figures 3.7a-d**). Additionally, we examined both the immediate downstream TCR signaling via phosphorylation of ERK (**Figure 3.8a**) and the proliferative capacity of wild-type and *Panx1*^{-/-} CD4⁺ T_{eff} cells (**Figure 3.8b**). Based on our data and under the conditions tested, we were unable to notice any differences between genotypes, suggesting that loss of Panx1 on CD4⁺ T_{eff} cells did not intrinsically affect their ability to activate.

It is known that *Cd4-Cre* mediated deletion will also delete floxed genes on T regulatory cells (T_{reg}), suggesting that Panx1 deletion on T_{reg} cells could be responsible for the worsened disease during AAI. In fact, Panx1 is capable of releasing ATP, which can be converted to the anti-inflammatory molecule adenosine via the two ectonucleotides CD39 (which converts ATP/ADP to AMP) and CD73 (which converts AMP to adenosine) (Antonioli et al., 2013). Moreover, T_{reg} cells express very high levels of both CD39 and CD73, hinting that ATP released from Panx1 channels has the potential to be converted to adenosine in the presence of regulatory T cells. Interestingly, T_{reg} cells make up about

~20% of the CD4⁺ T cell population within the lung during airway disease (**Figure 3.9a**), therefore, loss of Panx1 on T_{reg} cells could disrupt their suppressive function and lead to increased inflammation. To address whether loss of Panx1 specifically on T_{reg} cells would recapitulate the exacerbated inflammatory phenotype seen in global *Panx1*^{-/-} and *Panx1*^{fl/fl} *Cd4-Cre*⁺ mice, we generated animals with T_{reg} specific Panx1 deletion using *Foxp3-Cre* (**Figure 3.9b**). Surprisingly, *Panx1*^{fl/fl} *Foxp3-Cre*⁺ mice had a similar extent of immune cell infiltration and disease severity as wild-type mice (**Figures 3.9c, d**), suggesting that loss of Panx1 exclusively on T_{reg} cells had no effect on their ability to control inflammation during AAI. Consistent with this observation, when we tested *in vitro*, both wild-type or *Panx1*^{-/-} T_{reg} cells were able to comparably suppress the proliferation of wild-type CD4⁺ T_{eff} cells (**Figures 3.10a, b** grey and orange graphs/lines). Overall, Panx1 deletion exclusively on T_{reg} cells did not intrinsically affect their ability to optimally suppress inflammation or T cell proliferation.

Figure 3.7: Panx1 deletion does not intrinsically effect T effector cell activation.

a, Time course expression analysis of the CD69 activation marker in wild-type and *Panx1*^{-/-} CD4 T effector cells (CD4⁺ CD25⁻)(right) and representative FACS histograms at t=0 or t=12 hours after CD3/CD28 mediated T cell activation (left). **b**, Time course expression analysis of the CD62 naïve T cell marker in wild-type and *Panx1*^{-/-} CD4 T effector cells (CD4⁺ CD25⁻)(right) and representative FACS histograms at t=0 or t=12 hours (left). **c**, Time course expression analysis of the CD25 activation marker in wild-type and *Panx1*^{-/-} CD4 T effector cells (CD4⁺ CD25⁻)(right) and representative FACS histograms at t=0 or t=12 hours (left). **d**, Time course expression analysis of the CD44 activation marker in wild-type and *Panx1*^{-/-} CD4 T effector cells (CD4⁺ CD25⁻)(right) and representative FACS histograms at t=0 or t=12 hours (left). (n=3) Two-way ANOVA.

a

0 hr *Panx1^{fl/fl}Cd4-Cre -* *Panx1^{fl/fl}Cd4-Cre +*
 12 hr *Panx1^{fl/fl}Cd4-Cre -* *Panx1^{fl/fl}Cd4-Cre +*

Panx1^{fl/fl}Cd4-Cre - *Panx1^{fl/fl}Cd4-Cre +*

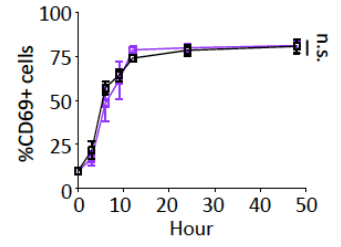
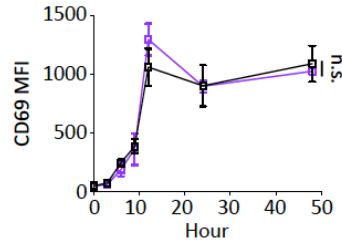
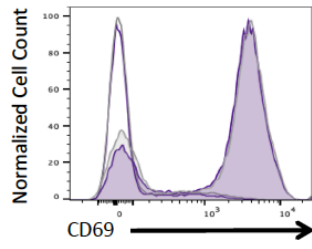
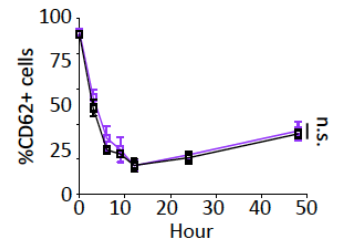
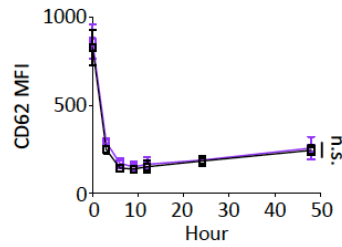
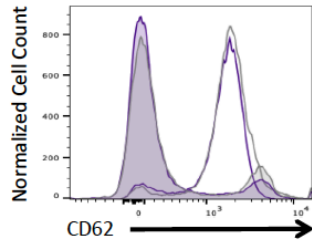
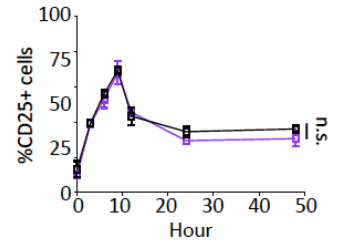
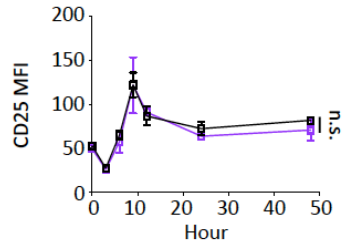
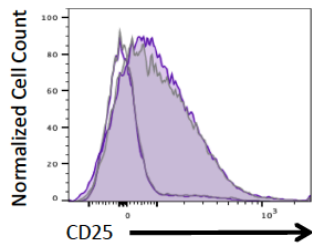
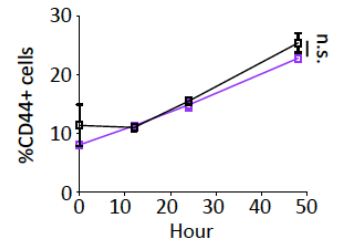
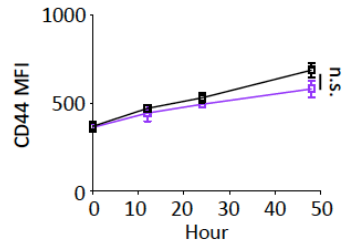
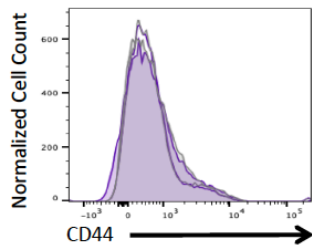
**b****c****d**

Figure 3.8: Panx1 deletion does not intrinsically affect CD4 T effector cell downstream TCR signaling or proliferation.

a, Western blot time course analysis of downstream TCR signaling via p-ERK in wild-type and *Panx1*^{-/-} CD4 T effector cells (CD4⁺ CD25⁻) (right) and quantitative analysis after CD3/CD28 mediated T cell activation (right). **b**, Representative FACS histograms of Cell Trace Violet dilution as a measurement of T cell proliferation after CD3/CD28 mediated activation in wild-type and *Panx1*^{-/-} CD4 T effector cells (CD4⁺ CD25⁻) (left). Normalized proliferative index between wild-type (*n*=9) and *Panx1*^{-/-} (*n*=10) CD4 T effector cells. Data are mean ± s.d. Unpaired student's t-test.

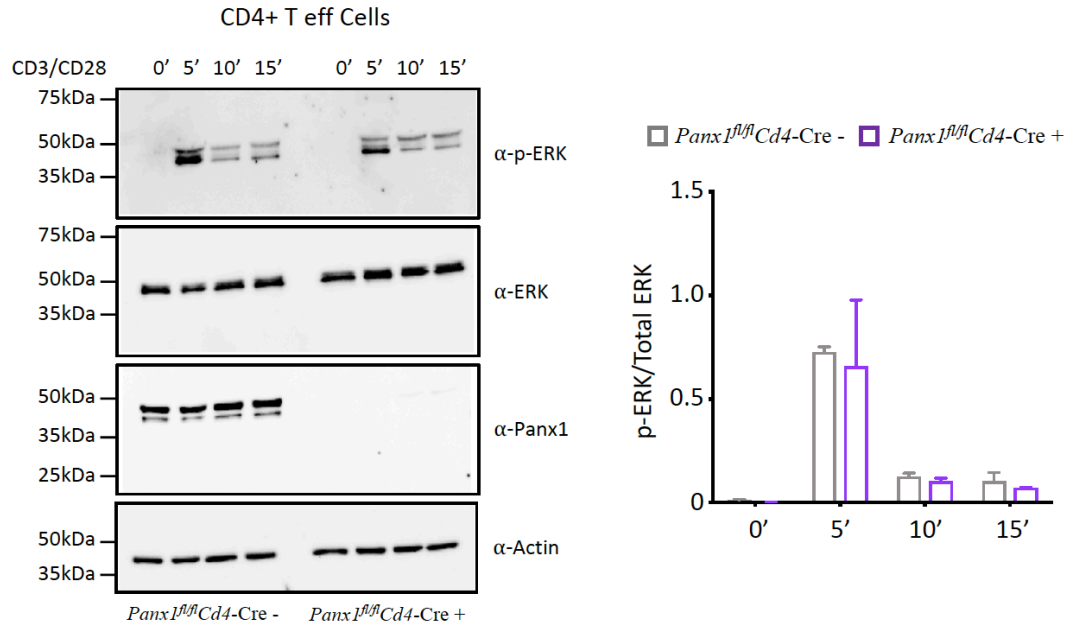
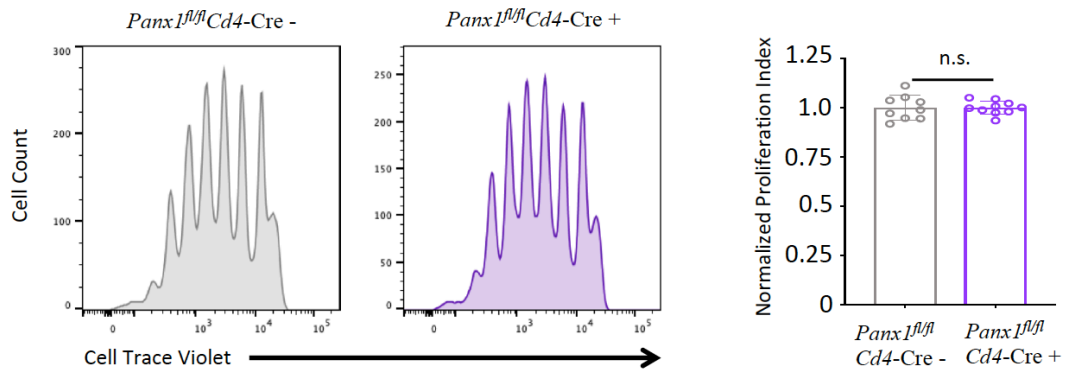
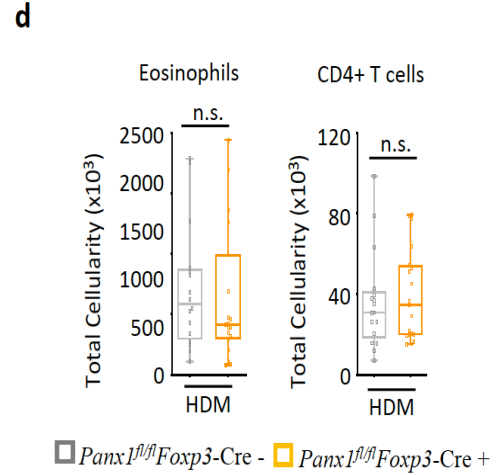
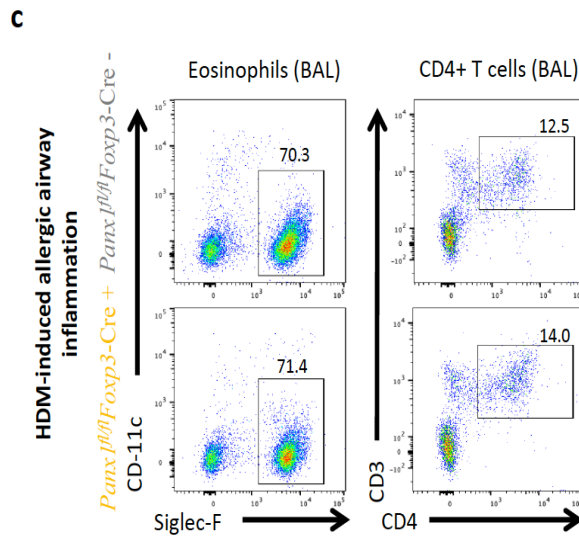
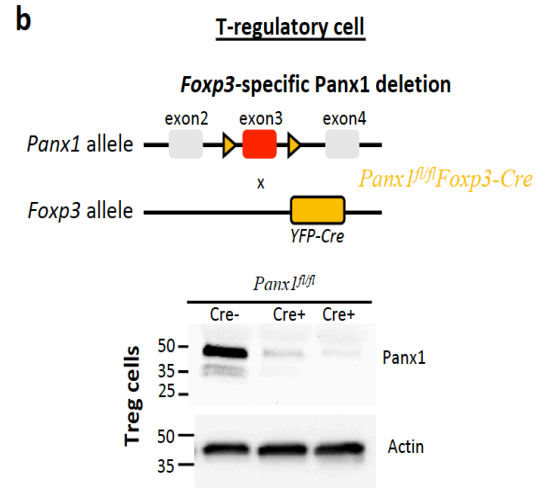
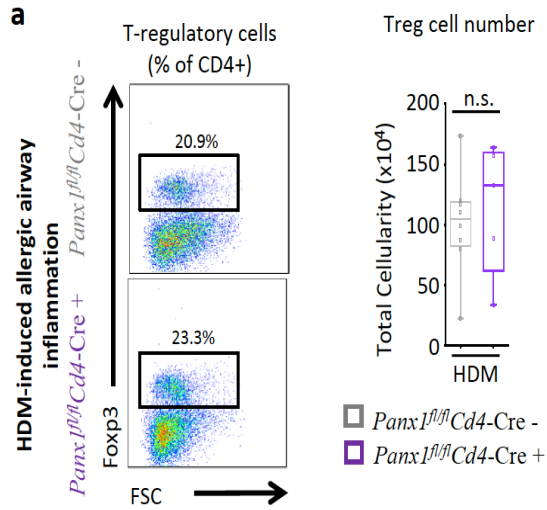
a**b**

Figure 3.9: T regulatory cell Panx1 deletion does not affect inflammation during airway inflammation.

a, Representative flow plots showing the number of Treg cells in the lung during AAI (*Panx1^{fl/fl}Cd4-cre⁻* $n=8$, *Panx1^{fl/fl}Cd4-cre⁺* $n=5$) (left). Absolute cellularity of Treg cells (right). **b**, Schematic representation of *Foxp3-cre* mediated Panx1 deletion and efficiency of knockout. **c**, Representative flow plots showing the extent of eosinophil and CD4 T cell infiltration into the bronchoalveolar space after HDM challenge (*Panx1^{fl/fl}Foxp3-cre⁻* $n=17$, *Panx1^{fl/fl}Foxp3-cre⁺* $n=19$). **d**, Absolute cellularity of eosinophils (left) and CD4 T cells (right). Unpaired student's t-test.



3.4.4. Intercellular T cell communication via Panx1 optimizes the suppressive capacity of T_{reg} cells

Panx1 deletion on T_{reg} cells (via *Foxp3-cre*) did not result in increased inflammation during allergic airway disease, however, Panx1 deletion on both T_{eff} and T_{reg} cells (via *Cd4-cre*) did. Given that Panx1 is responsible for the extracellular release of ATP, the channel could be functioning through a cell extrinsic communication mechanism between these two cells to limit inflammation. Of note, it has been shown that during antigen presentation by dendritic cells (DC) to T_{eff} cells, T_{reg} cells also ‘dock’ to the same DC. This is thought to occur in order to simultaneously inhibit T_{eff} activation and control excessive inflammation (Liu et al., 2015). Therefore, a non-cell autonomous mechanism for Panx1 at the T_{reg}-T_{eff} cell microenvironmental interface may be important for proper control of T_{eff} activation. To determine if Panx1 expression on either T_{eff} or T_{reg} is sufficient to mediate optimal suppression and if loss of Panx1 on both cells results in the reduced suppressive capacity of T_{reg} cells, we performed combinatorial suppression assays with either wild-type or Panx1^{-/-} T_{eff} and T_{reg} cells. Suppression assays with wild-type T_{eff} (WT-T_{eff}) and wild-type T_{reg} (WT-T_{reg}) resulted in optimal suppression (**Figures 3.10a, b** grey). Interestingly, during suppression assays when Panx1 was present on only T_{eff} cells or only T_{reg} cells (WT-T_{eff}/Panx1^{-/-}T_{reg} or Panx1^{-/-}T_{eff}/WT-T_{reg}), suppression was not significantly affected (**Figures 3.10a, b** orange and red). However, during suppression assays in which Panx1 was deleted on both cells (Panx1^{-/-}T_{eff}/Panx1^{-/-}T_{reg}), the suppressive capacity of T_{reg} cells was diminished and the T_{eff} cells proliferated to a greater extent (**Figures 3.10a, b** purple). These data suggest that Panx1 is playing a non-cell autonomous role during T cell suppression and when Panx1 is absent from the T_{eff}-T_{reg} communication interface,

uncontrolled proliferation of T cells and detrimental inflammation can occur (**Figure 3.10c**).

To confirm this was occurring *in vivo* during allergic airway inflammation, we tracked CD4⁺ T cell proliferation after HDM challenge in our *Panx1^{fl/fl} Cd4-Cre⁺* mice, in which Panx1 is deleted from both T_{eff} and T_{reg} populations. At 12 hours after the first challenge dose of HDM (day 10 of the model) mice received intraperitoneal injection of the thymidine analog, 5'-ethynyl-2'-deoxyuridine (EdU). On Day 11, 24 hours after the first HDM challenge (12 hours after EdU injection), lungs were harvested and the extent of EdU incorporation was analyzed as a measure of T cell proliferation (**Figures 3.11a, b**). Similar to *in vitro* experiments, lack of Panx1 on T cells resulted in increased CD4⁺ T cell proliferation (and total CD3⁺ T cell proliferation), when compared to wild-type littermate controls (**Figures 3.10d, e** and **Figure 3.11c**), suggesting inefficient suppression by T_{reg} cells during disease.

The non-cell autonomous role of Panx1 during T cell activation and the known role of Panx1 in the release of ATP, even during non-apoptotic conditions (Billaud et al., 2015), led us to examine whether loss of extracellular ATP in *Panx1^{-/-}* settings was mechanistically responsible for the lack of suppression in knockout mice. As mentioned above, extracellular ATP can be converted to the immunosuppressive molecule adenosine via CD39 and CD73, which are both highly expressed on T_{reg} cells (Dwyer et al., 2007). Therefore, without Panx1, lack of eATP could hinder the optimal suppressive capacity of T_{reg} cells. As demonstrated previously, lack of Panx1 on both T_{eff} and T_{reg} cells resulted in the decreased suppressive function of T_{reg} cells, however, supplementation of ATP to Panx1^{-/-} T cell cultures rescued suppression significantly (**Figure 3.10f**). These data

indicate that loss of Panx1 results in decreased T_{reg} suppressive potential. Supplementation with ATP could partially rescue this phenotype, further implicating the importance of Panx1-dependent eATP for the optimal suppressive function of T_{reg} cells at this immune microenvironment. Importantly, during the T_{eff} and T_{reg} interface, both cells can contribute to the extracellular accumulation of ATP as loss of Panx1 on only one cell type is not sufficient to affect proper suppression.

Figure 3.10: A non-cell autonomous role for Panx1-released extracellular ATP during Treg dependent suppression of T effector cell proliferation.

a, Representative histograms of combinatorial suppression assays with wild-type and *Panx1*^{-/-} T effector and T regulatory cells at indicated cell ratios (left). Individual experimental line plots demonstrating extent of suppression across Teff: Treg cell ratios (right). **b**, Quantitative analysis of suppression across the different cellular combinations ($n=3$) (* $p=0.047$). **c**, Summary of suppressive efficiency in different combinatorial suppression assays. **d**, Representative flow plots and **e**, quantitative analysis of *in vivo* T cell proliferation using Edu incorporation during AAI in *Panx1*^{fl/fl}*Cd4-cre*⁺ ($n=5$) and wild-type littermate controls ($n=6$) (* $p=0.028$). **f**, ATP supplementation during wild-type or *Panx1*^{-/-} T cell suppression assays ($n=3$) (** $p=0.001$). Data are mean \pm s.d. Two-way ANOVA (b), Unpaired student's t-test (e,f).

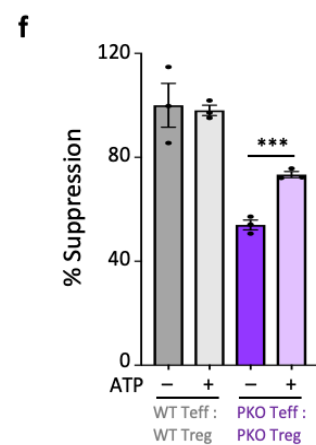
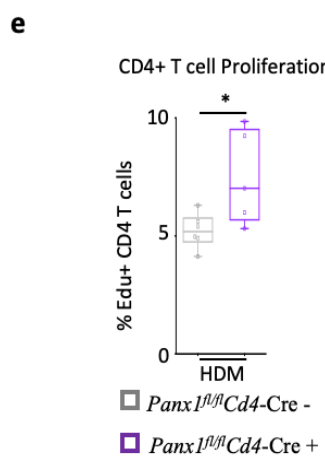
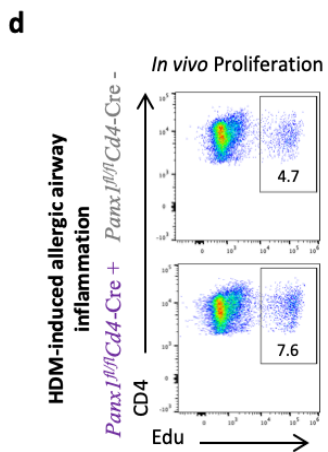
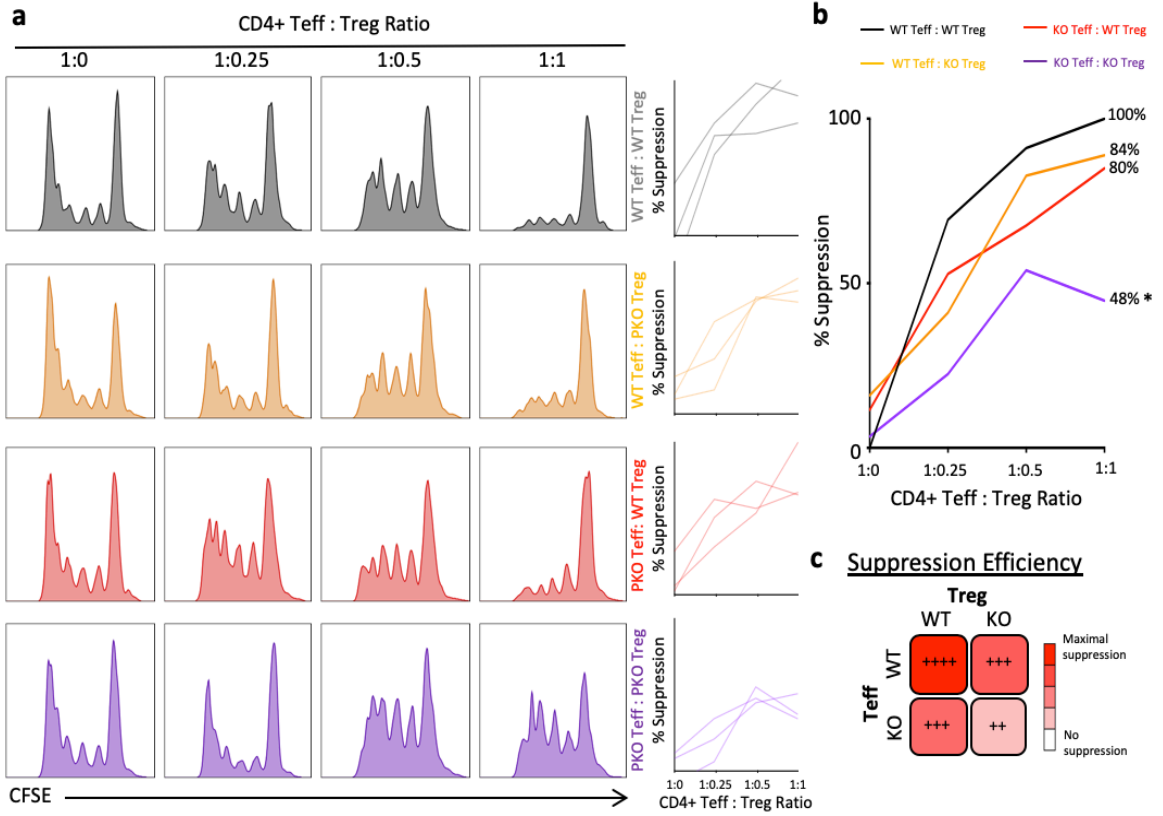
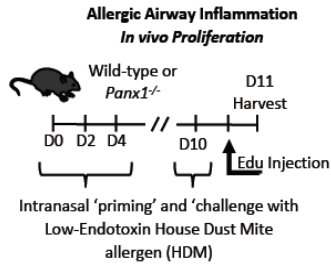
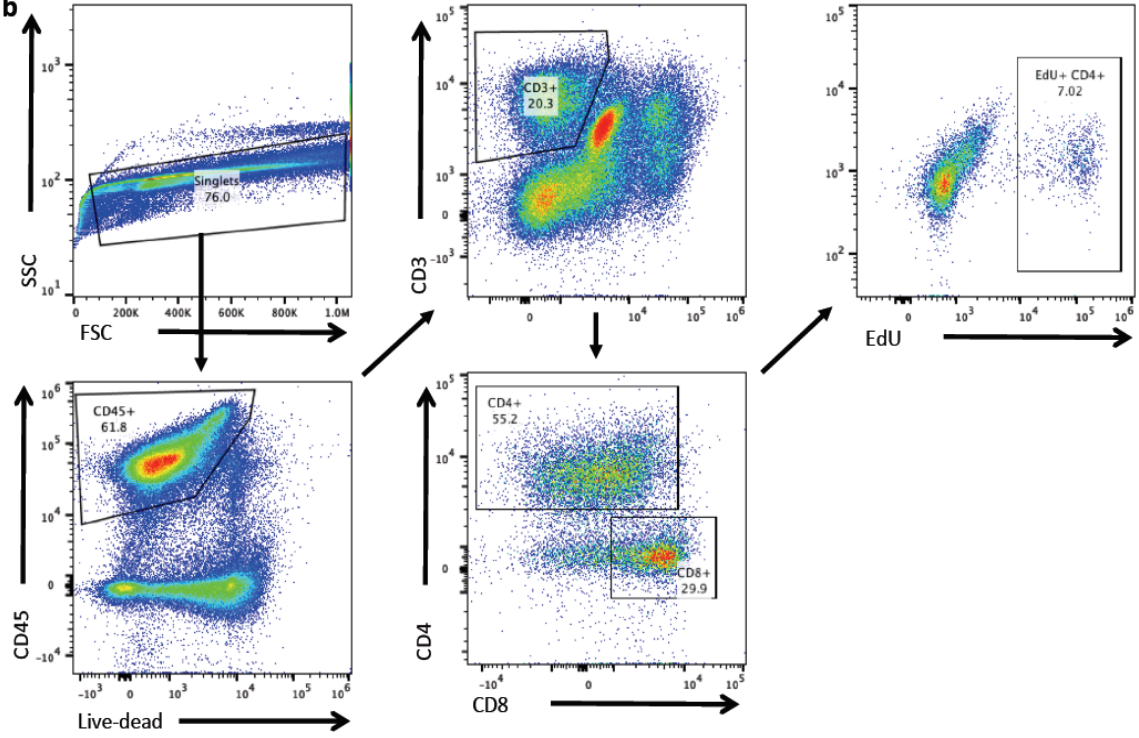
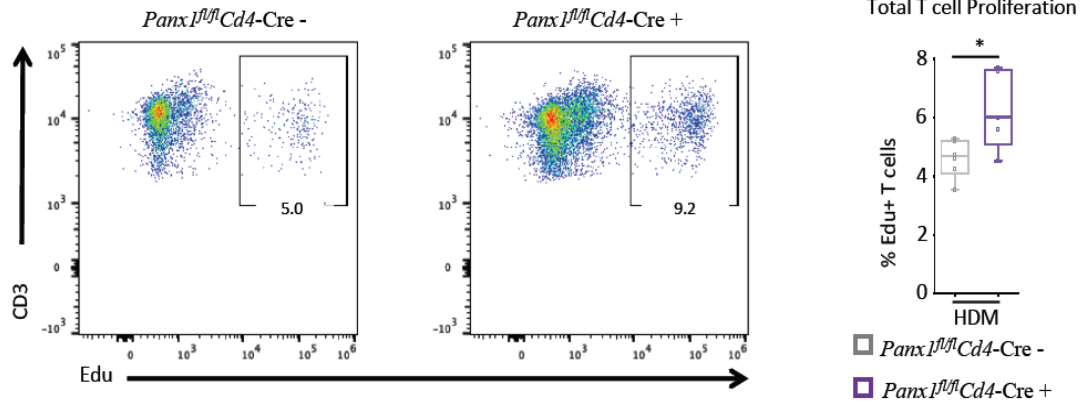


Figure 3.11: *In vivo* T cell proliferation.

a, Schematic representation for the modified mouse model of house dust mice induced allergic airway inflammation to measure T cell proliferation *in vivo*. **b**, Representative flow plots demonstrating the gating strategy used to determine the EdU+ (cells that have proliferated) T cells. **c**, Quantitative analysis of total CD3+ EdU+ T cells in *Panx1^{fl/fl}Cd4-cre-* ($n=6$) and *Panx1^{fl/fl}Cd4-cre+* ($n=5$) mice during HDM. Unpaired student's t-test.

a**b****c**

3.4.5. *Panx1* expression on T cells is sufficient to control AAI

After discovering that *Panx1* on T cells is necessary to inhibit disease severity during allergic airway inflammation, we asked whether *Panx1* exclusively on T cells was sufficient to inhibit the observed exacerbated inflammatory phenotype. We therefore generated a novel *Panx1* transgenic mice (*Panx1^{Tg}*). I used the CAG-STOP-eGFP-ROSA26TV (CTV) vector to insert our *Panx1* transgene into the endogenous safe harbor ROSA26 locus (Soriano, 1999; Xiao et al., 2007). Additionally, a floxed stop cassette upstream of the transgene allowed us to cell-specifically overexpress *Panx1*. Furthermore, the downstream internal ribosome entry site (IRES)-GFP allowed us to track transgene expression (**Figure 3.12a**). Mouse validation at the DNA level was confirmed via PCR (**Figure 3.13a**). In order to validate overexpression of *Panx1* protein, *Panx1^{Tg}* mice were crossed to *E2a-cre* mice for global expression. Western blot analysis of mouse spleen confirmed overexpression of *Panx1* (~8 fold compared to wild-type mice) and flow cytometry was used to detect GFP expression as a secondary validation of the newly generated mice (**Figure 3.13b, c**). Furthermore, by crossing the *Panx1^{Tg}* mice to *Cd4-cre* mice we were able to generate mice that specifically overexpressed *Panx1* in the CD4 compartment (**Figure 3.13d**). Functional testing of the transgene by measuring TO-PRO-3 dye uptake (a measurement of *Panx1* activity) was able to confirm that upon *Panx1* activation during apoptosis, the transgenic mice had increased *Panx1* channel activity relative to wild-type littermate controls (**Figure 3.13e, f**).

To investigate whether *Panx1* re-expression in T cells was sufficient to inhibit the increased inflammation seen in the global *Panx1^{-/-}*, we first crossed our *Panx1^{Tg}* mice to global *Panx1^{-/-}* mice. Then, by crossing the *Panx1^{-/-} Panx1^{Tg}* mice to *Cd4-cre* we could

exclusively express Panx1 on T cells, within a global *Panx1*^{-/-} background (**Figure 3.12a**). When we induced allergic airway inflammation in *Panx1*^{-/-} *Panx1*^{Tg} *Cd4-cre*⁺ mice, we were able to essentially reverse the increased inflammatory phenotype seen in global *Panx1*^{-/-} (*Panx1*^{-/-} *Panx1*^{Tg} *Cd4-cre*⁻) littermate controls. Decreased eosinophil and CD4⁺ T cell numbers in the BALF indicated a reduced inflammatory response in these mice (**Figure 3.12b, c**). These data, along with the previous results in *Panx1*^{fl/fl} *Cd4-Cre*⁺, indicate that Panx1 expression on T cells is both necessary and sufficient to limit disease severity during HDM-induced allergic airway inflammation.

Figure 3.12: Panx1 expression on T cells is sufficient to limit excessive inflammation during AAI.

a, Schematic representation of *Cd4-cre* mediated Panx1 transgene re-expression into global *Panx1*^{-/-} mice. **b**, Representative flow plots showing the extent of eosinophil and CD4 T cell infiltration into the bronchoalveolar space (*Panx1*^{-/-} *Panx1*^{Tg} *Cd4-cre*⁻ *n*=5, *Panx1*^{fl/fl} *Foxp3-cre*⁺ *n*=4). **c**, Absolute cellularity of eosinophils (**p*=0.048) (left) and CD4 T cells (***p*=0.002) (right). Unpaired student's t-test.

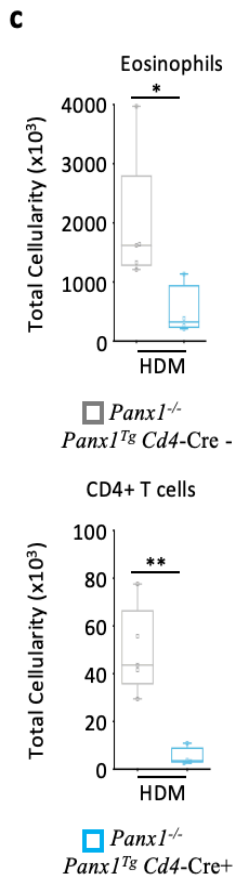
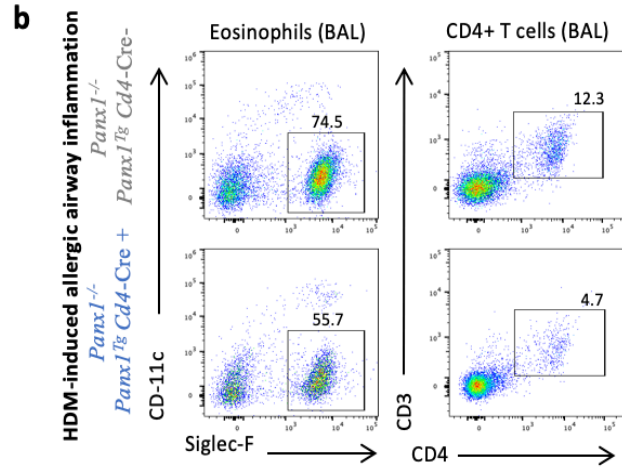
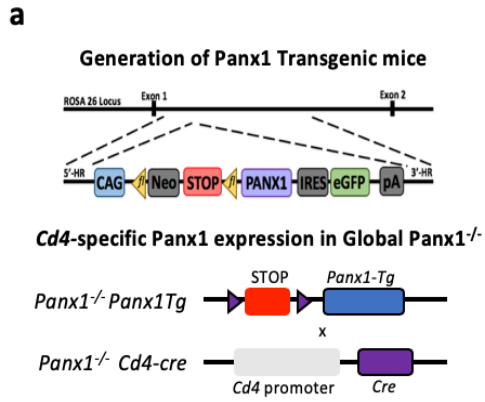
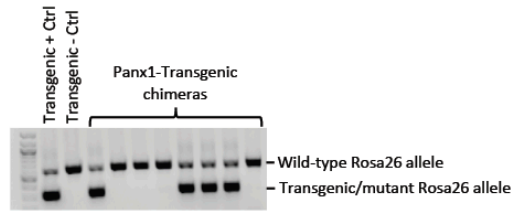
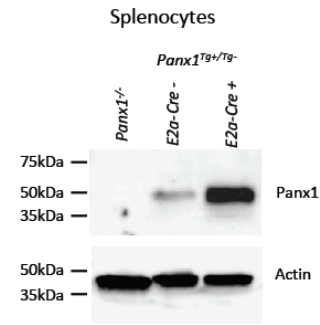
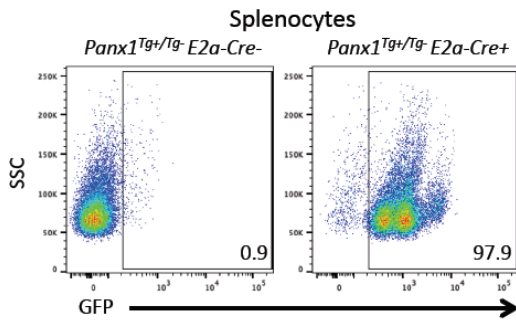
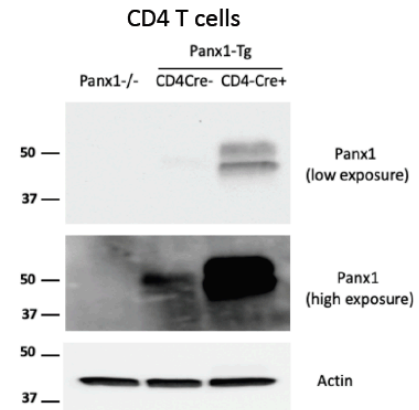
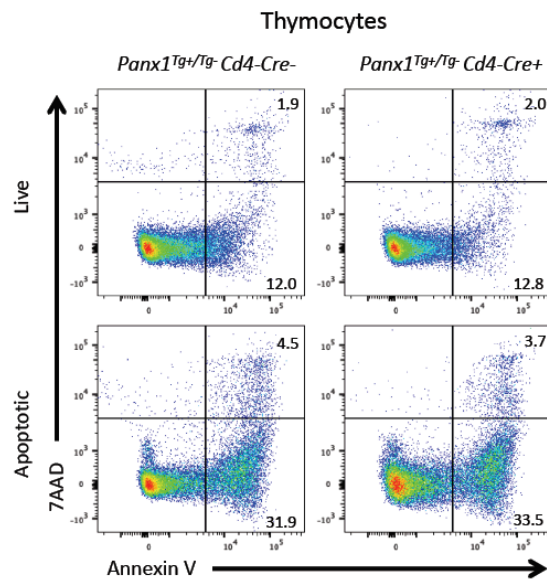
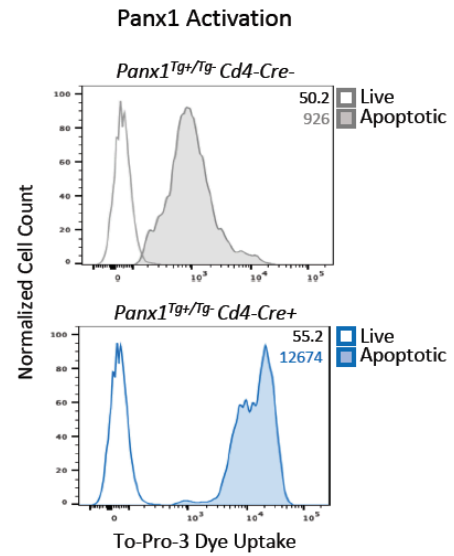


Figure 3.13: Generation and validation of *Panx1^{Tg}* mice.

a, PCR analysis of *Panx1^{Tg}* chimeric mouse genomic DNA to ensure proper integration of the transgene into the ROSA-26 locus. **b**, Western blot validation of Panx1 over-expression mice by crossing the *Panx1^{Tg}* mice to *E2a-cre* mice (express cre globally) and assessing Panx1 protein in the spleen. Actin expression was used as a loading control. **c**, Validation of eGFP expression in splenocytes from *Panx1^{Tg} E2a-cre* or wild-type GFP negative control mice. **d**, Western blot validation of Panx1 over-expression in CD4 T cells by crossing the *Panx1^{Tg}* mice to *Cd4-cre* mice and assessing Panx1 protein from isolated CD4⁺ T cells. Actin expression was used as a loading control. **e,f**, Functional analysis of Panx1 overexpression as assessed by TO-PRO-3 dye uptake during apoptosis. *Panx1^{Tg} Cd4-cre⁺* and control *Panx1^{Tg} Cd4-cre⁻* thymocytes were analyzed for apoptosis induction via annexin V and 7AAD staining (**e**). Representative histograms and MFI of TO-PRO-3 dye uptake within apoptotic cells of respective mice (**f**).

a**b****c****d****e****f**

3.5. Discussion

Overall, we have highlighted a Panx1-dependent extracellular immunoregulatory axis important for proper control and suppression of T cell proliferation. Initial observations in asthmatic humans suggested that Panx1 may be relevant during AAI. In a mouse model of HDM-driven allergic airway inflammation, global *Panx1*^{-/-} mice exhibited significantly heightened inflammation. Subsequent analysis indicated that T cells express very high levels of Panx1 and do not express other pannexin family proteins. In fact, we show that Panx1 expression on T cells (both T_{eff} and T_{reg}) is both necessary and sufficient to properly control inflammation during AAI. Mechanistically, Panx1 function seems to be independent of caspase-mediated activation and apoptotic cell clearance, as we did not see a clear correlation between *Panx1*^{-/-} mice and an increased presence of apoptotic cells. Instead, we show that Panx1 is acting in a non-cell autonomous manner via the extracellular accumulation of adenosine nucleotides during the T_{eff}-T_{reg} interplay for optimal T_{reg} suppression.

It has been shown that adenosine is a potent anti-inflammatory molecule capable of inhibiting T_{eff} cell proliferation and function, while simultaneously increasing the suppressive properties of T_{reg} cells (Haskó and Cronstein, 2004). Additionally, in many situations of inflammation, nucleotides have been proposed to be involved in both the development of inflammation, but also its resolution (Adamson and Leitinger, 2014). This temporal duplicity is thought to occur due to the initial pro-inflammatory extracellular functions of ATP; however, ATP is rapidly degraded unlike the much more stable and immunosuppressive adenosine, which accumulates at sites of inflammation to aid resolution of the inflammatory response. Interestingly, the mechanisms by which ATP and

its derivatives can accumulate in the extracellular environment, especially in inflammatory settings that lack cell death, remains an open question. In our study, we have identified Panx1 as one mechanism by which extracellular nucleotides can accumulate at a certain immune microenvironment to regulate inflammation. More specifically, given that T_{reg} cells, in addition to Panx1, also highly express CD39 and CD73 to break down ATP, it seems likely that adenosine can accumulate in these specific settings. We therefore propose a model that during T_{eff} cell activation, T_{reg} cells present in the same microenvironment will generate high levels of adenosine to suppress uncontrolled T_{eff} cell activation and unwanted or excess inflammation.

Surprisingly, we found that Panx1 deletion exclusively on T_{reg} cells did not affect their ability to limit inflammation or T cell proliferation as long as T_{eff} cells still expressed Panx1. This suggests that it is possible for T_{reg} cells to salvage ATP released from Panx1 on T_{eff} cells to limit activation. Of note, loss of Panx1 on T_{reg} cells did not affect T_{reg} CD39 or CD73 expression (data not shown). Overall this is consistent with a model of extracellular adenosine accumulation in the T cell communication interface to help T_{reg} cells control inflammation. The exact mechanisms that could lead to Panx1 activation on both T cell types is still unknown. Although our cleaved caspase data suggest that Panx1 activation in our model may be independent of apoptosis, it has been shown that apoptotic Tregs can be highly immunosuppressive due to ATP release from Panx1 (Maj et al., 2017). Besides caspase-mediated activation of Panx1 during cell death, reports have also demonstrated that GPCRs can lead to intracellular signaling that ends in the phosphorylation of Panx1 and channel activation. Such is the case in smooth muscle cells where adrenergic signaling can facilitate Src-mediated activation of Panx1 (Billaud et al.,

2015; Lohman et al., 2015). Whether a specific GPCR and kinase(s) are responsible for Panx1 phosphorylation and activation in T cells remains to be determined.

Extracellular ATP has long been considered as a pro-inflammatory stimulus, and this was often in the context of cell death and significant release of large amounts of cellular nucleotide content. However, more recent information begins to describe a much more dynamic picture. Additionally, extracellular ATP is difficult to study given the inability to remove it from a system and its extremely unstable nature outside of cells. Therefore, to understand the functions of eATP, studies have focused on different proteins involved in the generation and metabolism of this extracellular metabolite such as Panx1 and ectonucleotidases, respectively. We can now appreciate that the pro- or anti-inflammatory role of ATP and its derivatives are highly dependent on the tissue context and the cellular composition at sites of extracellular nucleotides. Our work suggest that the extracellular accumulation of nucleotides via Panx1 in the context of the $T_{\text{eff}}-T_{\text{reg}}$ communication axis is important to properly regulate T_{reg} mediated suppression as lack of Panx1 from this immune synapse can result in greater than intended T cell proliferation and consequently heightened airway inflammation.

3.6. Acknowledgements and Author Contributions

C.B.M. and K.S.R designed the experiments. C.B.M. performed majority of the experiments. C.D.L. assisted with the *in vivo* EdU T cell proliferation experiment. K.S.L scored the H&E pathology slides. U.L. provided mice and conceptual advice on T_{reg}: T_{eff} studies. C.B.M. and K.S.R wrote the manuscript with input from coauthors.

Chapter IV

Significance and future directions

The work described in Chapter II and Chapter III have resulted in several key observations, however it has also led to new avenues of research for future work. Below I describe the significance of these findings and the future directions aimed at elucidating these important biological processes.

4.1. Metabolites released from apoptotic cells

4.1.1. Significance of findings – apoptosis

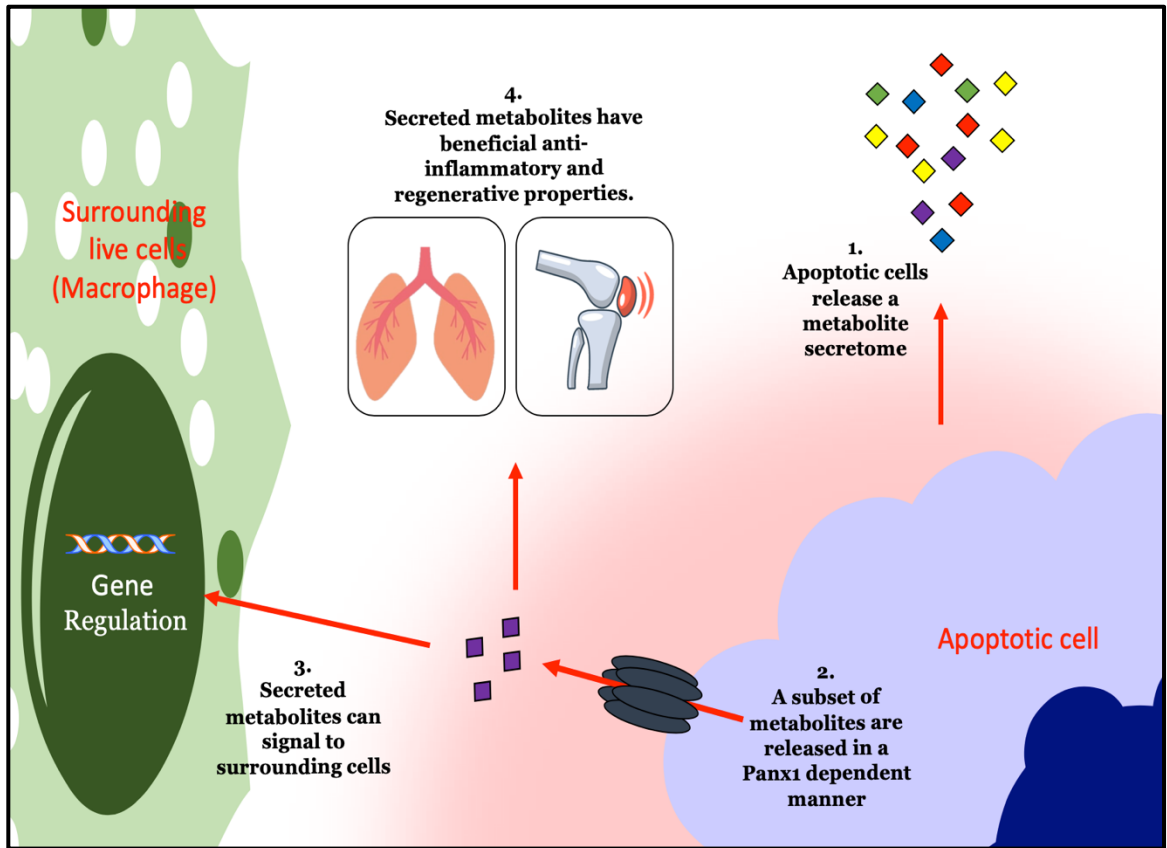
Chapter II covers several novel findings that have the capability of moving the field forward. It has long been known that apoptosis is an essential, evolutionarily conserved process. In fact, the redundancy of the apoptotic machinery suggests that organisms have developed ways to execute programmed cell death, regardless if one specific protein or pathway is disrupted (Elmore, 2007; Nagata, 2018). More recently, with the use of double and triple genetic knockout mice, we can appreciate both the compensatory mechanisms that exist within apoptosis, but also the effects that can occur once apoptosis is completely inhibited. For example, it was recently described that knockout of two intrinsic apoptosis effector molecules did not result in a severe phenotype, however, >99% embryonic lethality occurred upon deletion of a third apoptosis effector molecule (Ke et al., 2018). This is one of several reports that have identified apoptosis as an essential process. Even more so, apoptosis can be beneficial in several disease settings, such as regeneration and inflammation (Bergmann and Steller, 2010; Thompson, 1995). Albeit, a full understanding of the exact mechanisms that explain how apoptosis can mediate these effects has been unclear.

At the moment, in the apoptosis field, one explanation for its importance focuses on the need to remove excess and unwanted cells. While this is certainly true, this portrays a mechanism whereby apoptotic cells are inert, awaiting removal, and therefore, do not direct effects on their own. Consistent with this, much of the beneficial effects of apoptosis has been attributed to their engulfment or clearance by phagocytes, which are then able to mediate important biological functions. More recently, it is being appreciated that the apoptotic cells themselves may directly mediate some pro-regenerative effects through the release of certain proteins (Li et al., 2010; Tseng et al., 2007). However, it is known that apoptotic cells maintain their membrane integrity and a new quantitative report has highlighted that apoptotic cells do not release many proteins at all (Tanzer et al., 2020). Therefore, other mechanisms besides proteins through which these dying cells can communicate to the tissue neighborhood and regulate physiological functions remains unknown.

In this work, I was able to discover that apoptotic cells release a conserved metabolite secretome. As metabolites are much smaller than proteins, they are able to exit the cell, even while the membrane remains intact. This work, for the first time, revealed the ability of dying cells to release an array of molecules for the specific purpose of signaling to the tissue environment. Additionally, we show that these dying cells are not inert, but instead they can orchestrate the release of these signals through metabolic modulation and specific channel activation. Lastly, we demonstrate that these released metabolites have potent extracellular signaling capabilities and can even be harnessed for therapeutic potential (**Figure 4.1**). This has the ability to move the field forward in several directions. First, in the past we have understood that apoptotic cells can have specific

transcriptional and translation changes, but now, as identified here, metabolic alterations are also actively regulated rather than solely a consequence of cell demise. Secondly, we show that these released metabolites have powerful functions extracellularly and may be able to mediate very important physiological processes, which has never been shown before. This also begins to highlight the importance of metabolites as extracellular signaling molecules and not only an energy source for cells.

Figure 4.1: Summary of Findings – metabolites released from apoptotic cells



4.1.2. Future direction – metabolic adaptations during apoptosis

As described in Chapter II, spermidine was a metabolite that continued to be generated within apoptotic cells and this is one possible mechanism by which dying cells may dictate which metabolite is to be released. However, the polyamine pathway may not be the only metabolic change that occurs during cell death. In fact, other metabolites are released from apoptotic cells in a Panx1 dependent manner such as UDP-sugars. Given the several different UDP-sugar metabolites released, it seems plausible that this could be an additional metabolic pathway that is rewired during apoptosis. Interestingly, when we examine the cell pellet data for UDP-sugars we can see that during cell death these metabolites are decreased in the pellet, however, when we inhibit Panx1 channels and therefore their release, the intracellular levels of some UDP-sugars are higher than live cells control. This indicates that apoptotic cells are possibly increasing their production of UDP-sugars, as with polyamines, however, as it is simultaneously being released this is only observed when we inhibit Panx1 activation.

These two metabolic changes that occur within the apoptotic cells indicate a preference for certain pathways over others. While the increased metabolite production renders these molecules more readily available for release, it does not necessarily mean that they were generated for that purpose. One possible explanation for the preferential metabolic changes could be that certain pathways are inactivated during apoptosis, therefore, shuttling metabolites into a different pathway. This could be the scenario with UDP-sugar production as it has been shown that important glycolysis enzymes can be directly cleaved and inactivated by executioner caspases during apoptosis (Pradelli et al., 2014). UDP-sugar metabolism stems off the glycolytic pathway indicating that extra

glucose within the cell may accumulate during cell death (as it can no longer be used for glycolysis) and could be shifted towards the production of UDP-sugars.

Another explanation as to why these metabolites are specifically produced during cell death could be their protective effects. For example, spermidine has long been known to stabilize DNA and RNA (Madeo et al., 2018; Pegg, 2016; Pietrocola et al., 2015). During the apoptotic process it is understood that DNA is cleaved and degraded, however, whether a dying cell is trying to increase polyamine production to stabilize this DNA damage in an attempt to stay alive, is a fascinating question. A sort of internal ‘fight to the death’. UDP-sugars and the pentose phosphate pathway can also have pro-survival roles during different cell death modalities (Hao et al., 2018a). Therefore, whether an apoptotic cell is skewing its metabolic activity in an attempt to avoid cell death remains to be assessed.

Lastly, it would be interesting to determine if the specific metabolic changes that occur within a dying cell is an attempt to remain immunologically silent. It is understood that apoptosis does not elicit an immune response. In fact, we demonstrate that they are actively anti-inflammatory via specific metabolite release. However, this is not the case during other forms of cell death such as pyroptosis or necroptosis, which are known to be pro-inflammatory. Therefore, certain metabolic adaptations during apoptosis may have evolved to help the apoptotic cell itself maintain tissue homeostasis and dampen the inflammatory insult of a dying cell.

On this note, I was able to identify another pattern in the metabolomics data of apoptotic cells that provides a proof of concept for this hypothesis. More specifically, we are able to detect an increased presence of acetylated metabolites within the apoptotic samples. This is interesting, as a recent paper identified that one mechanism by which

necrotic cells can result in inflammation is through macrophage recognition of the dying cell derived histones (Lai et al., 2020). Clec2d receptors on macrophages can specifically recognize polybasic lysine residues on necrotic cell histones and elicit an immune response. However, this receptor was unable of recognizing histones that have had their lysine residues acetylated (thereby removing the positive charge) (Lai et al., 2020). It could be that apoptotic cells are creating acetylated metabolites to serve as substrates for histone acetylation during the cell death process, and therefore, inhibiting their ability to elicit an immune response through Clec2d. In fact, in a preliminary experiment we are able to detect increased histone lysine acetylation in apoptotic cells relative to live cell controls, which does not occur during cell necrosis. Overall, these metabolic adaptations that are occurring within an apoptotic cell are very interesting and they could occur for several reasons including an attempt to stave off cell death, but also a way in which the apoptotic cells can maintain their silent death.

4.1.3. Future directions – metabolites as extracellular signaling molecules

Following the identification of orchestrated apoptotic cell metabolite release, we further demonstrate that these metabolites can influence the surrounding tissue environment. This is an exciting observation as only recently are we understanding the potential of metabolites as extracellular signaling molecules (Husted et al., 2017). In this work we focused exclusively on the ability of these extracellular metabolites to mediate anti-inflammatory effects, specifically during arthritis and a lung transplant rejection model. It is very possible that these metabolites could have a more encompassing and global anti-inflammatory effect. One reason being that these metabolites were not administered locally, but instead intraperitoneally. This could have led to a global

attenuation of inflammatory signaling in many different tissues and therefore, has the potential to become a more general anti-inflammatory therapeutic. It will be interesting to continue to test the metabolite mixtures in different inflammatory conditions.

However, one can imagine that this type of anti-inflammatory signaling from metabolites may not be beneficial in all settings. Take for example a tumor microenvironment, an area where cancer cells are constantly undergoing cell death. Metabolites released from the dying cancer cells may help a specific tumor remain immunologically 'cold'. Therefore, inhibition of this extracellular metabolite signaling axis may be important to induce a proper immune response within tumors. Overall, we identify an important biological process in which apoptotic cell released metabolites can have anti-inflammatory effects in a given tissue neighborhood. During inflammatory diseases and normal homeostatic tissue turnover, this could be very important for proper control of inflammation, however during tumor progression it may be detrimental. Therefore, more research in specific tissues and settings in which apoptosis occurs will be instrumental to uncover the specific roles of these released metabolites.

Another interesting observation was that these released metabolites were not only signaling in an anti-inflammatory manner, but they could also signal in a wound-healing or regenerative fashion (among many others), indicating that these metabolites could be harnessed for other purposes such as injuries and muscle regeneration. Given this exciting possibility, we adapted our metabolite mixtures for use in regeneration models to see whether they could also have beneficial effects in these settings. One model organism used to assess tissue regeneration after injury is the zebrafish. The tail fin of the zebrafish can be cut off and after a period of time it will regenerate to form a fully recovered fin.

However, regeneration is not always complete and it can often take long periods of time to regain full function (Chera et al., 2009; Tseng et al., 2007). To address whether the purified metabolites released from apoptotic cells could influence regeneration, we incubated the zebrafish in different concentrations of the metabolite mixtures and assessed tail growth after cutting. Surprisingly, the metabolites were able to increase the speed in which the tail fins recovered and also seemed to influence the extent of recovery based on tail fin size. Therefore, these data indicate that released metabolites may not only function in an anti-inflammatory setting, but may also be involved in regenerative responses during which cell death is known to occur. Additionally, this provides a proof of concept for the therapeutic potential of apoptotic cell released metabolites in different pathologies. These are exciting areas of research that continue to move forward and figuring out the exact mechanisms through which these metabolites mediate their effects also need to be defined.

In general, our observations suggest that apoptotic cells are able to release a select subset of metabolites that can influence certain tissues in positive, immunologically silent modes (although the outcomes depend on setting as described above with cancer). However, other forms of cell death do exist, which are known to be more inflammatory. For example, pyroptosis occurs during infection with activation of caspase-1 and caspase-11 (Bergsbaken et al., 2009), necroptosis occurs through caspase-independent, RIPK3-MLKL-mediated cell lysis (Pasparakis and Vandenabeele, 2015; Weinlich et al., 2017), and ferroptosis is an iron-dependent cell death modality occurring via lipid peroxidation overload (Hao et al., 2018b). As these different forms of cell death are all thought to elicit inflammation, it would be interesting to investigate if and what metabolites are released under these conditions. Given that apoptosis does not elicit an immune

response and these other forms do, we could imagine that they may release a different set of metabolites during cell death. However, another scenario could be that these cell death modalities also release similar apoptotic metabolites, but on top of that also release other, more dangerous metabolites. The uncontrolled release of metabolites, some of which may be danger-associated molecular patterns (DAMPs) could occur during inflammatory cell death, as they, unlike apoptotic cells, lose membrane integrity. These remain interesting possibilities and avenues of research to fully understand and characterize cell death and its implications.

A big gap in our understanding of the biological process discovered in Chapter II is how these extracellular metabolites are actually signaling. We understand that they can signal, based on gene expression analysis and functional outcomes in live cells and disease settings, respectively. However, the molecular details underpinning the routes by which these metabolites mediate these effects is a current future direction in the lab. There are several different ways in which these extracellular metabolites may be signaling. For example, different receptors may recognize these signals, or these released metabolites may be taken up to change the metabolic state of the cell that is exposed to them.

Receptors on the cell surface of live surrounding cells could be a major mechanism by which the tissue neighborhood is able to respond to these signals. In fact, receptors such as GPCRs are one of the largest family of proteins that exist, making them an ideal avenue for further exploration to gain mechanistic insight into how the apoptotic secreted metabolites signal. Even more intriguing is the fact that many GPCRs, at the moment, are orphan receptors, meaning they do not have a known ligand. This creates a great opportunity to identify new and impactful discoveries on both the metabolic signaling axis

and the GPCR field. Therefore, to further these studies on the apoptotic secretome we have taken several steps in this direction.

In order to investigate novel metabolite::GPCR interactions we have decided to take a screening approach. A recent report used a novel GPCR screening method called PRESTO-TANGO in order to investigate any GPCRs that may be responding to bacterial metabolites in the gut lumen (Chen et al., 2019; Kroeze et al., 2015). Using this same approach with our apoptotic secretome, we will be able to screen for metabolites that may be stimulating GPCRs in our context. This screen uses a mutant HEK293T cell line that contains a luciferase reporter plasmid and a mutant β -arrestin molecule linked to the TEV protease enzyme (TEVp). The screen involves individual chimeric GPCRs that are linked, via a TEV protease cleavage sequence, to a transcription factor that can mediate luciferase expression. Normally, upon GPCR activation, the conserved β -arrestin pathway will be activated and recruit specific molecules to the GPCR for internalization and desensitization to the ligand. Given that this cell line expresses a β -arrestin-TEVp mutant, upon β -arrestin recruitment to the activated GPCR, the TEVp will cleave off the transcription factor from the GPCR. This will allow translocation of the transcription factor to the nucleus for luciferase expression. Via this method, even a small response or brief recognition of a ligand by a receptor will result in a strong signal due to continued luciferase expression regardless of continued GPCR stimulation. This is currently being pursued by a new graduate student Sofia Gasperino in our laboratory to discover new apoptotic metabolite::GPCR signaling axes important for the effects of the apoptotic secretome.

It is important to realize that not all signals are going to be mediated through GPCRs as there are other types of receptors that could recognize these metabolites, for example

receptor tyrosine kinases (RTK). Therefore, the GPCR screen is not all encompassing. Due to this we also want to take a bioinformatical approach similar to the screen in an attempt to unravel the apoptotic metabolite – receptor interactome. Recently an exciting and very useful program was developed called NicheNet (Browaeys et al., 2020). By using this program, which utilizes several resource databases, we can use our RNA-seq of the differentially expressed genes on the phagocyte after apoptotic supernatant treatment. By using our differentially expressed RNA-seq dataset in this program, we can determine which upstream transcription factors, signaling cascades, and eventual receptors can induce these specific gene sets. Therefore, this bioinformatical approach can give us a list of candidate receptors (not only GPCRs) that may be responding on the surrounding live cells to induce specific gene changes. This will give us a different way to attack the problem of identifying the mechanism by which the apoptotic metabolite secretome is signaling.

Lastly, the extracellular metabolic signals don't necessarily need to mediate their effects directly via a receptor. Instead these metabolites could be taken up and used as an energy source or in other capacities by the cell that is exposed to them. In this scenario, certain solute carrier proteins (Slc) may be necessary to internalize these factors. Therefore, the specific Slc proteins that a cell expresses may indicate which metabolites it may actually use and also which ones it may 'leave behind' for the different cell types. Overall, in a tissue setting an array of receptors and slc proteins can dictate the response to the released metabolites. Additionally, the non-homogenous cell types within the vicinity may respond differently to select metabolites whether they recognize and how they respond to particular metabolite signals. It is a very tough, but exciting investigation that may require a better spatial understanding of cell death within the tissue.

4.1.4. Significance of findings – Panx1 field

Panx1 has gained much attention since its discovery, with a better understanding of the channel's characteristics uncovered every year. One facet of the Panx1 literature that has dominated the research field is the ability of the channel to release ATP into the extracellular milieu. In fact, >95% of the research on Panx1 focuses exclusively on the channels ability to release this specific nucleotide. As a result, the involvement of Panx1 in many different physiological and pathological settings has been mainly attributed to its ability to stimulate extracellular purinergic signaling. However, electrophysiology studies has suggested that the channel pore is non-selective (Chiu et al., 2018) and size exclusion studies have shown that the channel pore is large enough to allow the passage of molecules up to 1kDa in size (Wang et al., 2007). Therefore, a major question in the field remains; what other metabolites do Panx1 channels release? In this work I was able to demonstrate via untargeted metabolomics studies that Panx1 is much more than an ATP release channel. Instead, Panx1 channels can release, in addition to ATP, other nucleotides, nucleotide sugars, metabolites involved in different metabolic energy pathways (glycolysis and TCA cycle), and others from specific amino acid metabolism pathways such as spermidine. I believe this work can expand significantly on the knowledge of Panx1 channels and open new areas of research to move the field forward.

4.1.5. Future directions – Panx1-dependent metabolite release

We have now identified different metabolites that are capable of being released in a Panx1-dependent manner from dying cells. One of the major questions that arise from this work is whether these metabolites are being released directly through the channel pore, or if this is an indirect effect of channel activation. Interestingly, while it is accepted that

Panx1 releases ATP, it has also never been adequately proven, in a reductionist manner, whether ATP is directly permeating the channel pore. Therefore, a comprehensive minimalistic approach with the use of purified Panx1 channels and individual metabolites (or even metabolites in combination) is needed to fully address this issue and understand the channels properties. Excitingly, in a collaboration project led by Dr. Doug Bayliss and his graduate student Adi Narahari, they have focused on demonstrating metabolite release specifically through the channel pore. With the use of recombinant Panx1 reconstituted liposomes, they are able to show whether these metabolites are passing directly through the channel pore or if the metabolites identified here are an indirect effect of channel activation. This type of study will further advance our understanding of Panx1 channel properties and its role in physio(patho)logical settings.

In this study we focus on the metabolites that are released in a Panx1-dependent manner during apoptosis. The mechanism of channel activation in this setting is through caspase mediated Panx1 C-terminal cleavage. However, Panx1 can be activated during several different stimuli (in live cells) including, but not limited to, receptor mediated activation (direct or indirect), mechanical stress, and increases in intracellular calcium (Chiu et al., 2014). Therefore, whether the same metabolites are released across all different mechanisms of channel activation remains to be determined. It seems unlikely, as the different metabolic properties of a given cell may help dictate which metabolites are available for release. As we demonstrate in apoptotic cells, certain metabolic modules are differentially regulated during cell death, which may incline the cell to release a certain metabolite. Additionally, dying cells have a permeabilized outer mitochondrial membrane that may also enable these apoptotic cells to release certain metabolites. Live cells will

have a different metabolic state and an intact mitochondrial membrane; therefore, their Panx1-dependent metabolite release signature may be slightly different.

Moreover, live cells can activate Panx1 channels in a caspase-independent mechanism as mentioned above. These mechanisms, such as receptor mediated activation, are reversible, unlike caspase-mediated cleavage. Therefore, the exact channel properties that arise from different modes of activation could also mediate the specific metabolites released. Currently in the lab, we are interested in identifying metabolites released from Panx1 channels during receptor mediated activation; however, at the moment, we have not fully optimized the conditions for this. As mass-spectrometry approach of the supernatant requires large cell numbers and uniform activation of the channel, we are currently troubleshooting these experiments. Overall, we have identified several different metabolites released from Panx1 channels during apoptosis, however, whether this is occurring directly through the channel pore, and if these same metabolites are released during different mechanisms of channel activation remain as exciting avenues of future research.

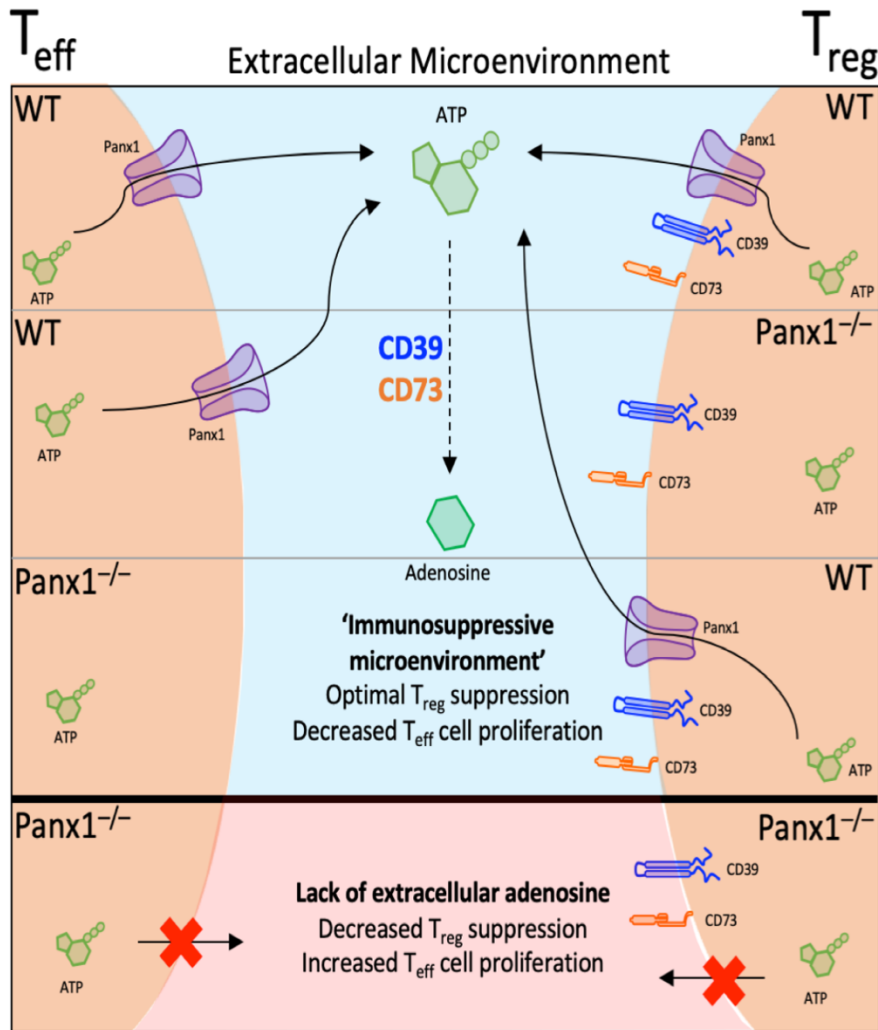
4.2. Panx1 in allergic airway inflammation

4.2.1. Significance of finding

In the extracellular nucleotide field, the role of ATP has predominantly been assigned an inflammatory outcome (Idzko et al., 2014). However, as we learn more about the ways in which ATP can be regulated, we begin to understand the dynamic impact it can have in many different settings. In fact, we now understand that ATP is most likely acting in small microenvironments to mediate its effects. Additionally, the different spatial

organization and duration of eATP can dictate whether it may have anti-inflammatory or suppressive actions. Extracellular ATP in the airways has been associated with an increased inflammatory response during allergic airway inflammation, however the long-term presence of eATP attenuated disease, demonstrating the dichotomy of this nucleotide (Idzko et al., 2013). In many cases that examine the effects of extracellular ATP accumulation, unregulated cell death is assumed to be the factor that results in the release of ATP, but in certain immunological pathologies, cell death rates and tissues damage are relatively low. Therefore, mechanisms that can control eATP in a regulated manner and in a local context, such as Panx1 channel mediated ATP release, are very important to the understating how eATP may act. In Chapter III, I describe a novel role for Panx1 and extracellular ATP during allergic airway inflammation. Panx1 at the $T_{\text{eff}} - T_{\text{reg}}$ interface is important for the suppressive function of T_{regs} (**Figure 4.2**). This work emphasizes the importance of considering the specific cellular microenvironments and which ATP regulating enzymes are present for a proper understanding of how this molecule can impact inflammation and in turn the therapeutic potential of this pathway.

Figure 4.2: Summary of Findings – Panx1 in allergic airway inflammation



4.2.2. Future directions

We were able to demonstrate that Panx1 expression on T cells was both necessary and sufficient to regulate the suppressive capacity of T_{reg} cells. Extracellular ATP released by Panx1 channels into this T_{eff} – T_{reg} microenvironment was essential. However, while ATP supplementation into Panx1 knockout cultures was able to rescue the suppressive function of T_{regs}, it does not necessarily mean that this was adenosine dependent. While T_{reg} cells express high levels of CD39 and CD73 to breakdown ATP into the immunosuppressive adenosine, I did not directly show that my phenotype was adenosine dependent. Future experiments will attempt to rescue the suppressive defects of Panx1 knockout cultures by supplementing back adenosine (instead of ATP), to help define the dependence on extracellular adenosine. Additionally, with the use of extracellular nucleotidase and adenosine receptor inhibitors in wild type cultures, I can further mechanistically test the importance of Panx1 in mediating the accumulation of extracellular adenosine for proper T_{reg} function. These experiments are currently being pursued.

Interestingly, ATP supplementation was only able to partially rescue the suppressive defect in Panx1 knockout cultures. This hints at the possibility that other metabolites released from Panx1 besides ATP and adenosine may also be important for the suppressive function of T_{reg}. In Chapter II we discover several metabolites that are released in a Panx1-dependent manner, although these were from apoptotic cells, it is possible that a subset may also be released from live T cells. It would be interesting to supplement different metabolites identified as Panx1-dependent (from Chapter II) to the Panx1 knockout T cell suppression cultures (in Chapter III), to investigate their role during T_{reg} function and in turn airway inflammation.

Lastly, we would like to try and determine the exact mechanism of Panx1 activation in this setting. We are able to show that very little apoptosis occurs in this disease model, making it less likely that much Panx1 activation via caspase-mediated cleavage is occurring. As mentioned in the introduction, other mechanisms of Panx1 activation can occur, including receptor mediated signaling that can result in Panx1 phosphorylation and channel activation. To this extent, our collaborators Bimal Desai and his graduate student Marta Stremaska have generated a mutant Panx1 mouse in which serine 205 on Panx1 has been mutated to an alanine. This is one phosphorylation site that has been shown to possibly mediate part of the phosphorylation dependent Panx1 activation mechanism. If Panx1 activation during allergic airway inflammation was occurring via this mechanism, then this mouse model should phenocopy the Panx1 knockout mice during AAI. However, preliminary experiments did not show this effect, suggesting that serine 205 on Panx1 may not be important in this setting (although repeats of this study are underway). It is important to note that recent unpublished work from the Doug Bayliss lab (who we are collaborating with) has suggested that several phosphorylation sites on Panx1 may exist to mediate its activation, therefore there is still much work to be done.

Although we were unable to determine the exact phosphorylation site on Panx1 that may be responsible for its activation during airway inflammation, we hypothesized that a specific kinase may be involved to mediate this effect. Ivan Poon, a post-doc in the Ravichandran lab performed a yeast-2-hybrid screen to identify possible Panx1 interacting proteins and identified salt inducible kinase 1 (SIK1) as a potential target. I went on to further characterize this Panx1-SIK1 interaction using ectopically expressed mammalian expression systems as well as endogenous protein interactions. Therefore, we hypothesized

that Panx1 phosphorylation, and in turn, its activation during airway inflammation may be SIK1 dependent due to the strong interaction data we were able to acquire *in vitro*. To investigate this, we crossed *SIK^{fl/fl}* mice to *Cd4-cre* mice to develop a model with SIK1 deleted in the CD4 compartment. If SIK1 is important on CD4 T cells for Panx1 activation and therefore extracellular ATP/adenosine accumulation for T_{reg} suppressive function in our AAI model, this mouse should phenocopy the Panx1 knockout mice. Unfortunately, preliminary experiments were not promising; however, more experiments are being carried out to confirm this initial result. Overall, while there still exists some mystery as to the specific mechanisms by which Panx1 may function during this T_{reg} – T_{eff} interface, we have uncovered a novel mechanism of action for T_{reg} mediated immunosuppression, which may also be important during other inflammatory diseases.

Collectively, in this dissertation I have made two major sets of observations: first, I uncovered a novel set of metabolites released from apoptotic cells, identified PANX1 as one modality by which some of these metabolites may be released, determined the effect of these metabolites on the neighboring live cells, and harnessed the ability of a select cocktail of these metabolites to function as anti-inflammatory mediators *in vivo* in two pre-clinical models of inflammatory diseases. Second, I have identified a novel role for PANX1 channels in allergic airway inflammation, and specifically showed that the expression of PANX1 in T cells help limit the severity of inflammation. Mechanistically, ATP released by either T_{reg} cells or the T_{eff} cells can facilitate the immunosuppression mediated by T_{reg} cells.

References

- Abascal, F., and Zardoya, R. (2012). LRRC8 proteins share a common ancestor with pannexins, and may form hexameric channels involved in cell-cell communication. *Bioessays* *34*, 551–560.
- Adamson, S.E., and Leitinger, N. (2014). The role of pannexin1 in the induction and resolution of inflammation. *FEBS Lett.* *588*, 1416–1422.
- Agrawal, D.K., and Shao, Z. (2010). Pathogenesis of allergic airway inflammation. *Curr Allergy Asthma Rep* *10*, 39–48.
- Ahmed, S.A., and Sriranganathan, N. (1994). Differential effects of dexamethasone on the thymus and spleen: alterations in programmed cell death, lymphocyte subsets and activation of T cells. *Immunopharmacology* *28*, 55–66.
- Aiello, R.J., Brees, D., Bourassa, P.-A., Royer, L., Lindsey, S., Coskran, T., Haghpassand, M., and Francone, O.L. (2002). Increased atherosclerosis in hyperlipidemic mice with inactivation of ABCA1 in macrophages. *Arterioscler. Thromb. Vasc. Biol.* *22*, 630–637.
- Allende, M.L., Sasaki, T., Kawai, H., Olivera, A., Mi, Y., van Echten-Deckert, G., Hajdu, R., Rosenbach, M., Keohane, C.A., Mandala, S., et al. (2004). Mice deficient in sphingosine kinase 1 are rendered lymphopenic by FTY720. *J. Biol. Chem.* *279*, 52487–52492.
- Ambrosi, C., Gassmann, O., Pranskevich, J.N., Boassa, D., Smock, A., Wang, J., Dahl, G., Steinem, C., and Sosinsky, G.E. (2010). Pannexin1 and Pannexin2 channels show quaternary similarities to connexons and different oligomerization numbers from each other. *J. Biol. Chem.* *285*, 24420–24431.
- Anselmi, F., Hernandez, V.H., Crispino, G., Seydel, A., Ortolano, S., Roper, S.D., Kessaris, N., Richardson, W., Rickheit, G., Filippov, M.A., et al. (2008). ATP release through connexin hemichannels and gap junction transfer of second messengers propagate Ca²⁺ signals across the inner ear. *Proc. Natl. Acad. Sci. U.S.a.* *105*, 18770–18775.
- Antonioli, L., Pacher, P., Vizi, E.S., and Haskó, G. (2013). CD39 and CD73 in immunity and inflammation. *Trends Mol Med* *19*, 355–367.
- Arandjelovic, S., and Ravichandran, K.S. (2015). Phagocytosis of apoptotic cells in homeostasis. *Nat. Immunol.* *16*, 907–917.
- Atsumi, G., Murakami, M., Tajima, M., Shimbara, S., Hara, N., and Kudo, I. (1997). The perturbed membrane of cells undergoing apoptosis is susceptible to type II secretory phospholipase A2 to liberate arachidonic acid. *Biochim. Biophys. Acta* *1349*, 43–54.

- Bao, L., Locovei, S., and Dahl, G. (2004a). Pannexin membrane channels are mechanosensitive conduits for ATP. *FEBS Lett.* *572*, 65–68.
- Bao, S., Miller, D.J., Ma, Z., Wohltmann, M., Eng, G., Ramanadham, S., Moley, K., and Turk, J. (2004b). Male mice that do not express group VIA phospholipase A2 produce spermatozoa with impaired motility and have greatly reduced fertility. *J. Biol. Chem.* *279*, 38194–38200.
- Baranova, A., Ivanov, D., Petrash, N., Pestova, A., Skoblov, M., Kelmanson, I., Shagin, D., Nazarenko, S., Geraymovych, E., Litvin, O., et al. (2004). The mammalian pannexin family is homologous to the invertebrate innexin gap junction proteins. *Genomics* *83*, 706–716.
- Bargiotas, P., Krenz, A., Hormuzdi, S.G., Ridder, D.A., Herb, A., Barakat, W., Penuela, S., Engelhardt, von, J., Monyer, H., and Schwaninger, M. (2011). Pannexins in ischemia-induced neurodegeneration. *Proc. Natl. Acad. Sci. U.S.A.* *108*, 20772–20777.
- Beck, G., Sugiura, Y., Shinzawa, K., Kato, S., Setou, M., Tsujimoto, Y., Sakoda, S., and Sumi-Akamaru, H. (2011). Neuroaxonal dystrophy in calcium-independent phospholipase A2 β deficiency results from insufficient remodeling and degeneration of mitochondrial and presynaptic membranes. *J. Neurosci.* *31*, 11411–11420.
- Behrendorf, H.A., van de Craen, M., Knies, U.E., Vandenabeele, P., and Clauss, M. (2000). The endothelial monocyte-activating polypeptide II (EMAP II) is a substrate for caspase-7. *FEBS Lett.* *466*, 143–147.
- Bergmann, A., and Steller, H. (2010). Apoptosis, stem cells, and tissue regeneration. *Sci Signal* *3*, re8–re8.
- Bergsbaken, T., Fink, S.L., and Cookson, B.T. (2009). Pyroptosis: host cell death and inflammation. *Nat. Rev. Microbiol.* *7*, 99–109.
- Billaud, M., Chiu, Y.-H., Lohman, A.W., Parpaite, T., Butcher, J.T., Mutchler, S.M., DeLalio, L.J., Artamonov, M.V., Sandilos, J.K., Best, A.K., et al. (2015). A molecular signature in the pannexin1 intracellular loop confers channel activation by the $\alpha 1$ adrenoceptor in smooth muscle cells. *Sci Signal* *8*, ra17–ra17.
- Birge, R.B., Boeltz, S., Kumar, S., Carlson, J., Wanderley, J., Calianese, D., Barcinski, M., Brekken, R.A., Huang, X., Hutchins, J.T., et al. (2016). Phosphatidylserine is a global immunosuppressive signal in efferocytosis, infectious disease, and cancer. *Cell Death Differ.* *23*, 962–978.
- Bond, S.R., and Naus, C.C. (2014). The pannexins: past and present. *Front Physiol* *5*, 58.
- Böing, A.N., Hau, C.M., Sturk, A., and Nieuwland, R. (2008). Platelet microparticles contain active caspase 3. *Platelets* *19*, 96–103.

- Browaeys, R., Saelens, W., and Saeys, Y. (2020). NicheNet: modeling intercellular communication by linking ligands to target genes. *Nat. Methods* *17*, 159–162.
- Bruzzone, R., Hormuzdi, S.G., Barbe, M.T., Herb, A., and Monyer, H. (2003). Pannexins, a family of gap junction proteins expressed in brain. *Proc. Natl. Acad. Sci. U.S.A.* *100*, 13644–13649.
- Calderón, M.A., Linneberg, A., Kleine-Tebbe, J., De Blay, F., Hernandez Fernandez de Rojas, D., Virchow, J.C., and Demoly, P. (2015). Respiratory allergy caused by house dust mites: What do we really know? *J. Allergy Clin. Immunol.* *136*, 38–48.
- Chekeni, F.B., Elliott, M.R., Sandilos, J.K., Walk, S.F., Kinchen, J.M., Lazarowski, E.R., Armstrong, A.J., Penuela, S., Laird, D.W., Salvesen, G.S., et al. (2010). Pannexin 1 channels mediate “find-me” signal release and membrane permeability during apoptosis. *Nature* *467*, 863–867.
- Chen, G., Li, J., Qiang, X., Czura, C.J., Ochani, M., Ochani, K., Ulloa, L., Yang, H., Tracey, K.J., Wang, P., et al. (2005). Suppression of HMGB1 release by stearyl lysophosphatidylcholine: an additional mechanism for its therapeutic effects in experimental sepsis. *J. Lipid Res.* *46*, 623–627.
- Chen, H., Nwe, P.-K., Yang, Y., Rosen, C.E., Bielecka, A.A., Kuchroo, M., Cline, G.W., Kruse, A.C., Ring, A.M., Crawford, J.M., et al. (2019). A Forward Chemical Genetic Screen Reveals Gut Microbiota Metabolites That Modulate Host Physiology. *Cell* *177*, 1217–1231.e1218.
- Chera, S., Ghila, L., Dobretz, K., Wenger, Y., Bauer, C., Buzgariu, W., Martinou, J.-C., and Galliot, B. (2009). Apoptotic cells provide an unexpected source of Wnt3 signaling to drive hydra head regeneration. *Dev. Cell* *17*, 279–289.
- Chiu, Y.-H., Jin, X., Medina, C.B., Leonhardt, S.A., Kiessling, V., Bennett, B.C., Shu, S., Tamm, L.K., Yeager, M., Ravichandran, K.S., et al. (2017). A quantized mechanism for activation of pannexin channels. *Nat Commun* *8*, 14324.
- Chiu, Y.-H., Ravichandran, K.S., and Bayliss, D.A. (2014). Intrinsic properties and regulation of Pannexin 1 channel. *Channels (Austin)* *8*, 103–109.
- Chiu, Y.-H., Schappe, M.S., Desai, B.N., and Bayliss, D.A. (2018). Revisiting multimodal activation and channel properties of Pannexin 1. *J. Gen. Physiol.* *150*, 19–39.
- Cho, J.-H., Gelinas, R., Wang, K., Etheridge, A., Piper, M.G., Batte, K., Dakhallah, D., Price, J., Bornman, D., Zhang, S., et al. (2011). Systems biology of interstitial lung diseases: integration of mRNA and microRNA expression changes. *BMC Med Genomics* *4*, 8.
- Christiansen-Weber, T.A., Voland, J.R., Wu, Y., Ngo, K., Roland, B.L., Nguyen, S., Peterson, P.A., and Fung-Leung, W.P. (2000). Functional loss of ABCA1 in mice causes severe placental malformation, aberrant lipid distribution, and kidney glomerulonephritis

as well as high-density lipoprotein cholesterol deficiency. *Am. J. Pathol.* *157*, 1017–1029.

Chung, E.Y., Liu, J., Homma, Y., Zhang, Y., Brendolan, A., Saggese, M., Han, J., Silverstein, R., Selleri, L., and Ma, X. (2007). Interleukin-10 expression in macrophages during phagocytosis of apoptotic cells is mediated by homeodomain proteins Pbx1 and Prep-1. *Immunity* *27*, 952–964.

Ciurana, C.L.F., Zwart, B., van Mierlo, G., and Hack, C.E. (2004). Complement activation by necrotic cells in normal plasma environment compares to that by late apoptotic cells and involves predominantly IgM. *Eur. J. Immunol.* *34*, 2609–2619.

Combadiere, C., Potteaux, S., Gao, J.-L., Esposito, B., Casanova, S., Lee, E.J., Debré, P., Tedgui, A., Murphy, P.M., and Mallat, Z. (2003). Decreased atherosclerotic lesion formation in CX3CR1/apolipoprotein E double knockout mice. *Circulation* *107*, 1009–1016.

Croset, M., Brossard, N., Polette, A., and Lagarde, M. (2000). Characterization of plasma unsaturated lysophosphatidylcholines in human and rat. *Biochem. J.* *345 Pt 1*, 61–67.

Dahl, G., and Locovei, S. (2006). Pannexin: to gap or not to gap, is that a question? *IUBMB Life* *58*, 409–419.

Dubyak, G.R., and el-Moatassim, C. (1993). Signal transduction via P2-purinergeric receptors for extracellular ATP and other nucleotides. *Am. J. Physiol.* *265*, C577–C606.

Dwyer, K.M., Deaglio, S., Gao, W., Friedman, D., Strom, T.B., and Robson, S.C. (2007). CD39 and control of cellular immune responses. *Purinergeric Signal.* *3*, 171–180.

Elliott, M.R., and Ravichandran, K.S. (2010). Clearance of apoptotic cells: implications in health and disease. *J. Cell Biol.* *189*, 1059–1070.

Elliott, M.R., Chekeni, F.B., Trampont, P.C., Lazarowski, E.R., Kadl, A., Walk, S.F., Park, D., Woodson, R.I., Ostankovich, M., Sharma, P., et al. (2009). Nucleotides released by apoptotic cells act as a find-me signal to promote phagocytic clearance. *Nature* *461*, 282–286.

Elmore, S. (2007). Apoptosis: a review of programmed cell death. *Toxicol Pathol* *35*, 495–516.

Eltzschig, H.K., Sitkovsky, M.V., and Robson, S.C. (2013). Purinergeric signaling during inflammation. *N. Engl. J. Med.* *368*, 1260–1260.

Evans, A.M., DeHaven, C.D., Barrett, T., Mitchell, M., and Milgram, E. (2009). Integrated, nontargeted ultrahigh performance liquid chromatography/electrospray ionization tandem mass spectrometry platform for the identification and relative quantification of the small-molecule complement of biological systems. *Anal. Chem.* *81*, 6656–6667.

Flannagan, R.S., Canton, J., Furuya, W., Glogauer, M., and Grinstein, S. (2014). The phosphatidylserine receptor TIM4 utilizes integrins as coreceptors to effect phagocytosis. *Mol. Biol. Cell* 25, 1511–1522.

Fonović, U.P., Jevnikar, Z., and Kos, J. (2013). Cathepsin S generates soluble CX3CL1 (fractalkine) in vascular smooth muscle cells. *Biol. Chem.* 394, 1349–1352.

Fransen, J.H., Hilbrands, L.B., Jacobs, C.W., Adema, G.J., Berden, J.H., and Van der Vlag, J. (2009a). Both early and late apoptotic blebs are taken up by DC and induce IL-6 production. *Autoimmunity* 42, 325–327.

Fransen, J.H., Hilbrands, L.B., Ruben, J., Stoffels, M., Adema, G.J., van der Vlag, J., and Berden, J.H. (2009b). Mouse dendritic cells matured by ingestion of apoptotic blebs induce T cells to produce interleukin-17. *Arthritis Rheum.* 60, 2304–2313.

Fu, M., Fan, P.-S., Li, W., Li, C.-X., Xing, Y., An, J.-G., Wang, G., Fan, X.-L., Gao, T.-W., Liu, Y.-F., et al. (2007). Identification of poly-reactive natural IgM antibody that recognizes late apoptotic cells and promotes phagocytosis of the cells. *Apoptosis* 12, 355–362.

Fuchs, Y., and Steller, H. (2011). Programmed cell death in animal development and disease. *Cell* 147, 742–758.

Furlow, P.W., Zhang, S., Soong, T.D., Halberg, N., Goodarzi, H., Mangrum, C., Wu, Y.G., Elemento, O., and Tavazoie, S.F. (2015). Mechanosensitive pannexin-1 channels mediate microvascular metastatic cell survival. *Nat. Cell Biol.* 17, 943–952.

Gandhi, V.D., Davidson, C., Asaduzzaman, M., Nahirney, D., and Vliagoftis, H. (2013). House dust mite interactions with airway epithelium: role in allergic airway inflammation. *Curr Allergy Asthma Rep* 13, 262–270.

Garton, K.J., Gough, P.J., Blobel, C.P., Murphy, G., Greaves, D.R., Dempsey, P.J., and Raines, E.W. (2001). Tumor necrosis factor-alpha-converting enzyme (ADAM17) mediates the cleavage and shedding of fractalkine (CX3CL1). *J. Biol. Chem.* 276, 37993–38001.

Gelman, A.E., Li, W., Richardson, S.B., Zinselmeyer, B.H., Lai, J., Okazaki, M., Kornfeld, C.G., Kreisel, F.H., Sugimoto, S., Tietjens, J.R., et al. (2009). Cutting edge: Acute lung allograft rejection is independent of secondary lymphoid organs. *J. Immunol.* 182, 3969–3973.

Goessling, W., North, T.E., Loewer, S., Lord, A.M., Lee, S., Stoick-Cooper, C.L., Weidinger, G., Puder, M., Daley, G.Q., Moon, R.T., et al. (2009). Genetic interaction of PGE2 and Wnt signaling regulates developmental specification of stem cells and regeneration. *Cell* 136, 1136–1147.

Gold, M., Marsolais, D., and Blanchet, M.-R. (2015). Mouse models of allergic asthma. *Methods Mol. Biol.* 1220, 503–519.

- Good, M.E., Chiu, Y.-H., Poon, I.K.H., Medina, C.B., Butcher, J.T., Mendu, S.K., DeLalio, L.J., Lohman, A.W., Leitinger, N., Barrett, E., et al. (2018). Pannexin 1 Channels as an Unexpected New Target of the Anti-Hypertensive Drug Spironolactone. *Circ. Res.* *122*, 606–615.
- Gorman, M.W., Feigl, E.O., and Buffington, C.W. (2007). Human plasma ATP concentration. *Clin. Chem.* *53*, 318–325.
- Gregory, C.D., and Paterson, M. (2018). An apoptosis-driven “onco-regenerative niche”: roles of tumour-associated macrophages and extracellular vesicles. *Philos. Trans. R. Soc. Lond., B, Biol. Sci.* *373*, 20170003.
- Gu, Y., Forostyan, T., Sabbadini, R., and Rosenblatt, J. (2011). Epithelial cell extrusion requires the sphingosine-1-phosphate receptor 2 pathway. *J. Cell Biol.* *193*, 667–676.
- Gu, Y., Shea, J., Slattum, G., Firpo, M.A., Alexander, M., Mulvihill, S.J., Golubovskaya, V.M., and Rosenblatt, J. (2015). Defective apical extrusion signaling contributes to aggressive tumor hallmarks. *Elife* *4*, e04069.
- Gude, D.R., Alvarez, S.E., Paugh, S.W., Mitra, P., Yu, J., Griffiths, R., Barbour, S.E., Milstien, S., and Spiegel, S. (2008). Apoptosis induces expression of sphingosine kinase 1 to release sphingosine-1-phosphate as a “come-and-get-me” signal. *Faseb J.* *22*, 2629–2638.
- Guo, X., Harada, C., Namekata, K., Kimura, A., Mitamura, Y., Yoshida, H., Matsumoto, Y., and Harada, T. (2011). Spermidine alleviates severity of murine experimental autoimmune encephalomyelitis. *Invest. Ophthalmol. Vis. Sci.* *52*, 2696–2703.
- Hait, N.C., Oskeritzian, C.A., Paugh, S.W., Milstien, S., and Spiegel, S. (2006). Sphingosine kinases, sphingosine 1-phosphate, apoptosis and diseases. *Biochim. Biophys. Acta* *1758*, 2016–2026.
- Hanayama, R., Tanaka, M., Miwa, K., Shinohara, A., Iwamatsu, A., and Nagata, S. (2002). Identification of a factor that links apoptotic cells to phagocytes. *Nature* *417*, 182–187.
- Hanstein, R., Negoro, H., Patel, N.K., Charollais, A., Meda, P., Spray, D.C., Suadicani, S.O., and Scemes, E. (2013). Promises and pitfalls of a Pannexin1 transgenic mouse line. *Front Pharmacol* *4*, 61.
- Hao, S., Liang, B., Huang, Q., Dong, S., Wu, Z., He, W., and Shi, M. (2018a). Metabolic networks in ferroptosis. *Oncol Lett* *15*, 5405–5411.
- Hao, S., Liang, B., Huang, Q., Dong, S., Wu, Z., He, W., and Shi, M. (2018b). Metabolic networks in ferroptosis. *Oncol Lett* *15*, 5405–5411.

- Hardy, K., Handyside, A.H., and Winston, R.M. (1989). The human blastocyst: cell number, death and allocation during late preimplantation development in vitro. *Development* *107*, 597–604.
- Haskó, G., Kuhel, D.G., Salzman, A.L., and Szabó, C. (2000). ATP suppression of interleukin-12 and tumour necrosis factor-alpha release from macrophages. *Br. J. Pharmacol.* *129*, 909–914.
- Haskó, G., and Cronstein, B.N. (2004). Adenosine: an endogenous regulator of innate immunity. *Trends Immunol.* *25*, 33–39.
- Henson, P.M. (2005). Dampening inflammation. *Nat. Immunol.* *6*, 1179–1181.
- Henson, P.M., and Hume, D.A. (2006). Apoptotic cell removal in development and tissue homeostasis. *Trends Immunol.* *27*, 244–250.
- Honda, S., Sasaki, Y., Ohsawa, K., Imai, Y., Nakamura, Y., Inoue, K., and Kohsaka, S. (2001). Extracellular ATP or ADP induce chemotaxis of cultured microglia through Gi/o-coupled P2Y receptors. *J. Neurosci.* *21*, 1975–1982.
- Horino, K., Nishiura, H., Ohsako, T., Shibuya, Y., Hiraoka, T., Kitamura, N., and Yamamoto, T. (1998). A monocyte chemotactic factor, S19 ribosomal protein dimer, in phagocytic clearance of apoptotic cells. *Lab. Invest.* *78*, 603–617.
- Hou, Y., Plett, P.A., Ingram, D.A., Rajashekhar, G., Orschell, C.M., Yoder, M.C., March, K.L., and Clauss, M. (2006). Endothelial-monocyte-activating polypeptide II induces migration of endothelial progenitor cells via the chemokine receptor CXCR3. *Exp. Hematol.* *34*, 1125–1132.
- Hua, V.B., Chang, A.B., Tchieu, J.H., Kumar, N.M., Nielsen, P.A., and Saier, M.H. (2003). Sequence and phylogenetic analyses of 4 TMS junctional proteins of animals: connexins, innexins, claudins and occludins. *J. Membr. Biol.* *194*, 59–76.
- Huang, Y.H., Schäfer-Elinder, L., Wu, R., Claesson, H.E., and Frostegård, J. (1999). Lysophosphatidylcholine (LPC) induces proinflammatory cytokines by a platelet-activating factor (PAF) receptor-dependent mechanism. *Clin. Exp. Immunol.* *116*, 326–331.
- Huber, J., Vales, A., Mitulovic, G., Blumer, M., Schmid, R., Witztum, J.L., Binder, B.R., and Leitinger, N. (2002). Oxidized membrane vesicles and blebs from apoptotic cells contain biologically active oxidized phospholipids that induce monocyte-endothelial interactions. *Arterioscler. Thromb. Vasc. Biol.* *22*, 101–107.
- Hundhausen, C., Misztela, D., Berkhout, T.A., Broadway, N., Saftig, P., Reiss, K., Hartmann, D., Fahrenholz, F., Postina, R., Matthews, V., et al. (2003). The disintegrin-like metalloproteinase ADAM10 is involved in constitutive cleavage of CX3CL1 (fractalkine) and regulates CX3CL1-mediated cell-cell adhesion. *Blood* *102*, 1186–1195.

- Husted, A.S., Trauelsen, M., Rudenko, O., Hjorth, S.A., and Schwartz, T.W. (2017). GPCR-Mediated Signaling of Metabolites. *Cell Metab.* *25*, 777–796.
- Idzko, M., K Ayata, C., Müller, T., Dürk, T., Grimm, M., Baudiß, K., Vieira, R.P., Cicko, S., Boehlke, C., Zech, A., et al. (2013). Attenuated allergic airway inflammation in Cd39 null mice. *Allergy* *68*, 472–480.
- Idzko, M., Ferrari, D., and Eltzschig, H.K. (2014). Nucleotide signalling during inflammation. *Nature* *509*, 310–317.
- Idzko, M., Hammad, H., van Nimwegen, M., Kool, M., Willart, M.A.M., Muskens, F., Hoogsteden, H.C., Luttmann, W., Ferrari, D., Di Virgilio, F., et al. (2007). Extracellular ATP triggers and maintains asthmatic airway inflammation by activating dendritic cells. *Nat. Med.* *13*, 913–919.
- Ipseiz, N., Uderhardt, S., Scholtysek, C., Steffen, M., Schabbauer, G., Bozec, A., Schett, G., and Krönke, G. (2014). The nuclear receptor Nr4a1 mediates anti-inflammatory effects of apoptotic cells. *J. Immunol.* *192*, 4852–4858.
- Isenring, B., Robinson, C., Buergi, U., Schuurmans, M.M., Kohler, M., Huber, L.C., and Benden, C. (2017). Lung transplant recipients on long-term extracorporeal photopheresis. *Clin Transplant* *31*, e13041.
- Ishii, I., Fukushima, N., Ye, X., and Chun, J. (2004). Lysophospholipid receptors: signaling and biology. *Annu. Rev. Biochem.* *73*, 321–354.
- Ishimoto, Y., Ohashi, K., Mizuno, K., and Nakano, T. (2000). Promotion of the uptake of PS liposomes and apoptotic cells by a product of growth arrest-specific gene, gas6. *J. Biochem.* *127*, 411–417.
- Jankowski, J., Perry, H.M., Medina, C.B., Huang, L., Yao, J., Bajwa, A., Lorenz, U.M., Rosin, D.L., Ravichandran, K.S., Isakson, B.E., et al. (2018). Epithelial and Endothelial Pannexin1 Channels Mediate AKI. *J. Am. Soc. Nephrol.* *29*, 1887–1899.
- Jha, A.K., Huang, S.C.-C., Sergushichev, A., Lampropoulou, V., Ivanova, Y., Loginicheva, E., Chmielewski, K., Stewart, K.M., Ashall, J., Everts, B., et al. (2015). Network integration of parallel metabolic and transcriptional data reveals metabolic modules that regulate macrophage polarization. *Immunity* *42*, 419–430.
- Juncadella, I.J., Kadl, A., Sharma, A.K., Shim, Y.M., Hochreiter-Hufford, A., Borish, L., and Ravichandran, K.S. (2013). Apoptotic cell clearance by bronchial epithelial cells critically influences airway inflammation. *Nature* *493*, 547–551.
- Junger, W.G. (2011). Immune cell regulation by autocrine purinergic signalling. *Nat. Rev. Immunol.* *11*, 201–212.
- Kao, J., Fan, Y.G., Haehnel, I., Brett, J., Greenberg, S., Clauss, M., Kayton, M., Houck, K., Kisiel, W., and Seljelid, R. (1994). A peptide derived from the amino terminus of

endothelial-monocyte-activating polypeptide II modulates mononuclear and polymorphonuclear leukocyte functions, defines an apparently novel cellular interaction site, and induces an acute inflammatory response. *J. Biol. Chem.* *269*, 9774–9782.

Ke, F.F.S., Vanyai, H.K., Cowan, A.D., Delbridge, A.R.D., Whitehead, L., Grabow, S., Czabotar, P.E., Voss, A.K., and Strasser, A. (2018). Embryogenesis and Adult Life in the Absence of Intrinsic Apoptosis Effectors BAX, BAK, and BOK. *Cell* *173*, 1217–1230.e1217.

Kim, S.J., Gershov, D., Ma, X., Brot, N., and Elkon, K.B. (2002). I-PLA(2) activation during apoptosis promotes the exposure of membrane lysophosphatidylcholine leading to binding by natural immunoglobulin M antibodies and complement activation. *J. Exp. Med.* *196*, 655–665.

Kinchen, J.M., Doukoumetzidis, K., Almendinger, J., Stergiou, L., Tosello-Tramont, A., Sifri, C.D., Hengartner, M.O., and Ravichandran, K.S. (2008). A pathway for phagosome maturation during engulfment of apoptotic cells. *Nat. Cell Biol.* *10*, 556–566.

Kleeman, T.A., Wei, D., Simpson, K.L., and First, E.A. (1997). Human tyrosyl-tRNA synthetase shares amino acid sequence homology with a putative cytokine. *J. Biol. Chem.* *272*, 14420–14425.

Knies, U.E., Behrendorf, H.A., Mitchell, C.A., Deutsch, U., Risau, W., Drexler, H.C., and Clauss, M. (1998). Regulation of endothelial monocyte-activating polypeptide II release by apoptosis. *Proc. Natl. Acad. Sci. U.S.A.* *95*, 12322–12327.

Kobayashi, N., Karisola, P., Peña-Cruz, V., Dorfman, D.M., Jinushi, M., Umetsu, S.E., Butte, M.J., Nagumo, H., Chernova, I., Zhu, B., et al. (2007). TIM-1 and TIM-4 glycoproteins bind phosphatidylserine and mediate uptake of apoptotic cells. *Immunity* *27*, 927–940.

Kohno, M., Momoi, M., Oo, M.L., Paik, J.-H., Lee, Y.-M., Venkataraman, K., Ai, Y., Ristimaki, A.P., Fyrst, H., Sano, H., et al. (2006). Intracellular role for sphingosine kinase 1 in intestinal adenoma cell proliferation. *Mol. Cell. Biol.* *26*, 7211–7223.

Koizumi, S., Shigemoto-Mogami, Y., Nasu-Tada, K., Shinozaki, Y., Ohsawa, K., Tsuda, M., Joshi, B.V., Jacobson, K.A., Kohsaka, S., and Inoue, K. (2007). UDP acting at P2Y6 receptors is a mediator of microglial phagocytosis. *Nature* *446*, 1091–1095.

Korganow, A.S., Ji, H., Mangialaio, S., Duchatelle, V., Pelanda, R., Martin, T., Degott, C., Kikutani, H., Rajewsky, K., Pasquali, J.L., et al. (1999). From systemic T cell self-reactivity to organ-specific autoimmune disease via immunoglobulins. *Immunity* *10*, 451–461.

Kouskoff, V., Korganow, A.S., Duchatelle, V., Degott, C., Benoist, C., and Mathis, D. (1996). Organ-specific disease provoked by systemic autoimmunity. *Cell* *87*, 811–822.

Kroemer, G., Galluzzi, L., Vandenabeele, P., Abrams, J., Alnemri, E.S., Baehrecke, E.H., Blagosklonny, M.V., El-Deiry, W.S., Golstein, P., Green, D.R., et al. (2009).

Classification of cell death: recommendations of the Nomenclature Committee on Cell Death 2009. *Cell Death Differ.* 16, 3–11.

Kroeze, W.K., Sassano, M.F., Huang, X.-P., Lansu, K., McCorvy, J.D., Giguère, P.M., Sciaky, N., and Roth, B.L. (2015). PRESTO-Tango as an open-source resource for interrogation of the druggable human GPCRome. *Nat. Struct. Mol. Biol.* 22, 362–369.

Kronlage, M., Song, J., Sorokin, L., Isfort, K., Schwerdtle, T., Leipziger, J., Robaye, B., Conley, P.B., Kim, H.-C., Sargin, S., et al. (2010). Autocrine purinergic receptor signaling is essential for macrophage chemotaxis. *Sci Signal* 3, ra55–ra55.

Krupnick, A.S., Lin, X., Li, W., Okazaki, M., Lai, J., Sugimoto, S., Richardson, S.B., Kornfeld, C.G., Garbow, J.R., Patterson, G.A., et al. (2009). Orthotopic mouse lung transplantation as experimental methodology to study transplant and tumor biology. *Nat Protoc* 4, 86–93.

la Sala, A., Ferrari, D., Corinti, S., Cavani, A., Di Virgilio, F., and Girolomoni, G. (2001). Extracellular ATP induces a distorted maturation of dendritic cells and inhibits their capacity to initiate Th1 responses. *J. Immunol.* 166, 1611–1617.

la Sala, A., Ferrari, D., Di Virgilio, F., Idzko, M., Norgauer, J., and Girolomoni, G. (2003). Alerting and tuning the immune response by extracellular nucleotides. *J. Leukoc. Biol.* 73, 339–343.

Lai, J.-J., Cruz, F.M., and Rock, K.L. (2020). Immune Sensing of Cell Death through Recognition of Histone Sequences by C-Type Lectin-Receptor-2d Causes Inflammation and Tissue Injury. *Immunity* 52, 123–135.e126.

Lai, W.-Q., Irwan, A.W., Goh, H.H., Melendez, A.J., McInnes, I.B., and Leung, B.P. (2009). Distinct roles of sphingosine kinase 1 and 2 in murine collagen-induced arthritis. *J. Immunol.* 183, 2097–2103.

Lambrecht, B.N., and Hammad, H. (2015). The immunology of asthma. *Nat. Immunol.* 16, 45–56.

Lauber, K., Bohn, E., Kröber, S.M., Xiao, Y.-J., Blumenthal, S.G., Lindemann, R.K., Marini, P., Wiedig, C., Zobywalski, A., Baksh, S., et al. (2003). Apoptotic cells induce migration of phagocytes via caspase-3-mediated release of a lipid attraction signal. *Cell* 113, 717–730.

Lázár, Z., Cervenak, L., Orosz, M., Gálffy, G., Komlósi, Z.I., Bikov, A., Losonczy, G., and Horváth, I. (2010). Adenosine triphosphate concentration of exhaled breath condensate in asthma. *Chest* 138, 536–542.

Le Vasseur, M., Lelowski, J., Bechberger, J.F., Sin, W.-C., and Naus, C.C. (2014). Pannexin 2 protein expression is not restricted to the CNS. *Front Cell Neurosci* 8, 392.

Le, L.Q., Kabarowski, J.H., Weng, Z., Satterthwaite, A.B., Harvill, E.T., Jensen, E.R., Miller, J.F., and Witte, O.N. (2001). Mice lacking the orphan G protein-coupled receptor G2A develop a late-onset autoimmune syndrome. *Immunity* *14*, 561–571.

Lee, C.S., Penberthy, K.K., Wheeler, K.M., Juncadella, I.J., Vandenabeele, P., Lysiak, J.J., and Ravichandran, K.S. (2016). Boosting Apoptotic Cell Clearance by Colonic Epithelial Cells Attenuates Inflammation In Vivo. *Immunity* *44*, 807–820.

Lee, S.-J., So, I.-S., Park, S.-Y., and Kim, I.-S. (2008). Thymosin beta4 is involved in stabilin-2-mediated apoptotic cell engulfment. *FEBS Lett.* *582*, 2161–2166.

Leonardi-Essmann, F., Emig, M., Kitamura, Y., Spanagel, R., and Gebicke-Haerter, P.J. (2005). Fractalkine-upregulated milk-fat globule EGF factor-8 protein in cultured rat microglia. *J. Neuroimmunol.* *160*, 92–101.

Li, F., Huang, Q., Chen, J., Peng, Y., Roop, D.R., Bedford, J.S., and Li, C.-Y. (2010). Apoptotic cells activate the “phoenix rising” pathway to promote wound healing and tissue regeneration. *Sci Signal* *3*, ra13–ra13.

Li, P., Gao, Y., Cao, J., Wang, W., Chen, Y., Zhang, G., Robson, S.C., Wu, Y., and Yang, J. (2015). CD39+ regulatory T cells attenuate allergic airway inflammation. *Clin. Exp. Allergy* *45*, 1126–1137.

Liang, J., Nagahashi, M., Kim, E.Y., Harikumar, K.B., Yamada, A., Huang, W.-C., Hait, N.C., Allegood, J.C., Price, M.M., Avni, D., et al. (2013). Sphingosine-1-phosphate links persistent STAT3 activation, chronic intestinal inflammation, and development of colitis-associated cancer. *Cancer Cell* *23*, 107–120.

Lin, P., and Ye, R.D. (2003). The lysophospholipid receptor G2A activates a specific combination of G proteins and promotes apoptosis. *J. Biol. Chem.* *278*, 14379–14386.

Lindsten, T., Ross, A.J., King, A., Zong, W.X., Rathmell, J.C., Shiels, H.A., Ulrich, E., Waymire, K.G., Mahar, P., Frauwirth, K., et al. (2000). The combined functions of proapoptotic Bcl-2 family members bak and bax are essential for normal development of multiple tissues. *Mol. Cell* *6*, 1389–1399.

Liu, X., Fu, R., Pan, Y., Meza-Sosa, K.F., Zhang, Z., and Lieberman, J. (2018). PNPT1 Release from Mitochondria during Apoptosis Triggers Decay of Poly(A) RNAs. *Cell*.

Liu, Z., Gerner, M.Y., Van Panhuys, N., Levine, A.G., Rudensky, A.Y., and Germain, R.N. (2015). Immune homeostasis enforced by co-localized effector and regulatory T cells. *Nature* *528*, 225–230.

Locovei, S., Bao, L., and Dahl, G. (2006a). Pannexin 1 in erythrocytes: function without a gap. *Proc. Natl. Acad. Sci. U.S.A.* *103*, 7655–7659.

Locovei, S., Wang, J., and Dahl, G. (2006b). Activation of pannexin 1 channels by ATP through P2Y receptors and by cytoplasmic calcium. *FEBS Lett.* *580*, 239–244.

- Lohman, A.W., and Isakson, B.E. (2014). Differentiating connexin hemichannels and pannexin channels in cellular ATP release. *FEBS Lett.* *588*, 1379–1388.
- Lohman, A.W., Leskov, I.L., Butcher, J.T., Johnstone, S.R., Stokes, T.A., Begandt, D., DeLalio, L.J., Best, A.K., Penuela, S., Leitinger, N., et al. (2015). Pannexin 1 channels regulate leukocyte emigration through the venous endothelium during acute inflammation. *Nat Commun* *6*, 7965.
- Lutz, S.E., González-Fernández, E., Ventura, J.C.C., Pérez-Samartín, A., Tarassishin, L., Negro, H., Patel, N.K., Suadicani, S.O., Lee, S.C., Matute, C., et al. (2013). Contribution of pannexin1 to experimental autoimmune encephalomyelitis. *PLoS ONE* *8*, e66657.
- Ma, W., Compan, V., Zheng, W., Martin, E., North, R.A., Verkhratsky, A., and Surprenant, A. (2012). Pannexin 1 forms an anion-selective channel. *Pflugers Arch.* *463*, 585–592.
- Madeo, F., Eisenberg, T., Pietrocola, F., and Kroemer, G. (2018). Spermidine in health and disease. *Science* *359*, ean2788.
- Maj, T., Wang, W., Crespo, J., Zhang, H., Wang, W., Wei, S., Zhao, L., Vatan, L., Shao, I., Szeliga, W., et al. (2017). Oxidative stress controls regulatory T cell apoptosis and suppressor activity and PD-L1-blockade resistance in tumor. *Nat. Immunol.* *18*, 1332–1341.
- Marques-da-Silva, C., Burnstock, G., Ojcius, D.M., and Coutinho-Silva, R. (2011). Purinergic receptor agonists modulate phagocytosis and clearance of apoptotic cells in macrophages. *Immunobiology* *216*, 1–11.
- Medina, C.B., and Ravichandran, K.S. Do not let death do us part: 'find-me' signals in communication between dying cells and the phagocytes. *Cell Death Differ.* *23*, 979–989.
- Michalski, K., Syrjanen, J.L., Henze, E., Kumpf, J., Furukawa, H., and Kawate, T. (2020). The cryo-EM structure of a pannexin 1 reveals unique motifs for ion selection and inhibition. *Elife* *9*, 213.
- Miksa, M., Amin, D., Wu, R., Ravikumar, T.S., and Wang, P. (2007). Fractalkine-induced MFG-E8 leads to enhanced apoptotic cell clearance by macrophages. *Mol. Med.* *13*, 553–560.
- Miyaniishi, M., Tada, K., Koike, M., Uchiyama, Y., Kitamura, T., and Nagata, S. (2007). Identification of Tim4 as a phosphatidylserine receptor. *Nature* *450*, 435–439.
- Mizugishi, K., Yamashita, T., Olivera, A., Miller, G.F., Spiegel, S., and Proia, R.L. (2005). Essential role for sphingosine kinases in neural and vascular development. *Mol. Cell. Biol.* *25*, 11113–11121.

- Mizuno, T., Kawanokuchi, J., Numata, K., and Suzumura, A. (2003). Production and neuroprotective functions of fractalkine in the central nervous system. *Brain Res.* *979*, 65–70.
- Morioka, S., Maueröder, C., and Ravichandran, K.S. (2019). Living on the Edge: Efferocytosis at the Interface of Homeostasis and Pathology. *Immunity* *50*, 1149–1162.
- Morioka, S., Perry, J.S.A., Raymond, M.H., Medina, C.B., Zhu, Y., Zhao, L., Serbulea, V., Onengut-Gumuscu, S., Leitinger, N., Kucenas, S., et al. (2018). Efferocytosis induces a novel SLC program to promote glucose uptake and lactate release. *Nature* *16*, 907.
- Muehling, L.M., Lawrence, M.G., and Woodfolk, J.A. (2017). Pathogenic CD4+ T cells in patients with asthma. *J. Allergy Clin. Immunol.* *140*, 1523–1540.
- Muñoz, L.E., Peter, C., Herrmann, M., Wesselborg, S., and Lauber, K. (2010). Scent of dying cells: the role of attraction signals in the clearance of apoptotic cells and its immunological consequences. *Autoimmun Rev* *9*, 425–430.
- Murakami, N., Yokomizo, T., Okuno, T., and Shimizu, T. (2004). G2A is a proton-sensing G-protein-coupled receptor antagonized by lysophosphatidylcholine. *J. Biol. Chem.* *279*, 42484–42491.
- Murata, N., Sato, K., Kon, J., Tomura, H., Yanagita, M., Kuwabara, A., Ui, M., and Okajima, F. (2000). Interaction of sphingosine 1-phosphate with plasma components, including lipoproteins, regulates the lipid receptor-mediated actions. *Biochem. J.* *352 Pt 3*, 809–815.
- Müller, T., Robaye, B., Vieira, R.P., Ferrari, D., Grimm, M., Jakob, T., Martin, S.F., Di Virgilio, F., Boeynaems, J.-M., Virchow, J.C., et al. (2010). The purinergic receptor P2Y2 receptor mediates chemotaxis of dendritic cells and eosinophils in allergic lung inflammation. *Allergy* *65*, 1545–1553.
- Nagata, S. (2018). Apoptosis and Clearance of Apoptotic Cells. *Annu. Rev. Immunol.* *36*, annurev-immunol-042617-053010.
- Nagata, S., Hanayama, R., and Kawane, K. (2010). Autoimmunity and the clearance of dead cells. *Cell* *140*, 619–630.
- Nakayama, M., Akiba, H., Takeda, K., Kojima, Y., Hashiguchi, M., Azuma, M., Yagita, H., and Okumura, K. (2009). Tim-3 mediates phagocytosis of apoptotic cells and cross-presentation. *Blood* *113*, 3821–3830.
- Nishimura, T., Horino, K., Nishiura, H., Shibuya, Y., Hiraoka, T., Tanase, S., and Yamamoto, T. (2001). Apoptotic cells of an epithelial cell line, AsPC-1, release monocyte chemotactic S19 ribosomal protein dimer. *J. Biochem.* *129*, 445–454.

Nishiura, H., Shibuya, Y., and Yamamoto, T. (1998). S19 ribosomal protein cross-linked dimer causes monocyte-predominant infiltration by means of molecular mimicry to complement C5a. *Lab. Invest.* *78*, 1615–1623.

Nishiura, H., Tanase, S., Sibuya, Y., Nishimura, T., and Yamamoto, T. (1999). Determination of the cross-linked residues in homo-dimerization of S19 ribosomal protein concomitant with exhibition of monocyte chemotactic activity. *Lab. Invest.* *79*, 915–923.

Noda, M., Doi, Y., Liang, J., Kawanokuchi, J., Sonobe, Y., Takeuchi, H., Mizuno, T., and Suzumura, A. (2011). Fractalkine attenuates excitotoxicity via microglial clearance of damaged neurons and antioxidant enzyme heme oxygenase-1 expression. *J. Biol. Chem.* *286*, 2308–2319.

Obinata, H., Hattori, T., Nakane, S., Tatei, K., and Izumi, T. (2005). Identification of 9-hydroxyoctadecadienoic acid and other oxidized free fatty acids as ligands of the G protein-coupled receptor G2A. *J. Biol. Chem.* *280*, 40676–40683.

Ojala, P.J., Hermansson, M., Tolvanen, M., Polvinen, K., Hirvonen, T., Impola, U., Jauhiainen, M., Somerharju, P., and Parkkinen, J. (2006). Identification of alpha-1 acid glycoprotein as a lysophospholipid binding protein: a complementary role to albumin in the scavenging of lysophosphatidylcholine. *Biochemistry* *45*, 14021–14031.

Okajima, F. (2002). Plasma lipoproteins behave as carriers of extracellular sphingosine 1-phosphate: is this an atherogenic mediator or an anti-atherogenic mediator? *Biochim. Biophys. Acta* *1582*, 132–137.

Okita, M., Gaudette, D.C., Mills, G.B., and Holub, B.J. (1997). Elevated levels and altered fatty acid composition of plasma lysophosphatidylcholine(lysoPC) in ovarian cancer patients. *Int. J. Cancer* *71*, 31–34.

Park, D., Tosello-Tramont, A.-C., Elliott, M.R., Lu, M., Haney, L.B., Ma, Z., Klibanov, A.L., Mandell, J.W., and Ravichandran, K.S. (2007). BAI1 is an engulfment receptor for apoptotic cells upstream of the ELMO/Dock180/Rac module. *Nature* *450*, 430–434.

Park, S.-Y., Jung, M.-Y., Kim, H.-J., Lee, S.-J., Kim, S.-Y., Lee, B.-H., Kwon, T.-H., Park, R.-W., and Kim, I.-S. (2008a). Rapid cell corpse clearance by stabilin-2, a membrane phosphatidylserine receptor. *Cell Death Differ.* *15*, 192–201.

Park, S.-Y., Kang, K.-B., Thapa, N., Kim, S.-Y., Lee, S.-J., and Kim, I.-S. (2008b). Requirement of adaptor protein GULP during stabilin-2-mediated cell corpse engulfment. *J. Biol. Chem.* *283*, 10593–10600.

Pasparakis, M., and Vandenabeele, P. (2015). Necroptosis and its role in inflammation. *Nature* *517*, 311–320.

Pegg, A.E. (2016). Functions of Polyamines in Mammals. *J. Biol. Chem.* *291*, 14904–14912.

Penberthy, K.K., and Ravichandran, K.S. (2016). Apoptotic cell recognition receptors and scavenger receptors. *Immunol. Rev.* 269, 44–59.

Penberthy, K.K., Rival, C., Shankman, L.S., Raymond, M.H., Zhang, J., Perry, J.S.A., Lee, C.S., Han, C.Z., Onengut-Gumuscu, S., Palczewski, K., et al. (2017). Context-dependent compensation among phosphatidylserine-recognition receptors. *Sci Rep* 7, 14623–14.

Penuela, S., Bhalla, R., Gong, X.-Q., Cowan, K.N., Celetti, S.J., Cowan, B.J., Bai, D., Shao, Q., and Laird, D.W. (2007). Pannexin 1 and pannexin 3 are glycoproteins that exhibit many distinct characteristics from the connexin family of gap junction proteins. *J. Cell. Sci.* 120, 3772–3783.

Penuela, S., Bhalla, R., Nag, K., and Laird, D.W. (2009). Glycosylation regulates pannexin intermixing and cellular localization. *Mol. Biol. Cell* 20, 4313–4323.

Penuela, S., Harland, L., Simek, J., and Laird, D.W. (2014). Pannexin channels and their links to human disease. *Biochem. J.* 461, 371–381.

Peter, C., Waibel, M., Keppeler, H., Lehmann, R., Xu, G., Halama, A., Adamski, J., Schulze-Osthoff, K., Wesselborg, S., and Lauber, K. (2012). Release of lysophospholipid “find-me” signals during apoptosis requires the ATP-binding cassette transporter A1. *Autoimmunity* 45, 568–573.

Peter, C., Waibel, M., Radu, C.G., Yang, L.V., Witte, O.N., Schulze-Osthoff, K., Wesselborg, S., and Lauber, K. (2008). Migration to apoptotic “find-me” signals is mediated via the phagocyte receptor G2A. *J. Biol. Chem.* 283, 5296–5305.

Peter, C., Wesselborg, S., and Lauber, K. (2010a). Apoptosis: opening PANDora's BoX. *Curr. Biol.* 20, R940–R942.

Peter, C., Wesselborg, S., Herrmann, M., and Lauber, K. (2010b). Dangerous attraction: phagocyte recruitment and danger signals of apoptotic and necrotic cells. *Apoptosis* 15, 1007–1028.

Pietrocola, F., Lachkar, S., Enot, D.P., Niso-Santano, M., Bravo-San Pedro, J.M., Sica, V., Izzo, V., Maiuri, M.C., Madeo, F., Mariño, G., et al. (2015). Spermidine induces autophagy by inhibiting the acetyltransferase EP300. *Cell Death Differ.* 22, 509–516.

Poon, I.K.H., Chiu, Y.-H., Armstrong, A.J., Kinchen, J.M., Juncadella, I.J., Bayliss, D.A., and Ravichandran, K.S. (2014a). Unexpected link between an antibiotic, pannexin channels and apoptosis. *Nature* 507, 329–334.

Poon, I.K.H., Lucas, C.D., Rossi, A.G., and Ravichandran, K.S. (2014b). Apoptotic cell clearance: basic biology and therapeutic potential. *Nat. Rev. Immunol.* 14, 166–180.

- Pradelli, L.A., Villa, E., Zunino, B., Marchetti, S., and Ricci, J.-E. (2014). Glucose metabolism is inhibited by caspases upon the induction of apoptosis. *Cell Death Dis* 5, e1406–e1406.
- Qu, Y., Misaghi, S., Newton, K., Gilmour, L.L., Louie, S., Cupp, J.E., Dubyak, G.R., Hackos, D., and Dixit, V.M. (2011). Pannexin-1 is required for ATP release during apoptosis but not for inflammasome activation. *J. Immunol.* 186, 6553–6561.
- Quinn, M.T., Parthasarathy, S., and Steinberg, D. (1988). Lysophosphatidylcholine: a chemotactic factor for human monocytes and its potential role in atherogenesis. *Proc. Natl. Acad. Sci. U.S.a.* 85, 2805–2809.
- Raedler, D., Ballenberger, N., Klucker, E., Böck, A., Otto, R., Prazeres da Costa, O., Holst, O., Illig, T., Buch, T., Mutius, von, E., et al. (2015). Identification of novel immune phenotypes for allergic and nonallergic childhood asthma. *J. Allergy Clin. Immunol.* 135, 81–91.
- Ramirez-Ortiz, Z.G., Pendergraft, W.F., Prasad, A., Byrne, M.H., Iram, T., Blanchette, C.J., Luster, A.D., Hacohen, N., Houry, El, J., and Means, T.K. (2013). The scavenger receptor SCARF1 mediates the clearance of apoptotic cells and prevents autoimmunity. *Nat. Immunol.* 14, 917–926.
- Ransford, G.A., Fregien, N., Qiu, F., Dahl, G., Conner, G.E., and Salathe, M. (2009). Pannexin 1 contributes to ATP release in airway epithelia. *Am. J. Respir. Cell Mol. Biol.* 41, 525–534.
- Ravichandran, K.S. (2003). “Recruitment Signals” from Apoptotic Cells. *Cell* 113, 817–820.
- Ravichandran, K.S. (2011). Beginnings of a good apoptotic meal: the find-me and eat-me signaling pathways. *Immunity* 35, 445–455.
- Ravichandran, K.S., and Lorenz, U. (2007). Engulfment of apoptotic cells: signals for a good meal. *Nat. Rev. Immunol.* 7, 964–974.
- Rayah, A., Kanellopoulos, J.M., and Di Virgilio, F. (2012). P2 receptors and immunity. *Microbes Infect.* 14, 1254–1262.
- Riederer, M., Ojala, P.J., Hrzenjak, A., Graier, W.F., Malli, R., Tritscher, M., Hermansson, M., Watzer, B., Schweer, H., Desoye, G., et al. (2010). Acyl chain-dependent effect of lysophosphatidylcholine on endothelial prostacyclin production. *J. Lipid Res.* 51, 2957–2966.
- Rosen, H., Gonzalez-Cabrera, P.J., Sanna, M.G., and Brown, S. (2009). Sphingosine 1-phosphate receptor signaling. *Annu. Rev. Biochem.* 78, 743–768.
- Rothlin, C.V., Carrera Silva, E.A., Bosurgi, L., and Ghosh, S. (2015). TAM receptor signaling in immune homeostasis. *Annu. Rev. Immunol.* 33, 355–391.

Ryoo, H.D., Gorenc, T., and Steller, H. (2004). Apoptotic cells can induce compensatory cell proliferation through the JNK and the Wingless signaling pathways. *Dev. Cell* 7, 491–501.

Saederup, N., Chan, L., Lira, S.A., and Charo, I.F. (2008). Fractalkine deficiency markedly reduces macrophage accumulation and atherosclerotic lesion formation in CCR2^{-/-} mice: evidence for independent chemokine functions in atherogenesis. *Circulation* 117, 1642–1648.

Sandilos, J.K., Chiu, Y.-H., Chekeni, F.B., Armstrong, A.J., Walk, S.F., Ravichandran, K.S., and Bayliss, D.A. (2012). Pannexin 1, an ATP release channel, is activated by caspase cleavage of its pore-associated C-terminal autoinhibitory region. *J. Biol. Chem.* 287, 11303–11311.

Sang, Q., Zhang, Z., Shi, J., Sun, X., Li, B., Yan, Z., Xue, S., Ai, A., Lyu, Q., Li, W., et al. (2019). A pannexin 1 channelopathy causes human oocyte death. *Science Translational Medicine* 11, eaav8731.

Schenk, U., Westendorf, A.M., Radaelli, E., Casati, A., Ferro, M., Fumagalli, M., Verderio, C., Buer, J., Scanziani, E., and Grassi, F. (2008). Purinergic control of T cell activation by ATP released through pannexin-1 hemichannels. *Sci Signal* 1, ra6–ra6.

Scher, J.U., and Pillinger, M.H. (2009). The anti-inflammatory effects of prostaglandins. *J. Investig. Med.* 57, 703–708.

Schulte, A., Schulz, B., Andrzejewski, M.G., Hundhausen, C., Mletzko, S., Achilles, J., Reiss, K., Paliga, K., Weber, C., John, S.R., et al. (2007). Sequential processing of the transmembrane chemokines CX3CL1 and CXCL16 by alpha- and gamma-secretases. *Biochem. Biophys. Res. Commun.* 358, 233–240.

Segawa, K., and Nagata, S. (2015). An Apoptotic “Eat Me” Signal: Phosphatidylserine Exposure. *Trends Cell Biol.* 25, 639–650.

Segundo, C., Medina, F., Rodríguez, C., Martínez-Palencia, R., Leyva-Cobián, F., and Brieva, J.A. (1999). Surface molecule loss and bleb formation by human germinal center B cells undergoing apoptosis: role of apoptotic blebs in monocyte chemotaxis. *Blood* 94, 1012–1020.

Seminario-Vidal, L., Okada, S.F., Sesma, J.I., Kreda, S.M., van Heusden, C.A., Zhu, Y., Jones, L.C., O'Neal, W.K., Penuela, S., Laird, D.W., et al. (2011). Rho signaling regulates pannexin 1-mediated ATP release from airway epithelia. *J. Biol. Chem.* 286, 26277–26286.

Shao, Q., Lindstrom, K., Shi, R., Kelly, J., Schroeder, A., Juusola, J., Levine, K.L., Esseltine, J.L., Penuela, S., Jackson, M.F., et al. (2016). A germline variant in PANX1 has reduced channel function and is associated with multisystem dysfunction. *J. Biol. Chem.* jbc.M116.717934.

- Sharma, A.K., Charles, E.J., Zhao, Y., Narahari, A.K., Baderdinni, P.K., Good, M.E., Lorenz, U.M., Kron, I.L., Bayliss, D.A., Ravichandran, K.S., et al. (2018). Pannexin-1 channels on endothelial cells mediate vascular inflammation during lung ischemia-reperfusion injury. *Am. J. Physiol. Lung Cell Mol. Physiol.* *315*, L301–L312.
- Shayakul, C., Cl emen on, B., and Hediger, M.A. (2013). The urea transporter family (SLC14): physiological, pathological and structural aspects. *Mol. Aspects Med.* *34*, 313–322.
- Shinzawa, K., Sumi, H., Ikawa, M., Matsuoka, Y., Okabe, M., Sakoda, S., and Tsujimoto, Y. (2008). Neuroaxonal dystrophy caused by group VIA phospholipase A2 deficiency in mice: a model of human neurodegenerative disease. *J. Neurosci.* *28*, 2212–2220.
- Shrestha, A., Shiokawa, M., Nishimura, T., Nishiura, H., Tanaka, Y., Nishino, N., Shibuya, Y., and Yamamoto, T. (2003). Switch moiety in agonist/antagonist dual effect of S19 ribosomal protein dimer on leukocyte chemotactic C5a receptor. *Am. J. Pathol.* *162*, 1381–1388.
- Silverman, W.R., de Rivero Vaccari, J.P., Locovei, S., Qiu, F., Carlsson, S.K., Scemes, E., Keane, R.W., and Dahl, G. (2009). The pannexin 1 channel activates the inflammasome in neurons and astrocytes. *J. Biol. Chem.* *284*, 18143–18151.
- Snider, A.J., Kawamori, T., Bradshaw, S.G., Orr, K.A., Gilkeson, G.S., Hannun, Y.A., and Obeid, L.M. (2009). A role for sphingosine kinase 1 in dextran sulfate sodium-induced colitis. *Faseb J.* *23*, 143–152.
- Soriano, P. (1999). Generalized lacZ expression with the ROSA26 Cre reporter strain. *Nat. Genet.* *21*, 70–71.
- Steinke, J.W., and Borish, L. (2001). Th2 cytokines and asthma. Interleukin-4: its role in the pathogenesis of asthma, and targeting it for asthma treatment with interleukin-4 receptor antagonists. *Respir. Res.* *2*, 66–70.
- Stewart, S., Fishbein, M.C., Snell, G.I., Berry, G.J., Boehler, A., Burke, M.M., Glanville, A., Gould, F.K., Magro, C., Marboe, C.C., et al. (2007). Revision of the 1996 working formulation for the standardization of nomenclature in the diagnosis of lung rejection. pp. 1229–1242.
- Tabas, I. (2010). Macrophage death and defective inflammation resolution in atherosclerosis. *Nat. Rev. Immunol.* *10*, 36–46.
- Taniuchi, M., Otani, H., Kodama, N., Tone, Y., Sakagashira, M., Yamada, Y., Mune, M., and Yukawa, S. (1999). Lysophosphatidylcholine up-regulates IL-1 beta-induced iNOS expression in rat mesangial cells. *Kidney Int. Suppl.* *71*, S156–S158.
- Tanzer, M.C., Frauenstein, A., Stafford, C.A., Phulphagar, K., Mann, M., and Meissner, F. (2020). Quantitative and Dynamic Catalogs of Proteins Released during Apoptotic and Necroptotic Cell Death. *Cell Rep* *30*, 1260–1270.e1265.

- Taylor, K.A., Wright, J.R., and Mahaut-Smith, M.P. (2015). Regulation of Pannexin-1 channel activity. *Biochem. Soc. Trans.* *43*, 502–507.
- Teupser, D., Pavlides, S., Tan, M., Gutierrez-Ramos, J.-C., Kolbeck, R., and Breslow, J.L. (2004). Major reduction of atherosclerosis in fractalkine (CX3CL1)-deficient mice is at the brachiocephalic artery, not the aortic root. *Proc. Natl. Acad. Sci. U.S.A.* *101*, 17795–17800.
- Thompson, C.B. (1995). Apoptosis in the pathogenesis and treatment of disease. *Science* *267*, 1456–1462.
- Thompson, R.J., Jackson, M.F., Olah, M.E., Rungta, R.L., Hines, D.J., Beazely, M.A., MacDonald, J.F., and MacVicar, B.A. (2008). Activation of pannexin-1 hemichannels augments aberrant bursting in the hippocampus. *Science* *322*, 1555–1559.
- Tibes, U., Hinder, M., Scheuer, W., Friebe, W.G., Schramm, S., and Kaiser, B. (1999). Phospholipase A2 is involved in chemotaxis of human leukocytes. *Adv. Exp. Med. Biol.* *469*, 189–197.
- Timmins, J.M., Lee, J.-Y., Boudyguina, E., Kluckman, K.D., Brunham, L.R., Mulya, A., Gebre, A.K., Coutinho, J.M., Colvin, P.L., Smith, T.L., et al. (2005). Targeted inactivation of hepatic Abca1 causes profound hypoalphalipoproteinemia and kidney hypercatabolism of apoA-I. *J. Clin. Invest.* *115*, 1333–1342.
- Truman, L.A., Ford, C.A., Pasikowska, M., Pound, J.D., Wilkinson, S.J., Dumitriu, I.E., Melville, L., Melrose, L.A., Ogden, C.A., Nibbs, R., et al. (2008). CX3CL1/fractalkine is released from apoptotic lymphocytes to stimulate macrophage chemotaxis. *Blood* *112*, 5026–5036.
- Tseng, A.-S., Adams, D.S., Qiu, D., Koustubhan, P., and Levin, M. (2007). Apoptosis is required during early stages of tail regeneration in *Xenopus laevis*. *Dev. Biol.* *301*, 62–69.
- Umetsu, D.T., and Dekruyff, R.H. (2006). The regulation of allergy and asthma. *Immunol. Rev.* *212*, 238–255.
- Van Opdenbosch, N., Van Gorp, H., Verdonckt, M., Saavedra, P.H.V., de Vasconcelos, N.M., Gonçalves, A., Vande Walle, L., Demon, D., Matusiak, M., Van Hauwermeiren, F., et al. (2017). Caspase-1 Engagement and TLR-Induced c-FLIP Expression Suppress ASC/Caspase-8-Dependent Apoptosis by Inflammasome Sensors NLRP1b and NLRC4. *Cell Rep* *21*, 3427–3444.
- Veras, F.P., Peres, R.S., Saraiva, A.L.L., Pinto, L.G., Louzada-Junior, P., Cunha, T.M., Paschoal, J.A.R., Cunha, F.Q., and Alves-Filho, J.C. (2015). Fructose 1,6-bisphosphate, a high-energy intermediate of glycolysis, attenuates experimental arthritis by activating anti-inflammatory adenosinergic pathway. *Sci Rep* *5*, 15171.

- Voll, R.E., Herrmann, M., Roth, E.A., Stach, C., Kalden, J.R., and Girkontaite, I. (1997). Immunosuppressive effects of apoptotic cells. *Nature* 390, 350–351.
- Wakasugi, K., and Schimmel, P. (1999). Two distinct cytokines released from a human aminoacyl-tRNA synthetase. *Science* 284, 147–151.
- Walker, C., Kaegi, M.K., Braun, P., and Blaser, K. (1991). Activated T cells and eosinophilia in bronchoalveolar lavages from subjects with asthma correlated with disease severity. *J. Allergy Clin. Immunol.* 88, 935–942.
- Wang, H., Xing, Y., Mao, L., Luo, Y., Kang, L., and Meng, G. (2013). Pannexin-1 influences peritoneal cavity cell population but is not involved in NLRP3 inflammasome activation. *Protein Cell* 4, 259–265.
- Wang, J., and Dahl, G. (2010). SCAM analysis of Panx1 suggests a peculiar pore structure. *J. Gen. Physiol.* 136, 515–527.
- Wang, J., Ma, M., Locovei, S., Keane, R.W., and Dahl, G. (2007). Modulation of membrane channel currents by gap junction protein mimetic peptides: size matters. *American Journal of Physiology - Cell Physiology* 293, C1112–C1119.
- Wang, Y., Subramanian, M., Yurdagul, A., Barbosa-Lorenzi, V.C., Cai, B., de Juan-Sanz, J., Ryan, T.A., Nomura, M., Maxfield, F.R., and Tabas, I. (2017). Mitochondrial Fission Promotes the Continued Clearance of Apoptotic Cells by Macrophages. *Cell* 171, 331–345.e22.
- Weaver, J.L., Arandjelovic, S., Brown, G., K Mendu, S., S Schappe, M., Buckley, M.W., Chiu, Y.-H., Shu, S., Kim, J.K., Chung, J., et al. (2017). Hematopoietic pannexin 1 function is critical for neuropathic pain. *Sci Rep* 7, 42550.
- Weigert, A., Cremer, S., Schmidt, M.V., Knethen, von, A., Angioni, C., Geisslinger, G., and Brüne, B. (2010). Cleavage of sphingosine kinase 2 by caspase-1 provokes its release from apoptotic cells. *Blood* 115, 3531–3540.
- Weigert, A., Johann, A.M., Knethen, von, A., Schmidt, H., Geisslinger, G., and Brüne, B. (2006). Apoptotic cells promote macrophage survival by releasing the antiapoptotic mediator sphingosine-1-phosphate. *Blood* 108, 1635–1642.
- Weigert, A., Tzieply, N., Knethen, von, A., Johann, A.M., Schmidt, H., Geisslinger, G., and Brüne, B. (2007). Tumor cell apoptosis polarizes macrophages role of sphingosine-1-phosphate. *Mol. Biol. Cell* 18, 3810–3819.
- Weinlich, R., Oberst, A., Beere, H.M., and Green, D.R. (2017). Necroptosis in development, inflammation and disease. *Nat. Rev. Mol. Cell Biol.* 18, 127–136.
- White, G.E., and Greaves, D.R. (2012). Fractalkine: a survivor's guide: chemokines as antiapoptotic mediators. *Arterioscler. Thromb. Vasc. Biol.* 32, 589–594.

White, G.E., Tan, T.C.C., John, A.E., Whatling, C., McPheat, W.L., and Greaves, D.R. (2010). Fractalkine has anti-apoptotic and proliferative effects on human vascular smooth muscle cells via epidermal growth factor receptor signalling. *Cardiovasc. Res.* 85, 825–835.

Witte, O.N., Kabarowski, J.H., Xu, Y., Le, L.Q., and Zhu, K. (2005). Retraction. *Science* 307, 206–206b.

Wu, Y.C., and Horvitz, H.R. (1998). The *C. elegans* cell corpse engulfment gene *ced-7* encodes a protein similar to ABC transporters. *Cell* 93, 951–960.

Xiao, C., Calado, D.P., Galler, G., Thai, T.-H., Patterson, H.C., Wang, J., Rajewsky, N., Bender, T.P., and Rajewsky, K. (2007). MiR-150 controls B cell differentiation by targeting the transcription factor *c-Myb*. *Cell* 131, 146–159.

Yamaguchi, H., Maruyama, T., Urade, Y., and Nagata, S. (2014). Immunosuppression via adenosine receptor activation by adenosine monophosphate released from apoptotic cells. *Elife* 3, e02172.

Yamamoto, T. (2007). Roles of the ribosomal protein S19 dimer and the C5a receptor in pathophysiological functions of phagocytic leukocytes. *Pathol. Int.* 57, 1–11.

Yang, L.V., Radu, C.G., Wang, L., Riedinger, M., and Witte, O.N. (2005). Gi-independent macrophage chemotaxis to lysophosphatidylcholine via the immunoregulatory GPCR G2A. *Blood* 105, 1127–1134.

Zaiss, D.M.W., Gause, W.C., Osborne, L.C., and Artis, D. (2015). Emerging functions of amphiregulin in orchestrating immunity, inflammation, and tissue repair. *Immunity* 42, 216–226.

Zhang, S., Weinberg, S., DeBerge, M., Gainullina, A., Schipma, M., Kinchen, J.M., Ben-Sahra, I., Gius, D.R., Charvet, L.Y., Chandel, N.S., et al. (2018). Efferocytosis Fuels Requirements of Fatty Acid Oxidation and the Electron Transport Chain to Polarize Macrophages for Tissue Repair. *Cell Metab.* 29, 443–456.e445.

Zimmermann, H., Zebisch, M., and Sträter, N. (2012). Cellular function and molecular structure of ecto-nucleotidases. *Purinergic Signal.* 8, 437–502.

Zujovic, V., Benavides, J., Vigé, X., Carter, C., and Taupin, V. (2000). Fractalkine modulates TNF- α secretion and neurotoxicity induced by microglial activation. *Glia* 29, 305–315.

Zwart, B., Ciurana, C., Rensink, I., Manoe, R., Hack, C.E., and Aarden, L.A. (2004). Complement activation by apoptotic cells occurs predominantly via IgM and is limited to late apoptotic (secondary necrotic) cells. *Autoimmunity* 37, 95–102.